NTNU – Trondheim
Norwegian University of
Science and Technology

Specialized Alginates and Microcapsules for Cell Therapy and Tissue Engineering

Focus on Immunological Properties in a
Whole Blood Model

Kine Samset Hoem

Biotechnology (5 year)
Submission date: May 2013
Supervisor: Gudmund Skjåk-Bræk, IBT
Co-supervisor: Berit Strand, IBT
Anne Mari Rokstad, IKM

Norwegian University of Science and Technology
Department of Biotechnology

Preface

This Master of Science thesis in biotechnology was submitted to the Department of Biotechnology at the Norwegian University of Science and Technology. The laboratory work was carried out at the Department of Cancer Research and Molecular Medicine in the time periods September 2011 to December 2011, and September 2012 to March 2013.

First of all I would deeply like to thank my skilled supervisors, Anne Mari Rokstad and Berit L. Strand. You have been so optimistic, enthusiastic and supportive throughout this process, and always helpful with the laboratory work as well as during the writing. I am very thankful for having been introduced into the fascinating world of biomaterials, and in particular alginate.

I would also like to express my gratitude towards senior engineers Bjørg Steinkjer and Liv Ryan for training and guidance at the lab, and senior engineer Kjartan W. Egeberg for help with using the confocal microscope. A thank you is directed towards the people who have been kind enough to donate blood – this thesis wouldn't have been much without you. In addition, I would like to thank professor Gudmund Skjåk-Bræk for being my supervisor at the Department of Biotechnology.

Last but not least, I would like to thank Olav Martin for his encouragement, care and understanding, as well as friends and family for their support.

Abstract

Alginates are a group of abundant natural polysaccharides with excellent gel-forming capacity and good biocompatibility, provided they are sufficiently well purified. Alginate shows great promise as an encapsulation material for the purpose of immunoisolating therapeutic cell transplants, such as insulin-producing cells for the treatment of type 1 diabetes mellitus. Recently, alginates have also been implicated for making novel extracellular matrix (ECM)-like bioscaffolds in tissue engineering.

An absolute requirement for successful graft function is that the biomaterial or microcapsule itself does not evoke inflammatory reactions. Thus, developing an understanding of the basic mechanisms leading to bioincompatibility of biomaterials *in vivo* is necessary in order to create improved artificial organs and tissue. To do this, the stimulatory properties of different biomaterials can be explored *in vitro*.

A lepirudin-based human whole blood model was used to demonstrate the inflammatory potential of a set of different alginate microcapsules and microbeads. This was done in order to elucidate the effect of introducing different properties into the alginate system, e.g. hydroxyapatite (HA) mineralization – as intended for uses in bone tissue engineering , and covalent grafting with peptides – as intended for producing ECM-like materials for general tissue engineering strategies. Furthermore, other microcapsules and microbeads proposed as immunoisolation devices in transplantation were also examined. Complement activation in terms of sTCC, secretion of chemokines, pro- and anti-inflammatoy cytokines and growth factors, as well as leukocyte activation in terms of CD11b-expression was measured. Confocal laser scanning microscopy (CLSM) was used in order to visualize receptor expression on attached cells and protein deposition on the capsule surfaces.

The HA-containing microbeads were found to possess slight immunostimulatory properties. This was especially true for microbeads mineralized through counter-diffusion precipitation, which induced significant leukocyte activation in terms of CD11b-expression, and also noticeably high levels of certain cytokines, e.g. the chemokine MCP-1. Furthermore, these microbeads significantly induced complement activation in terms of sTCC, which was also true for the microbeads mineralized by the use of alkaline phosphatase enzymes. Ca/Ba alginate microbeads (TAM) generally appeared non-inflammatory, and did not induce leukocyte activation, complement or cytokine secretion. Peptide-coupled microbeads covalently grafted with the cell adhesion motifs RGD and REDV, respectively, did generally not induce complement or leukocyte activation, nor cytokine induction, and were overall considered as non-inflammatory. Only the microbeads made from REDV-coupled alginate induced significant cytokine secretion, in terms of IFN-γ and IL-10. On the other hand, microbeads made from VAPG-coupled alginate induced potent inflammatory responses; however, this effect was most likely linked to a substantial endotoxin contamination. In comparison, polycation-containing microcapsules induced potent inflammatory responses in terms of significant levels of leukocyte (CD11b) and complement activation, as well as elevated cytokine levels.

Another part of this thesis aimed to get a mechanistic understanding of phenomena related to differences in the stimulatory effects of solid versus hollow microcapsules. Liquefying the capsule core was observed to decrease the immunostimulatory properties of PLL-containing microcapsules in terms of reduced complement protein deposition, cell adhesion and IL-8 secretion. In contrast, a more potent sTCC increase was detected for these hollow PLL-containing microcapsules as compared to those with a solid core. This could potentially be due to a hypothesized soluble molecule leaking out from the hollow microcapsules and triggering TCC formation in the fluid phase. By employing the C3-specific complement inhibitor compstatin, microcapsules with a liquefied core were further demonstrated to rely on complement activation for cytokine induction. Moreover, hollow microcapsules containing PLO as a polycation showed more promising properties in terms of lower complement activation as compared with PLL-containing hollow microcapsules.

In terms of studying the mechanisms leading to cytokine secretion, inhibiting the CD11b/CD18 complement receptor was not found to reduce IL-8 levels, likely due to a stimulatory effect of the CD11b-inhibitory antibody itself. Furthermore, whether the inhibition of phagocytosis with cytochalasin D affected the IL-8 release could not be concluded due to a toxic effect of the ethanol in which the cytochalasin was solubilized.

Sammendrag

Alginater er en gruppe naturlige polysakkarider som er vist å ha svært gode gelingsegenskaper og god biokompatibilitet, forutsatt at de er tilstrekkelig renset. Alginater er svært lovende som innkapslingsmaterialer for det formål å immunoisolere terapeutiske celletransplantater, som for eksempel insulinproduserende celler i behandling av type 1 diabetes mellitus. Nylig har alginater også blitt tatt i bruk i utviklingen av nye ekstracellulær matriks (ECM)-lignende biomaterialer innen vevsteknologi.

Et absolutt krav for vellykket transplantatfunksjon er at biomaterialet eller mikrokapselen i seg selv ikke framprovoserer inflammasjonsreaksjoner. For å kunne utvikle forbedrede kunstige organer og vev er det derfor helt nødvendig å forstå de grunnleggende mekanismene som fører til biomaterialers bioinkompatibilitet *in vivo*. For å oppnå dette kan de immunostimulerende egenskapene til ulike biomaterialer utforskes *in vitro*.

En lepirudin-basert human fullblodsmodell ble brukt for å demonstrere de inflammatoriske potensialene til forskjellige alginat-mikrokapsler og mikrokuler. Dette ble gjort for å utrede effekten av å introdusere ulike egenskaper inn i alginatsystemet, som f.eks. hydroxyapatitt (HA)-mineralisering – til bruk i benvevsteknologi, og kovalent påkobling av peptider – til bruk i produksjon av ECM-lignende materialer for generelle strategier innen vevsteknologi. Studier ble også foretatt av andre mikrokapsler og mikrokuler foreslått som immunoisolerende enheter for transplantasjon. Komplementaktivering i form av sTCC-dannelse, utskillelse av chemokiner, pro- og anti-inflammatoriske cytokiner og vekstfaktorer, såvel som leukocyttaktivering målt som CD11b-oppregulering ble undersøkt. Konfokal laser scanning mikroskopi (CLSM) ble brukt for å visualisere reseptorekspresjon på adherte celler og proteinnedslag på kapseloverflater.

De HA-mineraliserte mikrokulene ble observert å inneha lett immunostimulerende egenskaper. Dette var spesielt tydelig for mikrokuler mineralisert via diffusjonsbasert HA-utfelling, som induserte betydelig leukocyttaktivering i form av CD11b-oppregulering, og også merkbart høye nivåer av enkelte cytokiner, f.eks. chemokinet MCP-1. Videre stimulerte disse mikrokulene til en betydelig komplementaktivering i form av sTCC, noe som var tilfelle også for mikrokulene mineralisert ved hjelp av alkalisk fosfatase-enzymer. Ca/Ba-mikrokuler (TAM) fremstod generelt som ikke-inflammatoriske, og stimulerte ikke verken leukocyttaktivering, komplement eller cytokinsekresjon. Peptidkoblete mikrokuler med kovalent påkoblete celleadhesjonsligander – RGD og REDV – ble også generelt ansett som ikke-inflammatoriske, og stimulerte generelt ikke komplement, leukocyttaktivering eller cytokinsekresjon. Kun mikrokulene laget av REDV-koblet alginat induserte betydelig cytokinsekresjon i form av IFN-γ og IL-10. På den annen side stimulerte mikrokuler laget av VAPG-koblet alginat til kraftige inflammatoriske responser. Likevel var denne effekten høyst sannsynlig relatert til en påvist endotoksinkontaminering for det gjeldende alginatet. Til sammenligning induserte polykation-mikrokapsler kraftige inflammatoriske responser i form av betydelig leukocyttaktivering (CD11b) og komplementaktivering, så vel som forhøyete cytokinnivåer.

En annen del av denne avhandlingen tok sikte på å oppnå en mekanistisk forståelse av fenomener relatert til forskjeller i stimulerende effekter for mikrokapsler med fast versus løselig kjerne. Løseliggjøring av kapselkjernen førte til svakere immunostimulerende egenskaper for PLL-inneholdende mikrokapsler i form av redusert komplementproteinnedslag, celleadhesjon og IL-8 sekresjon. Derimot ble en kraftigere sTCC-økning detektert for disse hule PLL-mikrokapslene sammenlignet med PLL-mikrokapsler med fast kjerne. Dette kan potensielt skyldes et hypotetisk, løselig molekyl som lekker ut fra de hule mikrokapslene og trigger store mengder TCC-dannelse i løsning. Videre, ved å bruke den C3-spesifikke komplementinhibitoren compstatin ble mikrokapsler med løselig kjerne demonstrert å bero på komplementaktivering for cytokininduksjon. Hule mikrokapsler med PLO-polykationer fremviste mer lovende egenskaper enn hule PLL-mikrokapsler i form av en lavere komplementaktivering.

Når det gjaldt å studere mekanismer som fører til cytokinsekresjon, ble det ikke observert reduserte IL-8 nivåer ved inhibering av komplementreseptoren CD11b/CD18. Likevel, denne observasjonen skyldtes trolig en stimulerende effekt av det benyttede CD11b-inhiberende antistoffet i seg selv. Videre kunne det heller ikke konkluderes om inhibering av fagocytose ved hjelp av cytochalasin D påvirket IL-8 sekresjon, grunnet en toksisk effekt av etanolen som cytochalasinet var oppløst i.

Symbols and abbreviations

- (s)TCC – (soluble) Terminal complement complex
- ALP – Alkaline phosphatase
- AP – Alginate-poly-$_{L}$-lysine microcapsule
- APA – Alginate-poly-$_{L}$-lysine-alginate microcapsule
- APC – Allophycocyanin
- BSA – Bovine serum albumin
- Ca-bead – Calcium microbead
- CaP – Calcium phosphate microbeads HA-mineralized through counter-diffusion precipitation
- CLSM – Confocal laser scanning microscopy
- CR3 – Complement receptor 3 (CD11b/CD18)
- CS – Cellulose sulfate
- DIC – Differential interference contrast
- ECM – Extracellular matrix
- EDTA – Ethylenediaminetetraacetic acid
- ELISA – Enzyme-linked immunosorbent assay
- Enz-CaP – Calcium phosphate microbeads HA-mineralized through enzymatic control
- Epi – Epimerized alginate microbeads
- Epi-RGD – Epimerized alginate microbeads with covalently grafted RGD-peptides
- EU – Endotoxin units
- FBR – Foreign body response
- FITC – Fluorescein
- G – (α-L-guluronic acid)
- HA – Hydroxyapatite
- HEPES – 4-(2-hydroxyethyl)-1-piperazineethanesulfonic acid
- HRP – Horse radish peroxidase
- IFN-γ – Interferon-γ
- Ig – Immunoglobulin
- IL – Interleukin
- IL-1ra – Interleukin-1 receptor antagonist

- LAL – Limulus amebocyte lysate
- LPS – Lipopolysaccharide (endotoxin)
- M – (β-D-mannuronic acid)
- MAC – Membrane attack complex
- MCP-1 – Monocyte chemotactic protein-1
- MFI – Median fluorescence intensity
- MIP-1α – Macrophage inflammatory protein-1α
- M_w – Molecular weight
- PBS – Phosphate buffered saline
- PDGF-BB – Platelet-derived growth factor composed of two B-chains
- PE – Phycoerythrin
- PFA – Paraformaldehyde
- PLL – Poly-$_L$-lysine
- PLO – Poly-$_L$-ornithine
- PMCG – Polymethylene-*co*-guanidine
- RANTES – Regulated upon activation, normal T-cell expressed and secreted
- REDV – Arginine-glutamic acid-aspartic acid-valine (peptide sequence)
- RGD – Arginine-glycine-aspartic acid (peptide sequence)
- RT – Room temperature
- T0 – Baseline value
- TAM – Trondheim Alginate Microcapsule (Ca/Ba-microbead)
- TF – Tissue factor
- TLR – Toll-like receptor
- TMB – 3,3',5,5'-tetramethylbenzidine (ELISA A+B substrate)
- TNF-α – Tumor necrosis factor-α
- UP-LVG – Ultrapure low viscosity high G (alginate)
- UP-MVM – Ultrapure medium viscosity high M (alginate)
- VAPG – Valine-alanine-proline-glycine (peptide sequence)
- VEGF – Vascular endothelial growth factor
- wt% – Weight percent

Contents

1 INTRODUCTION

1.1 Cell encapsulation therapy

The use of biomaterials has great potential in a range of clinical applications including cell therapy and tissue engineering. Central to these approaches is cell encapsulation technology. Transplantation of healthy cells and tissue is proposed as a therapeutic option for a number of diseases. However, the benefits of transplantation are often outshone by the requirement for life-long immunosuppressive drug treatment in order to avoid rejection of the foreign tissue. In turn, these immunosuppressive drugs have significant toxicity which may give rise to other complications, such as increased susceptibility to infections, renal dysfunction, and a theoretically increased risk of cancer [1, 2]. Cell encapsulation therapy by the principle of immunoisolation aims to abolish the need for immunosuppressive drugs. The principle was first described by Lim and Sun in 1980 in terms of the so-called bioartificial pancreas, which aimed to provide a therapeutic option for type 1 diabetes mellitus [3]. The basis of immunoisolation is to enclose the cells for transplantation in a semipermeable membrane or matrix made of an inert biomaterial, in order to isolate and protect the cells from the host's immune system. Immunoisolating devices thus aim to prevent immunological attack and rejection of the encapsulated graft, thereby overcoming the need for immunosuppression [3-5]. The principle of immunoisolation of pancreatic islets containing insulin-producing β-cells is illustrated in figure 1.1. The membrane has pores which allow the passage of low molecular weight molecules such as insulin (~5808 Da) and glucose (~180 Da), but prevent the entry of immune cells (>7 µm), and potentially antibodies (~150-900 kDa) [2].

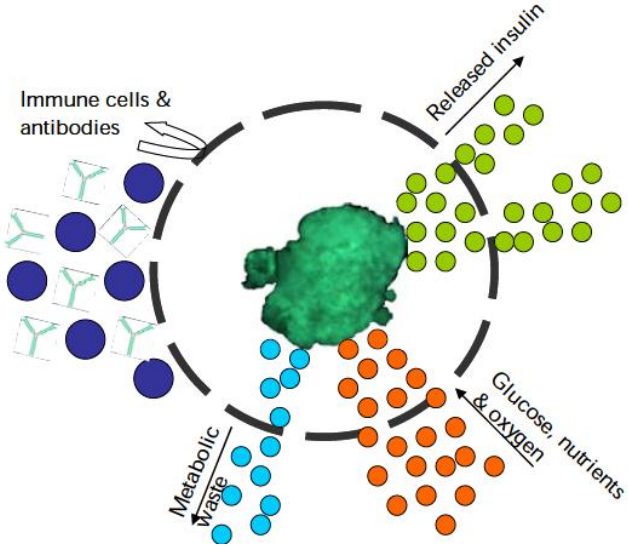

Figure 1.1. Principle for immunoisolation by encapsulation of insulin-producing cells and development of a bioartificial pancreas. The semi-permeable membrane allows the diffusion of insulin, metabolic waste, glucose, oxygen and nutrients, while at the same time preventing the entry of immune cells and antibodies. Adapted from [2].

Ideally, the encapsulated islets are kept viable and functional by access to nutrients, oxygen and stimulatory agents, which can easily diffuse across the membrane. However, in order to

ensure free diffusion it is crucial to avoid cellular and fibrotic overgrowth on the biomaterial surface, which will be discussed in section 1.2. Moreover, the cells present in an encapsulation device may themselves induce a host inflammatory response by releasing small molecules through the semipermeable membrane. These molecules are recognized as foreign, and therefore as a threat, by the host immune system. This facilitates the induction of an inflammatory response directed towards the encapsulation device in order to attack and kill the foreign body. The inflammatory response is generally comprised of a cellular and a humoral response, in which innate plasma cascades (e.g. complement and coagulation systems, discussed in sections 1.7-1.8) play a significant role. For some microencapsulation devices (e.g. TAM, se sections 1.3.1-1.3.2), antibodies may be able to diffuse through the semipermeable membrane. However, whether or not the diffusion of antibodies needs to be prevented is presently discussed. Regardless, successful immunoisolation will prevent the encapsulated cells from coming into direct contact with immune cells, which is a key event in immunological attack and graft rejection. An immunoisolating device can therefore prevent direct targeting of graft cells, but may still indirectly activate the host immune system. A range of immunoisolating devices may be used for the encapsulation of cells; however, the most intensively studied devices are the microcapsules. This is largely due to their spherical shape and small size, which offers an optimal surface to volume ratio and an optimal diffusion capacity [5].

Cell encapsulation technology is also applicable in tissue engineering. Tissue engineering is a cross between the science of the living organism and that of engineering, used to explore tissue function and to create artificial tissue [6]. Tissue engineering generally aims to replace, maintain or improve human tissue functions. This is achieved through combining biologically active factors (e.g. cells, growth factors, adhesion proteins) and materials (polymers or ceramics) into tissue-engineered implants. Bone tissue engineering has advanced most in this field, however, the applications are wide-ranging [7]. Figure 1.2 illustrates how facilitating a suitable microenvironment for cells may stimulate tissue development and remodeling. The properties of the employed biomaterial play an important role in creating an appropriate cell environment.

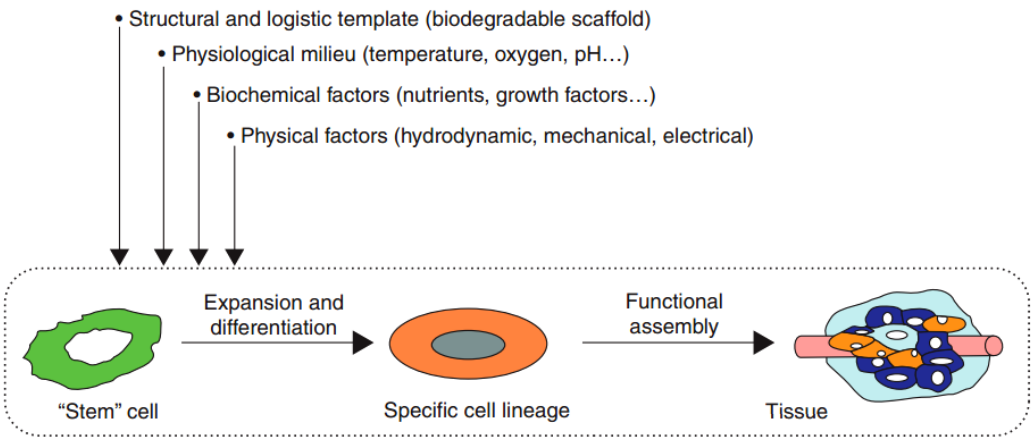

Figure 1.2. Tissue engineering, simplified illustration. Proliferation and differentiation of stem/progenitor cells and their subsequent assembly into tissues. A range of factors influence cell function and tissue assembly, including the cell-carrier scaffold design. A specially designed scaffold may facilitate controlled differentiation and proliferation of the scaffolded cells. Adapted and modified from [7].

1.2 Biocompatibility and the foreign body response

An absolute requirement for successful immunoisolation and optimal function of a microencapsulation device is that the employed biomaterial is fully biocompatible. Biocompatibility has for a long time been defined as the ability of a material to perform with an appropriate host response in a "specific application"[8]. However, more recent definitions stress further that the biomaterial should interact in a beneficial way with cells and tissues to optimize the clinical performance of the device [9-11]. Biocompatibility implies that the material in question does not evoke an undesirable immune response, such as fibrotic and cellular overgrowth, which is crucial in terms of preserving the viability and therapeutic function of the enclosed cells.

Depending on where they are implanted, biomaterials will come in contact with different bodily fluids, including blood, which contains inflammatory mediators. This contact, as well as the tissue injury that results from the implantation procedure, may induce acute inflammatory reactions followed by chronic inflammatory reactions. Indeed, this is the case whether or not the implanted biomaterial carries cells. The acute inflammatory response towards a biomaterial is generally characterized by the presence of neutrophils (a subgroup of granulocytes, or polymorphonuclear leukocytes), and is usually resolved within few days depending on the extent of injury at the implant site [12]. The continual presence of a foreign object will lead to chronic inflammation, which is normally associated with the so-called foreign body response (FBR). The FBR can be defined as the overall response of a host to the presence of a foreign body (e.g. an implanted biomaterial). In short, this host response is associated with the presence of macrophages and foreign body giant cells at the biomaterial surface, as well as fibrous capsule formation and the proliferation of blood vessels (angiogenesis) and connective tissue to restructure the affected area, as illustrated in figure 1.3 [12, 13].

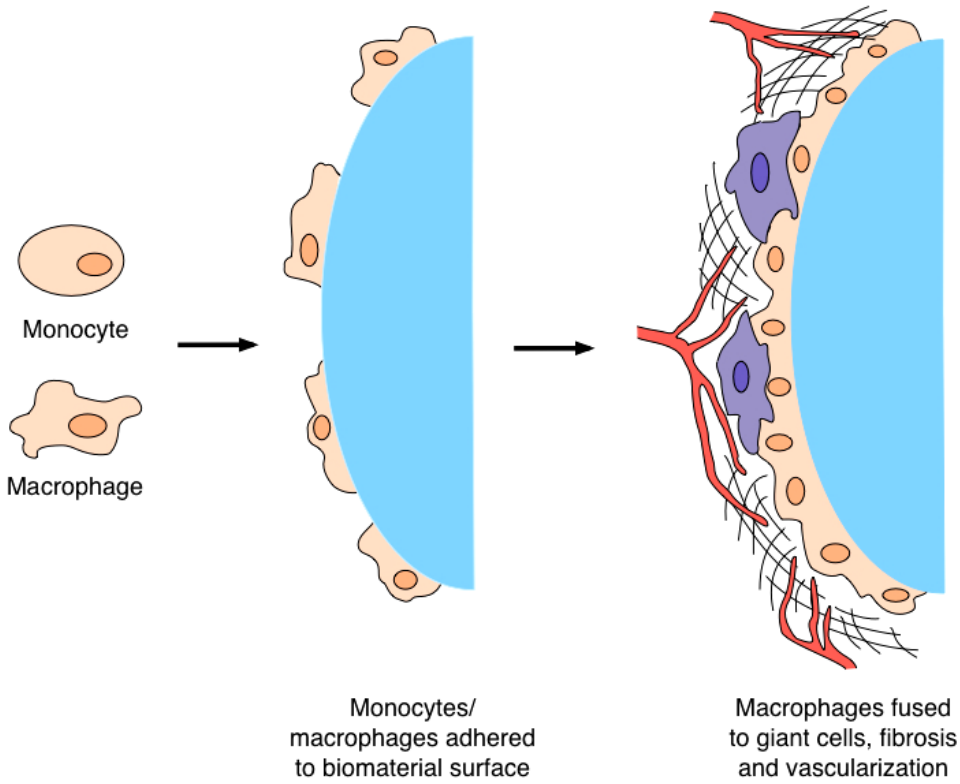

Figure 1.3. Simplified overview of the foreign body response. Monocytes and macrophages attach to the biomaterial surface, on which monocytes may further mature into macrophages. Macrophages may fuse into foreign body giant cells. Fibroblasts (in purple) produce extracellular matrix/fibrous tissue (illustrated as a mesh). New vascular tissue (in red) is formed by angiogenesis.

The FBR may thereby lead to cellular and fibrotic overgrowth of an implanted device. Cellular overgrowth results from immune cells attempting to rid of the foreign body through phagocytosis, which will be prevented by the large size of the capsule. Consequently, this may result in "frustrated phagocytosis" and fusion of macrophages into multinucleated foreign body giant cells which remain on the microcapsule surface [14]. Furthermore, activated leukocytes on the surface of a biomaterial may potentially secrete inflammatory mediators that can negatively affect the graft function. The FBR may also lead to formation of a tough fibrotic capsule around the encapsulation device (typically 50-200 mm in thickness) which aims to isolate the implant and prevent it from interacting with the surrounding environment [15]. In general, overgrowth of microencapsulation devices tends to impair the diffusion capacity and function of the capsules, effectively limiting the diffusion of oxygen, nutrients, waste and therapeutic molecules to and from the enveloped cells [16, 17]. Ultimately, this may lead to damage or necrosis of the encapsulated cells, which may impair or completely eliminate the therapeutic function of the graft. Indeed, evidence suggests that implanted biomaterials lead to ongoing, low-level inflammation which persists indefinitely, potentially resulting in an unexpected risk for patients [9]. Therefore, it is important to assess and optimize the biocompatibility of implantable devices and biomaterials in order to completely delete overgrowth and other adverse effects of host inflammation.

1.3 Alginate

Alginate, with its great capacity to form hydrogels, is by far the most frequently used biomaterial in the field of cell microencapsulation [8]. Moreover, alginate is shown to be of excellent biocompatibility in vivo [5, 8, 18]. However, its biocompatibility is strongly related to its substantial purity, which can be achieved through different purification protocols. Raw alginates extracted from seaweed contains contaminants such as proteins, endotoxins (LPS) and polyphenols [8, 19]. The presence of polyphenols may be harmful to immobilized cells and lead to oxidative-reductive free radical depolymerization (ORD) and a subsequent loss of viscosity of the alginates, while proteins and endotoxins may evoke inflammatory reactions [5, 19]. It is now possible to buy ultrapure alginates with notably low endotoxin levels.

The structure of alginate and the relationship of the chemical structure to its gel-forming abilities have been widely studied. Alginates are a group of unbranched polysaccharides primarily found as a structural component in brown seaweeds (such as *Macrycystis pyrifera* and *Laminaria hyperborea*) where it constitutes approximately 20-40% of the seaweed's total dry weight [8, 20, 21]. In addition, alginates are produced by certain bacterial species, such as *Pseudomonas aeruginosa* and *Azotobacter vinelandii* [20]. Alginate molecules are linear block co-polymers consisting of the monomers β-D-mannuronic acid (M) and α-L-guluronic acid (G), with a variation in composition and sequential arrangement depending on the source of isolation (figure 1.4).

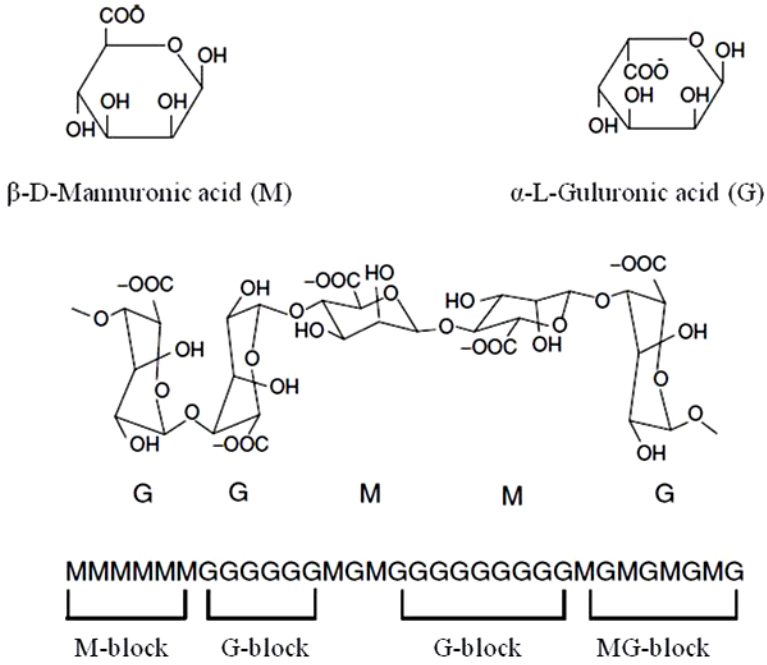

Figure 1.4. Chemical structure of alginate: 1-4 linked β-D-mannuronic acid (M) and α-L-guluronic acid (G). Respectively, from the top: constituent monomers of alginate, polymeric structure of alginate, and the alginate chain sequence. Modified and adapted from [18].

Naturally occurring alginates do not have regular repeating units, and the M- and G-units are either alternating or arranged in homopolymeric blocks of various lengths. The G and M units are C-5 epimers, which are only different in their conformations. The sequential structure of

alginate is generated in a post-polymerizing step involving polymer modifying enzymes called mannuronan C-5 epimerases, converting M-units to G-units [22]. It has also been demonstrated that C5-epimerases can be used in vitro to obtain tailored alginate gels with specialized properties [23, 24]. This epimerization process increases the G content and allows for alteration of important characteristics of the polymer gels. The G- and M-monomer distribution and the block structure is shown to be of great significance in terms of properties such as permeability, mechanical strength and stability, as well as the ion-binding capacity and capability to form gels. Overall, alginates with high content of G-units result in more stable gels of greater permeability than those with high M [8], as illustrated in figure 1.5.

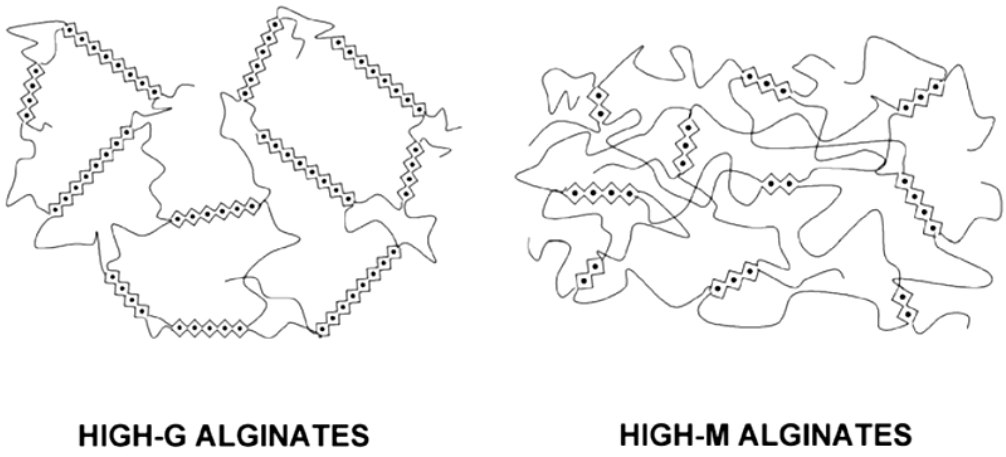

Figure 1.5. Model for network structure and porosity shown by hydrogels obtained from alginates of different composition. M-residues are known to provide elasticity to the gel. As a result, gels with high G content, possessing long G blocks and short elastic segments, produce rigid, open and static networks, while high M content alginates become more dynamic, containing more entangled networks due to their relative long elastic segments. Adapted from [8].

1.3.1 Alginate gels

Alginate exhibits excellent gel-forming properties, and forms stable hydrogels in the presence of divalent cations like Ca^{2+}, Ba^{2+} and Sr^{2+}. This is due to preferential binding of the divalent cations to G-blocks in alginate, which has been explained by the so-called "egg-box" model, shown in figure 1.6 [19, 25]. In this model, each divalent ion interacts with two adjacent G-residues as well as with two G-residues in an opposing chain. It has been widely accepted that the G-blocks are the main structural feature contributing to gel formation. However, recent findings show that not only G-blocks but also blocks of alternating M and G (MG-blocs) can form cross-links with calcium [26]. Thus, calcium junctions of GG-GG, MG-GG, and MG-MG must be held responsible for gel-formation.

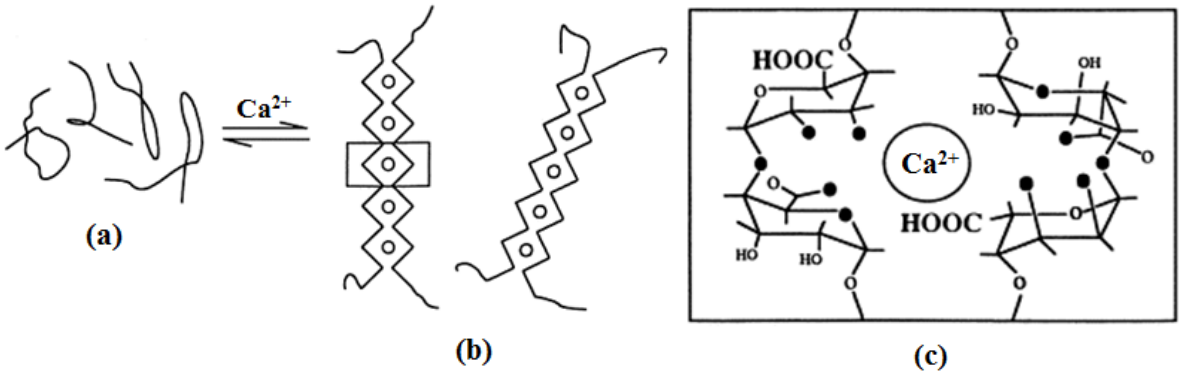

Figure 1.6. The egg box model. (a) Free alginate polymer chains. (b) Alginate chains are cross-linked with Ca^{2+}, forming an alginate gel with the "egg box junction" structure. These chains will have zig-zag as well as no zig-zag regions. (c) A section of the "egg box junction". Adapted and modified from [27].

The affinity of alginates toward the different divalent ions has been shown to increase in the following order: Mn<Co<Zn<Cd<Ni<Cu<Pb<Ca<Sr<Ba [8]. Nevertheless, most of them cannot be considered for therapeutic application of the microcapsules. Calcium is the most frequently used cation in alginate hydrogel formation, as it exists in large quantities in the human body and is generally considered biocompatible [18]. However, a downside to capsules made of Ca-alginate is their tendency to suffer osmotic swelling, partly as a result of constant interchange between Ca^{2+} and other nongelling ions (e.g. Na^{+}) [8]. Swelling of the capsules may lead to increased permeability, destabilization and finally, disruption of the gel matrix. As an alternative for calcium, other cross-linking ions have been used as well, in particular barium. Barium form stronger cross links with alginate, which results in stronger gels than with calcium [5]. Among other things, this knowledge has led to the development of a promising calcium/barium-containing alginate microbead which in this study is referred to as Trondheim Alginate Microcapsule (TAM) [28-31].

1.3.2 Microcapsule formation and properties

Although there is variation in the encapsulation processes performed by different research groups, the methods are all based on the same principle, illustrated in figure 1.7. A cell suspension is mixed with a sodium or potassium alginate solution. The mixture is subsequently dripped into a gelling solution containing divalent (e.g. Ca^{2+} or Ba^{2+}) or multivalent ions, which can react with the carboxyl groups of the alginate (as shown in figure 1.6) to quickly form rigid gel beads [18, 32]. Most commonly, encapsulation is carried out by dripping a suspension of cells and sodium alginate into a solution of $CaCl_2$ [5, 32]. Alginate is one of the few materials that allows for complete processing of the capsules at physiological conditions, enabling the whole encapsulation process to be performed with relative ease. This results in a higher viability of enclosed cells and a lower risk of releasing harmful products in vivo derived from the use of toxic components during capsule formation [8].

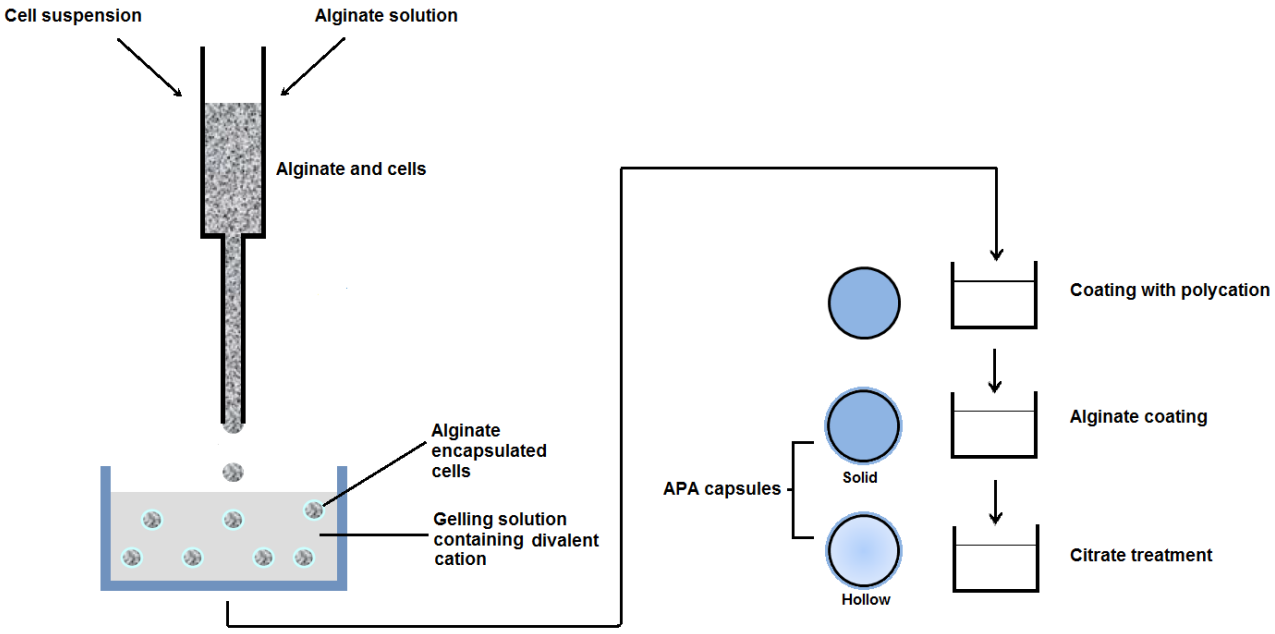

Figure 1.7. Basic principle for microencapsulation of cells in alginate (pancreatic islets, or other types of cells depending on purpose). A cell suspension and alginate solution is mixed, and transferred to a droplet-forming device. The cell-containing alginate solution will crosslink to form rigid beads upon contact with a divalent cation-containing gelling solution, such as calcium chloride ($CaCl_2$). Adapted and modified from [2]. Only empty capsules are employed in this study, which is achieved simply by excluding the first step of mixing cells and alginate.

Alginate itself is a polyanion, and coating with polycation provides a higher degree of mechanical stability and strength to the matrix and adjusts the permeability of the capsules [5, 16]. After formation, the microcapsules are coated with polycation by suspending the beads in polycation solutions such as poly-$_L$-lysine (PLL), as shown in figure 1.7. During this step, polycations bind to alginate molecules and induces the formation of alginate-polycation complexes at the capsule surface. An additional step of alginate coating may be applied to neutralize the positive charges of the polycation. The polycation PLL was initially used by Lim and Sum in 1980 to design the classical alginate-poly-$_L$-lysine-alginate microcapsules (APA) [3]. Several studies by different groups have demonstrated that the PLL coating may be the causative agent of cellular overgrowth [33-36]. Regardless, PLL is the most broadly studied and frequently employed polycation for alginate-based capsules. Other polycations are also evaluated, such as polyethyleneimine, poly-$_D$-lysine (PDL), poly-$_L$-ornithine (PLO), and polymethylene-*co*-guanidine (PMCG) [5]. Studies have shown that PLO capsules have better mechanical stability and are significantly more resistant to swelling and damage compared to the "classical" PLL microcapsules [34, 37]. In addition, PLO coating restricts more effectively the diffusion of higher molecular weight components than does PLL[38]. Direct comparisons of the biocompatibility of PLL vs PLO *in vivo* have shown varying results, although similar methods and materials have been employed. In one study, Ponce et al. observed a higher extent of cellular overgrowth on PLO-capsules than PLL-capsules [38], whereas a study performed by Tam et al. demonstrated the opposite result [34].

The PMCG capsule was first described by Wang et al. [39], and is comprised of a Ca^{+}/alginate core complexed with a PMCG polycation coat, with an outermost coat of cellulose sulfate (CS), as shown in figure 1.8. PMCG capsules are observed to have low permeability for inflammatory mediators, thus conferring good immunisolating properties [40, 41]. In addition, the capsules have shown a high degree of mechanical stability [42] and to be free from cellular overgrowth in canine and baboon studies [43, 44].

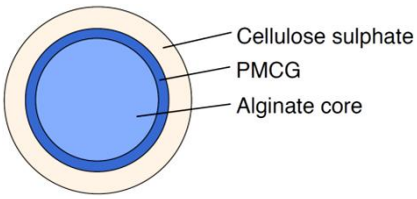

Figure 1.8. PMCG alginate microcapsule consisting of an alginate core, a polymethylene-*co*-guanidine (PMCG) polycation layer, and a cellulose sulfate layer.

Despite the potential of polycation capsules, it has been shown that polycation coatings may give rise to inflammatory reactions if brought into contact with the surrounding milieu. It has been reported that the PLL coating evokes a fibrotic overgrowth, making the capsules bioincompatible [33-36]. A study performed by Rokstad et al. demonstrated that polycation-containing APA and PMCG microcapsules triggered complement and leukocyte activation, while non-coated alginate microbeads (Trondheim Alginate Microcapsule, TAM) did not provoke complement reactions [45]. Indeed, the TAM microbeads have also been shown to evoke only minimal amounts of overgrowth in mouse studies [30, 31]. However, a recent study in cynomolgus monkeys did show that TAM induced increased overgrowth [46]. The reason for this is yet unknown, but could potentially be due to protein adsorption. Furthermore, a clinical trial in type 1 diabetes patients showed increased fibrosis when encapsulating human islet cells in barium alginate microbeads, implicating that barium-containing microbeads may need further improvement [47].

Implantation of alginate-based microcapsules in different animal models and at different implantation sites has produced variable results. A number of parameters can vary in this type of study (e.g. alginate composition, encapsulation protocol, animal model and host-implant-compatibility). Therefore, outcomes from the many performed experiments with alginate capsules *in vivo* cannot easily be compared. Several animal studies have been carried out using pancreatic islets encapsulated in APA microcapsules and transplanted into mice, rats, monkeys and dogs [2]. Transplantation of islets in alginate-based microcapsules has generally shown great promise in small animals, but less consistently in larger animals [30, 31, 48]. Moreover, a few clinical trials have been carried out in human patients, but so far without producing clinically significant outcomes. The results suggest that allografting of encapsulated human islets is safe; however, the graft function must be enhanced in order to improve the treatment and make it a desirable therapy [47, 49].

1.4 Alginate as extracellular matrix-like scaffolds

Until recently, biomaterials have been considered as inert, structural scaffolds in which cells were simply entrapped. However, it is becoming increasingly accepted that biocompatibility also involves a certain biofunctionality of the material [9-11]. According to this concept, the biomaterial should be able to support cell-biomaterial interactions and actively promote specific cell responses in a controllable manner. A desirable property for artificial cell carriers such as alginate microcapsules is to mimic the natural extracellular matrix (ECM). The ECM itself is not just a structural scaffold, but a complex structure with multiple specialized proteins providing specific binding sites for cell adhesion. The ECM provides cells with a wealth of information and encodes a myriad of mechanical and biochemical stimuli playing active roles in the regulation of cell behaviors [50]. Synthetic ECMs may replace many functions of natural ECM, including the organizing of cells into a three-dimensional architecture, providing mechanical integrity to the new tissue, and providing a hydrated space for the diffusion of nutrients and metabolites to and from the cell. In order to create a microenvironment that mimics the ECM, certain signaling factors recognized by cell receptors can be incorporated into suitable materials, such as alginate hydrogels.

Alginates possess many favorable properties as biomaterials. However, they are unable to specifically interact with mammalian cells. Cell adhesion is a strict requirement for survival for most cells, and also orchestrates critical roles in many cellular functions including migration, proliferation, differentiation, and apoptosis [51]. The alginate-cell interactions may be improved through the addition of macromolecules or peptides to the alginate, for instance, the cell-adhesive motif RGD (arginine-glycine-aspartic acid) can be conjugated directly to the alginate chains. This sequence is found in many ECM proteins, such as fibronectin, and acts as a binding site for integrins. Integrins are cell surface receptors involved in mediating attachment between cells and their surroundings—mostly the ECM, but in some cases other cells. Integrins are also important in signaling, and are involved in maintaining integrity as well as regulation of the cell cycle, shape and motility. The coupling of peptides containing the RGD sequence to a solid surface will promote cell adhesion through the binding to integrins (β1 and αvβ3, facilitating binding to many cell types). Indeed, it has been shown that RGD-alginates successfully initiate biological interactions between alginate hydrogels and cells [24, 50-52]. A study performed by Fonseca et al. showed that RGD-containing alginate hydrogels partially linked with matrix metalloproteinase (MMP) cleavable peptides significantly improved cell-matrix interactions (e.g. matrix degradation and reorganizing, through cleavage of the MMP-sensitive peptides by cell proteases) [50]. Indeed, these alginates provided an even more dynamic microenvironment that was beneficial to the cells than the controls with hydrogels containing only RGD. The experiment thus suggests that it is advantageous to make the cell carrier scaffold mimic the ECM to the greatest possible extent.

In addition to the RGD motif, a range of other ligands recognized by cell receptors can be employed to create a microenvironment that mimics the ECM. VAPG (valine-alanine-proline-glycine) is a sequence found in elastin, a structural protein found in connective tissue, and an important component of the ECM providing elasticity and robustness to tissues [53].

Coupling the VAPG sequence to alginates aims to stimulate cell proliferation and improve tissue repair. Similar to RGD, REDV (arginine-glutamic acid-aspartic acid-valine) is an adhesion motif which can be found in fibronectin, and is intended to stimulate cell adhesion [54, 55]. The VAPG and REDV sequences are ligands for binding respectively the integrins β3, found on smooth muscle cells, and α4β1 found on endothelial cells [53, 54].

1.5 Alginate in bone tissue engineering

Bone tissue engineering may be used to address destruction of bone tissue due to skeletal disease and inefficient bone healing after traumatic injury. Conventional treatment approaches involve bone grafting, however, there are drawbacks associated with bone grafting such as a high surgical risk and limited bone graft availability [48]. Bone substitute biomaterials are thus under current evaluation.

Bone tissue is an organic/inorganic composite, and consists of a collagen matrix mineralized with 50-60 wt% hydroxyapatite (HA, $Ca_{10}(PO_4)_6(OH)_2$) crystals [56]. It differs from other connective tissues due to its greater stiffness and strength, stemming from the great compression strength of HA and the elasticity of collagen. Inspired by the distinctive properties of bone tissue, alginate hydrogels can be mineralized with calcium phosphate for applications in bone tissue engineering. Alginate systems may function in guiding tissue repair by providing a temporary extracellular matrix for cells to infiltrate and migrate while depositing new bone tissue [48]. A number of cell types have been encapsulated in alginate hydrogels for the purpose of rapid regeneration of bone tissue, potentially at a rate faster than natural healing. These cell types include osteoblasts (bone-forming cells) and mesenchymal stem cells (MSCs, multipotent connective tissue cells, can differentiate into osteoblasts, cartilage cells etc.) [56]. Studies have shown that incorporation of HA in alginate hydrogels increases scaffold stability, facilitates cell attachment, speeds up cell proliferation and induces osteogenic differentiation by the addition of osteogenic supplements [57, 58]. Nanosized HA precipitation results from calcium phosphates, and can be achieved through several different techniques, e.g. counter-diffusion precipitation (one-step preparation of scaffolding and the mineral phase) [59] and by the use of alkaline phosphatase (ALP) [56]. ALP is an enzyme produced by osteoblasts which is important in bone formation, liberating phosphates necessary for mineralization. It is claimed that using ALP in biomineralization has considerable advantages compared to the gel diffusion approach, in terms of offering better control of the precipitation as well as requiring lower concentrations of $CaCl_2$, which is beneficial for encapsulated cell viability [56]. Moreover, this approach is seen to produce a more uniform distribution of HA crystals, most likely due to a uniform distribution of ALP throughout the beads. This is in contrast to the counter-diffusion approach, in which the nature of diffusion in a gel system creates a concentration gradient with relatively high levels of crystal formation on the bead surface [56].

A bone tissue engineering scaffold should possess a range of specific qualities, however, perhaps the most important one is biocompatibility. As of today, little is known about the inflammatory properties of calcium phosphate mineralized alginates. This study aims to

explore the inflammatory potential of mineralized alginate capsules made by counter-diffusion precipitation and by the use of ALP.

1.6 The whole blood model

The whole blood model is proposed by Rokstad et al. as an important and efficient screening tool for measuring and comparing inflammatory potentials of different capsules, which might be an important factor for their bio(in)compatibility [45]. The whole blood model may also be an important tool for determining the mechanisms leading to inflammatory reactions for different capsules. Information obtained from whole blood assays may help us develop fully biocompatible materials, and to determine the safety of different capsules for transplantation purposes. The sensitivity and efficiency of the whole blood model for screening microspheres and other biomaterials or their components has been demonstrated in recent studies [45, 60, 61].

The whole blood model is based upon using fresh, human whole blood that is anti-coagulated with lepirudin. Lepirudin interacts specifically with the coagulation component thrombin, while rendering other proteins intact and able to participate in host reactions (see figure 1.11). As previously mentioned, the initial contact of blood with a biomaterial may induce a host inflammatory response. The use of lepirudin as an anticoagulant in the whole blood assay is significant, as lepirudin does not interfere with the complement cascade [62]. Thus, lepirudin treated whole blood contains all the potential cellular and fluid phase mediators of inflammation. The whole blood model allows for screening different alginate microcapsules *in vitro* under identical conditions. This includes exploring the potential activation of different plasma cascade systems (e.g. complement and coagulation), interactions between cascade systems and blood cells, as well as leukocyte activation and cytokine profiles. The level of complement activation is a strong indicator on the ability of the capsules to trigger inflammatory reactions, as the complement system is a primary inductor of inflammation. Moreover, the fact that there is a high degree of interplay between the complement and coagulation cascades also needs to be taken into account when assessing inflammatory responses evoked by biomaterials (e.g. alginate microcapsules).

1.7 The Complement System

The complement system (figure 1.9) is the major effector of the humoral branch of the immune system, acting upstream of the leukocyte and cytokine responses. The complement system is a set of more than 30 plasma and membrane-bound proteins, constituting approximately 5% (by weight) of the serum globulin fraction [63]. Most are synthesized in the liver and circulate in plasma as inactive zymogens, activated only after cleavage [64]. This intricate network of proteins compose a cascade, in which a small number of proteins upstream in the reaction sequence are activated in a sequential manner, leading to cleavage and activation of a large number of downstream proteins. The end-result is a massive amplification of the complement response. Research has shown that complement activation is necessary for a number of inflammatory reactions, as blocking complement activation with

specific antibodies or peptides hampers or completely inhibits several secondary inflammatory responses [60, 65, 66].

The main event in the complement cascade is the enzymatic cleavage of complement component C3 into the anaphylatoxin C3a (so named because of its potential to cause anaphylactic shock) and C3b, the main effector molecule of the complement system. Depending on the activators, C3 is cleaved by the C3 convertase from the classical/lectin pathway (C4b2a) or from the alternative pathway (C3bBb). Both C3b and C3a play major roles in promoting inflammatory responses. C3b as well as inactivated C3b (iC3b) are major opsonins, and their deposition on foreign surfaces may enhance leukocyte adhesion and phagocytosis through the binding to complement receptor 1 (CR1) and 3 (CR3), expressed on monocytes and granulocytes [64]. It has been suggested that the ability of biomaterials to trigger complement activation is directly related to whether C3b is able to form covalent links to surface hydroxyl or amino groups on the material [67, 68]. C3b may further assemble with C3 convertase to form C5 convertase, initiating the final steps of the complement cascade called the terminal pathway. Moreover, the anaphylatoxins C3a, C4a and C5a are potent chemoattractants and mediate chemotaxis of leukocytes to the site of the ongoing inflammatory reaction . It has been suggested that C3a and C5a may be involved in regulating leukocyte gene expression, and thus cytokine production, through inducing activation of certain transcription factors [69, 70]. Indeed, the anaphylatoxins have been shown to stimulate production of certain cytokines (e.g. IL-1β and IL-8) in epithelial and endothelial cells [71, 72].

The complement cascade can be activated through any of three distinct pathways: the classical, alternative, and lectin pathways, which all require distinct molecular triggers for their activation. Figure 1.9 illustrates the complement cascade with its three activation pathways. The early steps of the complement cascade differ between each activation pathway. All three eventually converge into the terminal pathway (figure 1.10), resulting in deposition of C5b and ultimately formation of the cell-killing terminal complement complex (TCC), sometimes called the membrane-attack complex (MAC). This macromolecular structure may exist in the fluid phase (soluble TCC, or sTCC), but can also be inserted into a target membrane. Here it forms a transmembrane channel, leading to direct lysis and destruction of the target cell or microbe as a result of osmotic stress. The complement system is remarkable in its ability to distinguish "self" from "non-self", and is a powerful defense mechanism. Improper and uncontrolled complement activation may cause extensive damage to host cells and tissue, and complement activity is therefore under tight regulation.

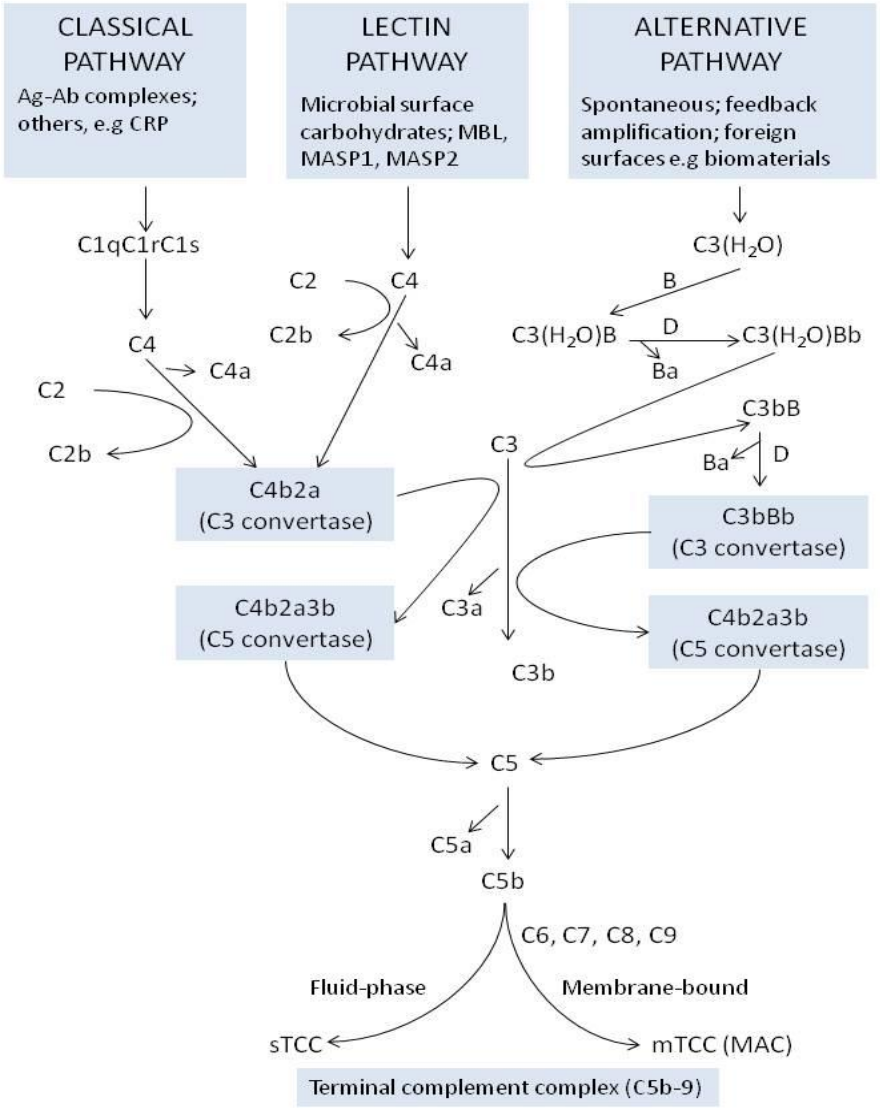

Figure 1.9. The complement cascade. The final result is formation of soluble and membrane-bound terminal complement complex (TCC), respectively sTCC and mTCC. Assembly of this complex is illustrated in figure 1.10. Modified and adapted from [73, 74]

1.7.1 The classical pathway

The classical pathway links the adaptive humoral immune response to the complement system and provides a more specific innate defense mechanism. The classical pathway is commonly activated by the formation of antigen-antibody complexes, but can also be triggered by acute phase proteins (e.g. bound C-reactive protein) and "self-structures" released from damaged cells [73]. Formation of Ag:Ab-complexes induces conformational changes in the immunoglobulin that exposes a binding site for C1, a complex consisting of the subunits C1q, C1r and C1s [64]. The binding of C1q to antigen-complexed antibodies induces a conformational change in the C1 complex. This converts C1r to an active serine protease, leading to activation of C1s through proteolytic cleavage. Activated C1s is able to cleave two substrates: C4 and C2. The cleavage of C4 by C1s will expose a binding site on the larger fragment of C4 (C4b) for the larger fragment of C2 (C2a). The smaller fragments, C2b and

the anaphylatoxin C4a, diffuse away. The C4b fragment binds the target surface and interacts with C2a to form the classical/lectin pathway C3 convertase (C4b2a). C3 convertase hydrolyzes many C3 molecules, resulting in a massive amplification of C3b. Some of the C3b molecules combine with C3 convertase to form C5 convertase (C4b2a3b). The C5 convertase is able to cleave C5 into C5b and the highly inflammatory anaphylatoxin C5a, which diffuses away [64]. The splitting of C5 initiates the terminal pathway of complement.

1.7.2 The lectin pathway

The lectin pathway, sometimes called the mannose-binding lectin (MBL) pathway, has a mechanism similar to that of the classical pathway. This pathway is activated by the binding of specific pattern recognition receptors circulating in blood and extracellular fluids (MBL or ficolins) to conserved carbohydrate structures on microorganism surfaces [75]. After binding to carbohydrate residues, MBL-associated serine proteases – MASP-1 and MASP-2 – will associate with the receptors. The result is activated MBL-MASP or ficolin-MASP which resemble the C1 complex in the classical complement pathway [64]. These complexes cleave C4 and C2 in the same fashion as C1, resulting in formation of the same C3 convertase as in the classical pathway, and a similar downstream mechanism.

1.7.3 The alternative pathway

The key features of the alternative pathway are its ability to be spontaneously activated and its alternative pathway C3 convertase. The alternative pathway targets any unprotected surface that is foreign to the host. This is the complement activation pathway most commonly associated with activation upon exposure to biomaterials [73, 76, 77]. The alternative pathway can be activated in two different ways. The first is by the action of the lectin or classical pathway, in which generated C3b covalently linked to a foreign surface can bind a serum protein called factor B. This alters the conformation of factor B, enabling an active serum protease called factor D to cleave factor B, releasing a small fragment (Ba) that diffuses away, and Bb. Fragment Bb remains stably associated with C3b, forming the alternative pathway C3bBb C3 convertase. Initiation of the alternative pathway is also associated with slow, spontaneous hydrolysis of unstable serum C3 molecules. This is the most abundant protein of the complement system, present in plasma at a concentration of approximately 1 mg/ml [78]. The spontaneous activation of C3 is also known as the "tick-over" process, and results in formation of C3(H_2O) [79]. This conformational change allows factor B to complex with C3(H_2O). Binding to C3(H_2O) exposes a site on factor B that serves as a substrate for the factor D. Factor D cleaves the C3(H_2O)-bound factor B into Ba and Bb. The Bb fragment remains bound to the C3(H_2O) complex to form fluid phase C3(H_2O)Bb, which has C3 convertase activity. The alternative pathway C3 convertases have a very limited half-life unless they are bound to and stabilized by the serum protein properdin (factor P). It has also been shown that properdin itself may act as a pattern recognition receptor and may bind certain biological surfaces where it can facilitate formation of alternative pathway C3 convertase [80, 81]. A special feature of the alternative C3 convertases is their ability to generate more of themselves, amplifying the initial steps of the activation pathway. In other words, once some C3b has been formed, by whichever pathway, the alternative pathway may

function as an amplification loop to rapidly increase C3b production and enhance an initially week complement system stimulus.

1.7.4 The terminal pathway

The final events in the complement cascade are initiated with the assembly the C5 convertases. These complexes are able to cleave C5 into a small C5a fragment, which diffuses away, and a larger C5b fragment, which binds to the target surface to facilitate assembly of the TCC. The C5b component is highly unstable, and rapidly becomes inactivated unless it is stabilized by the binding of component C6 [64]. The C5b6 assembly further complexes with C7, C8 and multiple copies of C9. The completed macromolecular structure, TCC (C5b-9), serves as a small pore spanning the target cell membrane. Formation of the TCC is illustrated in figure 1.10. Ions and small molecules can diffuse freely through this complex, resulting in osmotic instability and eventually lysis of the target cell due to water-influx and loss of electrolytes.

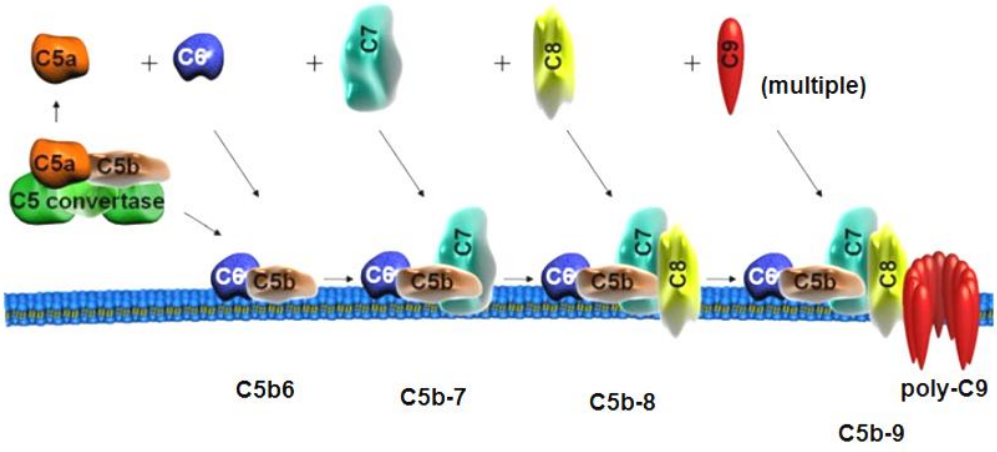

Figure 1.10. TCC formation. C5 convertases (surface-bound, although this is not illustrated) are generated through either the classical, alternative or lectin pathway. C5 convertase cleaves C5, generating C5a and C5b. C5b binds the microbial surface and is sequentially bound to C6, C7, C8, and C9. After the binding of one C9 molecule to membrane-inserted C8, polymerization of multiple C9 molecules occurs, resulting in formation of the complete C5b-9 complex, or TCC. Modified and adapted from [74].

1.7.5 Inhibitors of the complement system

The ability to regulate the human complement system is increasingly considered a promising approach for treating a number of pathological conditions. Several inhibitors of complement activity are currently in development, and identified inhibitors includes compstatin and Soliris®. Compstatin is a cyclic peptide which functions as a highly potent and selective C3-inhibitor. By binding directly to native C3, compstatin inhibits the cleavage of C3 into its active fragments C3a and C3b (see figure 4.1 in section 4.6) [82]. The proposed mechanism of action is that compstatin blocks the initial interaction between C3 and the C3 convertase [83]. This effectively prevents deposition of C3b, and the potent pro-inflammatory activity of the anaphylatoxin C3a, as well as other downstream complement actions. Several compstatin analogues have been identified and are currently in evaluation for therapeutical use [84]. Another complement inhibitor is Soliris® or Eculizumab, a humanized monoclonal antibody

that specifically binds to and inhibits complement component C5. This inhibits the C5 convertase-mediated cleavage of C5 into the anaphyatoxin C5a and C5b, the starting point for the terminal pathway and the formation of the terminal complement complex (TCC, C5b-9) [63]. This drug has recently been approved for clinical use, and is used for treating diseases such as paroxysmal nocturnal hemoglobinuria (PNH) and atypical hemolytic-uremic syndrome (aHUS).

1.8 The coagulation system

Another innate defense mechanism a pathogen or a biomaterial needs to overcome is the coagulation or clotting system (see figure 1.11). This is a mediator-producing system contained in plasma, which is fairly similar to and closely interconnected with the complement system [85]. Its activation leads to the formation of a fibrin clot, which is normally acting to prevent blood loss during vascular tissue damage. However, with regard to innate immunity, this fibrin clot acts to physically encase infectious microorganisms in a thick fibrin capsule to limit their spread and prevent their entry into the bloodstream [63]. The coagulation cascade can be activated by vascular injury or by the presence of blood-contacting foreign surfaces such as cardiovascular devices or biomaterials. The coagulation cascade has two known pathways leading to formation of fibrin: the contact activation pathway, also known as the intrinsic pathway, and the tissue factor (TF) pathway, also known as the extrinsic pathway. The primary pathway for the initiation of blood coagulation is the TF pathway, whereas amplification requires the intrinsic pathway [64].

The TF pathway is initiated by exposure of the plasma coagulation factor VII (fVII) to TF, for which TF is a receptor [86]. TF is expressed by connective tissue cells surrounding the blood vessels (e.g. vascular smooth muscle cells, pericytes and fibroblasts), and will be exposed to coagulation factors in plasma in case of vessel injury. In addition, so-called blood-borne TF circulates in the vasculature in the form of cell-derived microparticles [86]. Moreover, circulating monocytes can express TF on their surfaces upon activation, and may thus be associated with activation of the TF pathway [87, 88]. As fVII is brought into contact with TF, this results in formation of an activated complex fVIIa-TF. The sequential action of different coagulation factors leads to formation of fXa, initiating the final common pathway of the coagulation cascade.

Initiation of the contact dependent pathway occurs by surface-mediated contact activation. This pathway may be associated with biocompatibility, as high-molecular-weight kininogen (HMWK) adsorbs to the surface of biomaterials that come into contact with blood *in vivo*, and acts as a cofactor for prekallikrein. This pathway plays a relatively minor role in initiating clot formation, and is considered to be more involved in inflammation [89].

The two pathways converge into a final common pathway after formation of plasma factor Xa. The end result is cleavage of fibrinogen into fibrin and thrombin, and the subsequent cross-linking of the fibrin fibers by factor XIIIa, leading to formation of a stable fibrin clot. The formation of thrombin is a crucial step which contributes to a massive amplification of the coagulation response and a "thrombin burst" as indicated in figure 1.11. Thrombin exerts

many functions, including conversion of fibrinogen to fibrin and the activation of factor XIII, eventually leading to a hemostatic fibrin clot. Fibrinogen, which is abundant in plasma (3 mg/ml) [90] is known to adsorb to biomaterial surfaces and might further play a role in cell adhesion [73].

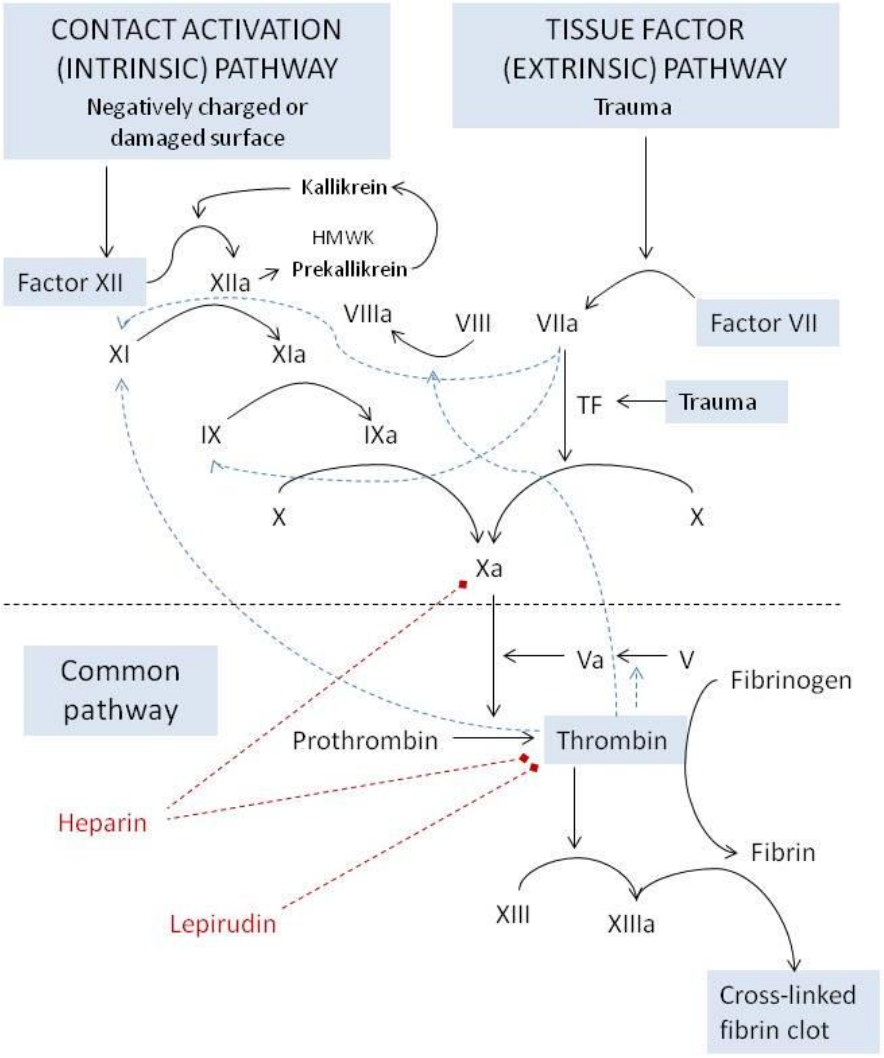

Figure 1.11. Simplified illustration of the coagulation cascade. The anticoagulants lepirudin and heparin, and their mechanism of action are shown in red. Feedback stimulation is indicated with blue arrows. Adapted and modified from [91]

Two well-known inhibitors of coagulation – lepirudin and heparin – are included in figure 1.11. Heparin is widely used as an injectable anticoagulant, and may also be used to form an inner heparin coating on the surface of various medical and experimental devices, e.g. test tubes. Heparin binds to the physiological enzyme inhibitor antithrombin III (ATIII) and increases the activity of ATIII, which will rapidly inactivate thrombin and other coagulation factors, most notably fXa [77]. However, heparin has been shown to possess complement inhibiting activity [92, 93]. Another anticoagulant is lepirudin – a potent and highly specific thrombin inhibitor, acting by binding directly to thrombin and blocking its enzymatic activity. Lepirudin has been shown not to interfere with complement activation, and enables complement to interact in the inflammatory network [93]. Lepirudin is therefore a suitable

anticoagulant for the purpose of studying the involvement of complement in inflammatory processes in whole blood.

1.9 Inflammatory responses upon implantation

1.9.1 Protein adsorption and interactions between plasma cascade systems

Immediately following implantation of alginate microcapsules, proteins from plasma or extracellular fluid are adsorbed onto the capsule surface. The nature of this protein film will influence host cell interactions and adhesion, and subsequent inflammatory responses [12]. In general, proteins often found on biomaterial surfaces are complement factors (e.g. C3 and its breakdown products), coagulation factors and proteins (e.g. fX and fibrinogen), extracellular matrix proteins (e.g. fibronectin and vitronectin), albumin, von Willebrand factor (involved in platelet activation and coagulation) and immunoglobulins (antibodies) [94, 95]. Several models describe how this protein coating contributes to activation of plasma cascades, cell adhesion and inflammation [94, 96, 97]. Figure 1.12 illustrates potential effects of the adsorbed protein film on implanted biomaterials.

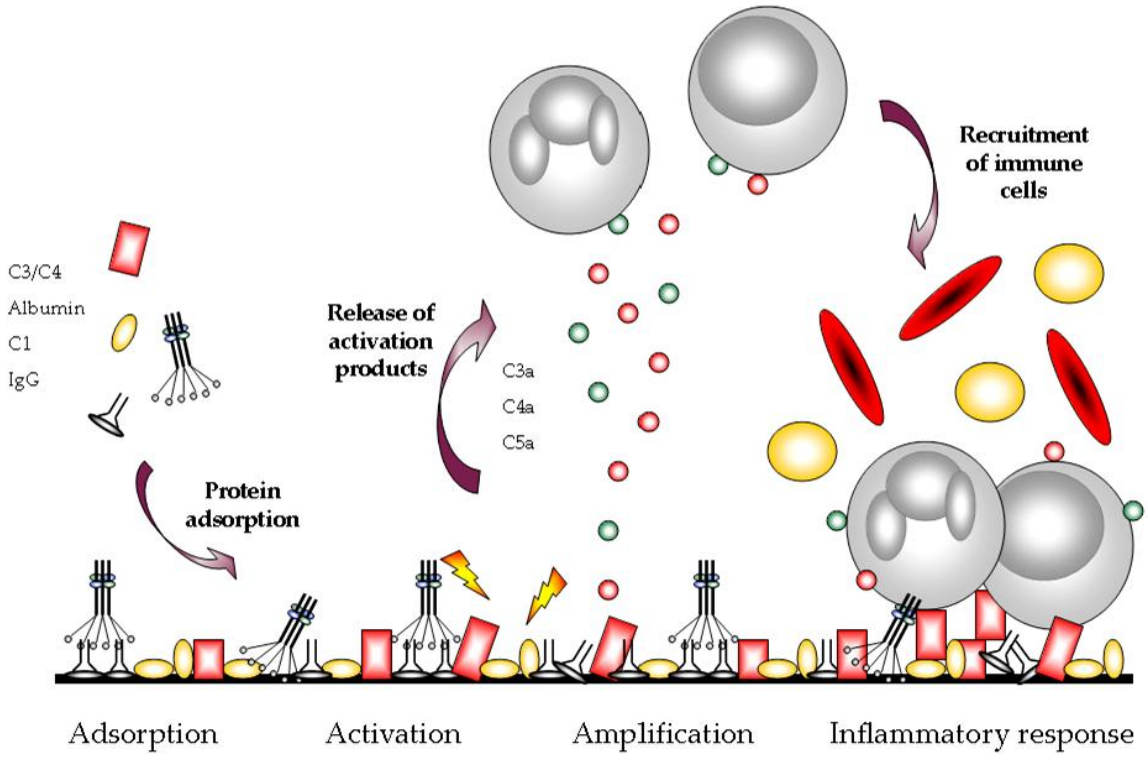

Figure 1.12. A schematic illustration of protein adsorption, complement activation and leukocyte recruitment induced on a biomaterial surface. Plasma proteins rapidly adsorb to the biomaterial surface. Interaction with the surface may trigger a conformational change in some of the proteins (e.g. C3 and IgG), which facilitate activation of the complement cascade. Once C3b is generated and covalently bound to the protein coat, the response is amplified through the alternative pathway [73]. Activation of the complement system leads to formation of the anaphylatoxins C3a, C4a and C5a. The anaphylatoxins induce recruitment and activation of leukocytes, which can attach to the plasma proteins deposited on the surface via surface receptors. Activated leukocytes will initiate an inflammatory response. Adapted from [94].

It is well established that the surface properties of a biomaterial may greatly influence protein adsorption and thus its biocompatibility. For instance, it is generally observed that positively

charged surfaces are more potent activators of complement than negatively charged ones, as positively charged surfaces show elevated levels of protein adsorption [96]. This is related to the fact that most proteins are negatively charged at physiological pH. Biomaterial surfaces with free OH and NH_3 are generally regarded as more prone to activate complement than others, since these groups are essential for the covalent binding of C3b [67, 68, 98]. Ferraz et al. also showed that complement activation could be depended on the nanoporesize of the biomaterial [99]. Moreover, a study performed by Xie et. Al suggests that microcapsules with a smoother surface have better biocompatibility compared to those with a rougher surface, which elicited a stronger immune response [100]. This is likely due to the fact that rough surfaces tend to absorb more proteins than smooth ones [101]. In this respect, capsule surface characteristics have significant effects on the activity of the plasma cascade systems and the subsequent inflammatory response.

The processes of complement and coagulation activation are closely interlinked, and will act synergistically to promote inflammation [102, 103]. For instance, the complement system is well known for its ability to recruit and activate leukocytes [77, 96, 104]. It is also shown that sTCC complexes may interact with and activate platelets [105]. Complement has also been found to facilitate coagulation activation, as C5a may result in upregulation of tissue factor (TF) – the potent initiator of the extrinsic pathway of coagulation – on both endothelial cells and circulating granulocytes [96]. Moreover, certain members of the coagulation cascade (e.g. fXII, kallikrein and thrombin) are able to directly cleave and activate complement components or fragments, thus bypassing convertases to directly generate anaphylatoxins [96]. Thrombin is also a powerful platelet activator. Activation of platelets will release mediators that further activate fluid phase complement, thus amplifying the ongoing inflammatory reaction.

1.9.2 Leukocytes and cytokine release

Activation of complement leads to generation of potent mediators such as the anaphylatoxins C3a and C5a, and soluble TCC. These will trigger activation of leukocytes (granulocytes and monocytes) as well as platelets, leading to inflammatory reactions [77, 96, 104]. Hence, there is an important link between complement (and coagulation) activation and leukocyte responses. The activation of leukocytes may lead to undesirable adhesion and cellular overgrowth of the capsule surface [14, 96].

Following initiation of an inflammatory response, activated leukocytes may remain attached to the microcapsule surface for extended periods of time, and can release a range of cytokines and other mediators. Cytokines are small signaling molecules used to direct an immune response. These include pro- and anti-inflammatory cytokines, chemokines (cytokines with chemotactic activity), growth factors as well as a range of other mediators [14, 63]. Some of these products have the ability to recruit additional macrophages to the biomaterial-tissue interface (e.g. MIP-1α and IL-8) while others can exert pro-inflammatory effects (e.g. IL-6, IL-1β and TNF-α). Table 1.1 below lists the cytokines screened for in the present study, with some of their properties. Some of these mediators may have a negative effect on the function of the enveloped graft.

Table 1.1. The cellular source and the main immunological functions of selected cytokines involved in inflammatory responses [63, 94].

Chemokines	Main cell source	Major immunological effect
Interleukin-8, IL-8	Macrophages, monocytes, epithelial and endothelial cells	Pro-inflammatory; recruitment and activation of neutrophils. Angiogenesis
Monocyte chemotactic protein-1, MCP-1	Macrophages, monocytes, endothelial cells and fibroblasts	Pro-inflammatory; recruits monocytes, T-cells, basophils, mast cells, dendritic cells, and activates macrophages.
Macrophage inflammatory protein-1α, MIP-1α	Macrophages, neutrophils	Pro-inflammatory; activation of granulocytes, induction of synthesis of pro-inflammatory cytokines
Inflammatory cytokines		
Interleukin-1β, IL-1β	Macrophages, monocytes, dendritic cells and epithelial cells	Pro-inflammatory; activation of T-cells and macrophages, induces fever, upregulates adhesion molecules on endothelial cells
Interleukin-6, IL-6	T-cells, macrophages, monocytes and endothelial cells	Pro-inflammatory; Induces synthesis of acute-phase proteins, fever, T- and B-cell growth and differentiation. Induces antibody secretion
Tumor necrosis factor-α, TNF-α	T-cells, natural killer (NK) cells and macrophages	Pro-inflammatory, activation of neutrophils, promotes endothelial activation and increases vascular permeability
Anti-inflammatory cytokines		
Interleukin-1 receptor antagonist, IL-1ra	Macrophages, monocytes, neutrophils	Anti-inflammatory; biologically inactive molecule and natural antagonist of IL-1 function, competitive binding to IL-1 receptor
Interleukin-10, IL-10	Macrophages, monocytes, lymphocytes and mast cells	Anti-inflammatory; inhibition of macrophage functions and release of several pro-inflammatory cytokines; downregulating the expression of co-stimulatory- and MHC(II) molecules on macrophages
Growth factors		
Platelet-derived growth factor, PDGF	Platelets and other cells, including eosinophils	Important for vasculogenesis, angiogenesis, and cell division
Vascular endothelial growth factor, VEGF	Mast cells, platelets and neutrophils	Important for vasculogenesis and angiogenesis. Stimulates monocytes and macrophages
Other cytokines		
Regulated upon activation, normal T-cell expressed and secreted, RANTES	Macrophages, T-cells, endothelial cells and platelets	Chemotactic activity - attracts T-cells, monocytes and other cells. Activates T-cells
Interferon-γ, IFN-γ	T-cells, NK cells	Pro-inflammatory; activation of macrophages, increased expression of MHC molecules, B-cell isotype switching

1.10 Aims of this study

The present work has several objectives, all revolving around inflammation and the mechanisms leading up to it.

The main objective was to explore the inflammatory properties of novel, specialized alginates intended for specific applications. These include hydroxyapatite mineralized alginates for uses in bone tissue engineering, and peptide-coupled alginates for producing new extracellular matrix-like bioscaffolds. To our knowledge, the inflammatory potential of these specialized alginates has not yet been assessed. To do this, a set of different alginate microbeads was screened for leukocyte and complement activation as well as cytokine induction by employing the whole blood model. High responses seen for these properties *in vitro* may imply an increased risk of overgrowth and inflammation directed towards the capsules *in vivo*. The obtained information may therefore give indications on the degree of bio(in)compatibility of the alginates in question.

Furthermore, this work aims to build further on information acquired through previous studies [45, 61, 106]. Ørning [106] studied the effects of soluble capsule cores, and found that alginate microcapsules with a liquefied core often induced a lower degree of immune stimulation than did those with a solid core. In order to further elaborate the inflammatory mechanisms induced by hollow microcapsules, these same microcapsules were screened for complement protein deposition on their surfaces, as well as cytokine induction in the presence of a specific complement inhibitor.

Mechanism studies were also performed on microcapsules with a solid core. These experiments aimed to provide information about the mechanisms leading up to inflammatory reactions. To do this, microcapsules were screened for protein deposition, surface adhesion of leukocytes, and cytokine production in the presence of specific inhibitors.

2 MATERIALS AND METHODS

2.1 Alginate microcapsule formation

A range of alginate microcapsules and microbeads were prepared with varying alginate types, gelling solutions, needle sizes as well as with different capsule coatings in accordance with figure 1.7. Only empty capsules with no enveloped cells are employed in this study. Table 1.2 shows the conditions under which the capsules were prepared.

Table 2.1. Alginate microcapsules and microbeads used throughout this study and the conditions under which they were prepared The employed alginate and gelling solutions are described in more detail in table 2.2 and section 2.1.2, respectively.

Micro-capsule	Alginate solution	Gelling solution	Size of needle (mm)	Polycation	Additional comments
Ca-bead	1.8% UP-LVG	50 mM $CaCl_2$	0.35		
CaP	1.8% UP-LVG, 100 mM $Na_2HPO_4*H_2O$ + $NaH_2PO_4*H_2O$	300 mM $CaCl_2$	0.35		Hydroxyapatite-mineralized microbeads prepared by counter-diffusion precipitation in accordance with [59].
Enz-CaP	1.8% UP-MVG	50 mM $CaCl_2$	0.35		Hydroxyapatite-mineralized microbeads made by using ALP (0.25 mg/ml). Prepared by Weshtrin [107] in accordance with [56].
TAM4	1.8% UP-LVG*	50 mM $CaCl_2$, 1 mM $BaCl_2$	0.35		New UP-LVG batch.
TAM3	1.8% UP-LVG	50 mM $CaCl_2$, 1 mM $BaCl_2$	0.35		Old UP-LVG batch.
PLL Solid	UP-100M	50 mM $CaCl_2$	0.40		Same as APA, but with a high M alginate core. Prepared by Ørning [106].
PLL Hollow	UP-100M	50 mM $CaCl_2$	0.40	0.14% PLL	Same as APA, but with a hollow core (citrate-treated). Prepared by Ørning [106].
PLO Hollow	UP-100M	50 mM $CaCl_2$	0.40	0.14% PLO	Similar to the classical APA-capsule, but with PLO as polycation instead of PLL, and with a hollow core (citrate-treated). Prepared by Ørning [106].
APA	1.8% UP-LVG	50 mM $CaCl_2$	0.40	0.1% PLL	Outer alginate coat UP-100M. High G.
AP	1.8% UP-LVG	50 mM $CaCl_2$	0.40	0.1% PLL	

AP 0.05% PLL	1.8% UP-LVG	50 mM $CaCl_2$	0.35	0.05% PLL	Employed only in one single whole blood experiment (section 3.1).
PMCG2	1.8% UP-LVG	50 mM $CaCl_2$		1.2% PMCG	Capsules prepared by Igor Lacík group (Polymer Institute of the Slovak Academy of Sciences, Bratislava, Slovakia).
G VAPG	1.8% G VAPG	50 mM $CaCl_2$, 1 mM $BaCl_2$	0.35		
G RGD	1.8% G RGD	50 mM $CaCl_2$, 1 mM $BaCl_2$	0.35		
M RGD	1.8% M RGD	50 mM $CaCl_2$, 1 mM $BaCl_2$	0.35		
M REDV	1.8% M REDV	50 mM $CaCl_2$, 1 mM $BaCl_2$	0.35		
UP-MVM	1.8% UP-MVM	50 mM $CaCl_2$, 1 mM $BaCl_2$	0.35		
Epi	1.8% Alg HG III	50 mM $CaCl_2$	0.35		Mannuronan C-5 epimerized alginates. Capsules prepared by Karstensen [24].
Epi-RGD	1.8% RGD HG I	50 mM $CaCl_2$	0.35		Mannuronan C-5 epimerized alginates. Capsules prepared by Karstensen [24].

2.1.1 Alginate solutions

The majority of the alginates used throughout this study are different types of ultrapure (endotoxins ≤ 100 EU/gram) sodium alginates from FMC BioPolymer AS (NovaMatrix, Norway). These include sodium alginates from the series Pronova, as well as peptide coupled sodium alginates from the series Novatach. Two Novatach-alginates coupled to RGD-containing peptides were employed, in addition to alginates coupled to the peptide sequences VAPG and REDV (see section 1.4). The intention of the peptide-coupled alginates used in this study is to facilitate and promote interaction with cells, and promote enhanced cell functionality and viability. A description of the employed alginates in this work is shown in table 2.2. For the calcium phosphate (CaP) microbeads, which are made by hydroxyapatite mineralization through counter-diffusion precipitation, the alginate solution contains UP-LVG alginate with phosphate (100 mM $Na_2HPO_4 \cdot H_2O$ + $NaH_2PO_4 \cdot H_2O$). UP-LVG is similar to UP-LVG* but of a newer batch, as the GMP license had expired for the older alginate. Batch variation may occur.

To prepare alginate solutions, freeze-dried alginate (1.8 g) was dissolved overnight in sterile, endotoxin free water (50 ml, B. Braun, Melsungen, Germany) with agitation. D-mannitol (50 ml, 0.6 M, BDH AnalaR., VWR International Ltd, Pool, England) was added, creating an alginate concentration of 1.8%. The pH of the solution was adjusted with sterile NaOH and HCl to within the physiological range of 7.2-7.4. Sterile filtration of the alginate solution was performed with a 0.2 mm filter, and the sterilized alginate solution was stored in 4 °C.

Table 2.2. Alginates used throughout this study. Mw = molecular weight, given in kilodaltons. EU/g = endotoxin units per gram. Data is provided by the manufacturer (NovaMatrix) when no other information is given.

Name	**Batch/lot**	**Endotoxins (EU/g)**	**Mw (kDa)**	**G/M Ratio**	**Additional comments**
Pronova UP-LVG*	FP-603-04	< 23	75-200	≥1.5	Old batch. Low viscosity, high G.
Pronova UP-LVG	BP-1108-01		75-200	≥1.5	New batch. Low viscosity, high G.
Pronova UP-MVG	FP-505-01	≤ 43	>200	≥1.5	Medium viscosity, high G.
Pronova UP-MVM	BP-0803-03	< 27	>200	≤1	Medium viscosity, high M.
Pronova UP-100M	FP-209-02				High M.
Novatach G RGD	BU-0805-02	0,00002		≥1.5	GRGDSP-coupled alginate, high G.
Novatach M RGD	FU-701-01	0,00359		≤1	GRGDSP-coupled alginate, high M.
Novatach G VAPG	CBIFMC01A 02122005	320,4		≥1.5	VAPG-coupled alginate, high G. Endotoxin level not provided by manufacturer, determined by LAL assay. Significant endotoxin levels.
Novatach M REDV	FU-612-01	0,00566		≤1	REDV-coupled alginate, high M.
Alg HG I	512-215-01	5233			Uncoupled alginate epimerized by C-5 mannuronan epimerases prepared by [24]. High G. Endotoxin levels determined by LAL assay. Significant endotoxin levels.
RGD HG I	512-215-01	721			Uncoupled alginate epimerized by C-5 mannuronan epimerases prepared by [24]. High G. Endotoxin levels determined by LAL assay. Significant endotoxin levels.

2.1.2 Gelling solutions

The gelling solution varied according to the type of capsule to be prepared. Three different gelling solutions were made by dissolving analytical grade $CaCl_2 \cdot 2H_2O$ and HEPES (Merck, Darmstadt, Germany), and D-mannitol (BDH AnalaR., VWR International Ltd, Pool, England) over night in sterile, endotoxin free water:

i) Without Ba: 50 mM $CaCl_2$, 0.15 M mannitol and 10 mM HEPES buffer
ii) With Ba: 50 mM $CaCl_2$, 1 mM $BaCl_2$, 0.15 M mannitol and 10 mM HEPES buffer
iii) High $CaCl_2$: 300 mM $CaCl_2$, 10 mM HEPES buffer

For the preparation of TAM (Ca/Ba) microbeads, the gelling solution was added analytical grade $BaCl_2$ (Merck, Darmstadt, Germany). The pH of the gelling solution was adjusted to lie within the range of 7.2-7.4 using sterile NaOH and HCl, followed by sterile filtration (0.2 mm filter) and storage (4 °C).

2.1.3 Capsule preparation

Alginate capsules were made by dripping alginate solution into a divalent cation-containing gelling solution to form a hydrogel, as described in section 1.3. The capsules were prepared by using an electrostatic bead generator as described by Strand et al [32]. All equipment used for capsule preparation was thoroughly washed with ethanol (70%), and all glassware, scissors etc. had been sterilized by autoclaving.

After formation, some capsules were coated with polycation, and added an outer alginate coating. Some of the capsules were treated with citrate so as to liquify the core of the capsules, then designated as hollow microcapsules, as illustrated in figure 1.7. The PLO and PLL Hollow microcapsules as well as PLL Solid were prepared by Ørning [106], as indicated in table 2.1. APA and AP microcapsules were coated in a bath with poly-L-lysine (PLL Hydrochloride, P2658, Sigma Aldrich, MO, USA, 25 ml, 0.05%, 0.1% or 0.14% in NaCl) or poly-L-ornithine (PLO Hydrobromide, P8954, Sigma Aldrich, MO, USA, 25 ml, 0.14% in NaCl) for 10 minutes. APA microcapsules were washed with 0. 9% NaCl (B. Braun, Melsungen, Germany) before being placed in an alginate coating bath (0.1 % Pronova UP-100M alginate in D-mannitol, 10 ml) on agitation for 10 minutes. In order to prepare hollow APA microcapsules, these were treated with citrate (0.055 M Na-citrate tribasic dihydrate, 20 ml, Merck, Darmstadt, Germany) on agitation for 10 minutes.

PMCG-microcapsules (see figure 1.8), initially described by Wang et al. [39], were prepared after the same protocol as described by Rokstad et al. [61] by the Igor Lacík group (Polymer Institute of the Slovak Academy of Sciences, Bratislava, Slovakia). These microcapsules were formed by polyelectrolyte complexation between sodium alginate/cellulose sulfate (CS) with polycation polymethylene-*co*-guanidine (PMCG) and calcium cations. The PMCG microcapsules were made using a multi-loop reactor with 40s complexation time and with following specifications: polyanion solution 0.90% UP-LVG alginate/0.90% CS in 0.9% NaCl; polycation solution 1.2% PMCG/1% $CaCl_2$/0.025% Tween 20 in 0.9% NaCl. The membrane composition was equilibrated by incubation in a 50 mM sodium citrate/0.9% NaCl solution for 10 min, with subsequent coating with 0.1% CS/0.9% NaCl for 10 min [61].

The epimerized microbeads (Epi and Epi-RGD) were prepared by Karstensen [24]. These microbeads were made by dripping epimerized alginate and epimerized alginate grafted with RGD into a solution of 50 mM $CaCl_2$ to give Epi and Epi-RGD, respectively (see table 2.1). Ca-bead, which is made by dripping a non-modified alginate solution into the same gelling solution, may represent a control capsule for the epimerized—as well as the HA-mineralized—microbeads. Furthermore, the calcium phosphate mineralized microbead (Enz-CaP) made using ALP (0.25 mg/ml) was prepared by Westhrin [107].

After formation, capsules were stored (4 °C) in 0.9% NaCl (5 ml). Capsules were further aliquoted by resuspending the capsules in the solution and transferring 1 ml of the mixture into four Eppendorf tubes, each now containing approximately 0.5 ml capsules in wash solution. Prior to performing experiments, capsules were aliquoted into smaller batches in tubes (1.8 ml, Nunc A/S, Roskilde, Denmark) containing 50 µl capsules and 0.9% NaCl for a

total volume of 100 µl. This was done by washing capsules twice in washing solution, prior to transfer into a sterile 15 ml tube and addition of wash solution for a total of 5,5 ml. Capsules were resuspended, and 500 µl capsule-containing solution was transferred into ten sterile 1.8 ml Nunc polypropylene vials. 400 µl supernatant was removed, leaving approximately 50 µl in a total volume of 100 µl wash solution.

Capsules studied in the preliminary whole blood assay (see section 3.1.1) were aliquoted by using 10 mM $CaCl_2$ in 0,9% NaCl, in order to avoid swelling of capsules by loss of Ca^{2+} from the gel matrix. After aliquoting, capsules were stored in NaCl.

2.1.4 LAL assay

Although the majority of the employed alginates were apparently ultrapure, a few alginates were suspected to be endotoxin contaminated. In order to verify this, a LAL assay was performed, in which endotoxins can be detected and quantified. The test is based on the fact that an aqueous extract of blood cells from the horseshoe crab (*Limulus polyphemus*), termed Limulus amebocyte lysate (LAL), reacts with bacterial endotoxins (LPS). The test was conducted by Bjørg Steinkjer at the department of Cancer Research and Molecular Medicine, NTNU, and the endotoxin levels present in the alginates were determined.

2.2 The whole blood model

In this study, the whole blood model has been employed in order to unmask differences in complement and leukocyte activation between various types of alginate microcapsules. The assay makes use of lepirudin anti-coagulated fresh, human whole blood. Low activating polypropylene tubes were used in order to minimize complement and coagulation activation by the containers themselves. To be able to do direct comparisons between samples, it was essential that the volume proportions between blood and additives were equal throughout the whole blood experiments.

The use of human whole blood for basal experiments was approved by the Regional Ethic Committee at the Norwegian University of Science and Technology in Norway. The experiments were performed in accordance with their guidelines.

2.2.1 General procedure

Single experiments were performed for different blood donors, as responses may vary significantly between individuals. Lepirudin (2.5 mg/ml, 80 µl, final concentration in blood 50 µg/ml, Celgene Europe, Switzerland) was added to polypropylene tubes (4.5 ml Nunc A/S, Denmark) using BD Vacutainer tops (BD Vacutainer Systems, UK), with vacuum achieved by retracting 19 ml air by a syringe. Whole blood was collected into the tubes from voluntary donors. Dulbecco's PBS with $MgCl_2$ and $CaCl_2$ (100 µl, Sigma-Aldrich, MO, USA) was added to Nunc tubes (1.8 ml) containing alginate capsules (50 µl capsules in a total volume of 100 µl sterile 0.9% NaCl) and controls. Positive controls contained 10 µg/ml Zymosan A (Sigma-Aldrich, MO, USA) in a total volume of 100 µl NaCl, and negative controls were T0

and saline, both containing only sterile NaCl (100 µl). Zymosan is derived from yeast cell walls and is commonly used to induce experimental sterile inflammation. The T0 samples represent the baseline values for the respective properties in question, that is, the level of cytokines etc. initially present in the whole blood of the respective donors. As complement activation in T0 is immediately activated, saline is generally regarded as the best negative control for the capsule samples, since the saline controls will get the same background stimulation from the polypropylene vials that the capsule samples do.

Fresh, anti-coagulated whole blood (500 µl) was added to each sample tube (preheated to 37 °C) immediately after collection, giving a total volume of 700 µl for each vial. T0 was immediately added ethylenediaminetetraacetic acid (EDTA,14 µl, final concentration 10 mM) to stop the reaction. EDTA acts by sequestering metal ions such as Ca^{2+} and Fe^{3+}, thus halting complement activation as many steps in the complement cascade are calcium-dependent. T0 was sebsequently kept on ice while incubating the remaining samples (37 °C) under constant rotation for 240 minutes before addition of EDTA (final concentration 10 mM). The tubes were treated with caution to avoid blood coming into contact with the screw cap, as this is made of a more activating material. After 60 minutes, some blood was taken out from each sample to be used in flow cytometry, as described in section 2.3. After inactivation with EDTA, all samples were centrifuged (3000 rpm, 15 minutes, 22 °C), and aliquots of plasma were harvested and stored (-20 °C) for subsequent analyses. It should be noted that the employed centrifugation speed does not separate blood platelets from plasma. For the T0 samples, which were kept on ice 4 hours, platelet activity might be affected by the exposure to low temperature, which may potentially further influence other inflammatory reactions.

2.2.2 Compstatin studies

When studying the effects of the C3-inhibitor compstatin on complement and cytokine response, compstatin analog 4(1MeW) (stock 2 mM, synthesized in the laboratory of Prof. John D. Lambris) was added to the samples before adding the blood (500 µl). A titration experiment prior to the whole blood assays gave an indication of appropriate compstatin concentrations. Hollow APA capsules were added compstatin in a concentration of 25 µM, and solid APA capsules 10 µM. A control peptide (Sar-Sar-Trp(Me)-Ala-Ala-Asp-Ile-His-Val-Gln-Arg-mlle-Trp-Ala-NH2, 10 mg/ml, Prof. John D. Lambris) was used as control for compstatin, in concentrations corresponding to the respective compstatin additions. Subsequent steps are similar to those described in section 2.2.1.

2.2.3 Inhibition studies

Whole blood assays were also performed in order to study the effect of cytochalasin D and CD11b-inhibitor on cytokine production. Cytochalasin D belongs to a class of fungal metabolites termed cytochalasins, and is a cell permeable potent inhibitor of actin cytoskeleton function. In phagocytic cells, one significant effect of cytochalasin D is the inhibition of phagocytosis [108].

Two of three experiments were performed with normal amounts of blood (500 µl), whereas in the first assay smaller volumes of blood were employed. In this case, NaCl (25 µl) was

removed from the respective capsule samples, and added whole blood (125 µl) after the addition of inhibitors (CD11b-inhibitor and cytochalasin D), giving a total volume of 200 µl for each vial. The aim was to explore the possibility for using smaller quantities of materials while still being able to study the effects of high concentrations of inhibitors. A titration experiment prior to the whole blood assays gave an indication of appropriate inhibitor concentrations. After incubation, EDTA was added (4 µl for 200 µl total volume; 14 µl for 700 µl total volume, final concentration 10 mM). Subsequent steps are similar to those described in section 2.2.1.

Cytochalasin D (1 mg/ml, Sigma-Aldrich, St. Louis, MO, USA) was dissolved in pure ethanol (197 µl) , giving a stock concentration of 10 mM. Cytochalasin D was then added vials for a total concentration of 20 µM and 40 µM. For use as controls, the corresponding masses of the standard protein BSA were added. Pure ethanol (197 µl) was added BSA (10%, 10 µl, R&D Systems, Minneapolis, MN, USA) to yield a mass of 1 mg BSA in the control stock, corresponding to a mass of 1 mg in the cytochalasin D stock. BSA controls were further prepared by adding to the capsules the same volumes of BSA in ethanol as cytochalasin D in ethanol. Ethanol controls were prepared by adding ethanol in the same volume as for 40 µM cytochalasin D.

CD11b-inhibitor (1 mg/ml, Merck Millipore KGaA, Darmstadt, Germany) was added to the vials for a total concentration of 60 µg/ml. No controls were prepared for these samples.

2.3 Flow cytometry

Flow cytometry was used in order to measure leukocyte activation after whole blood incubation with alginate microcapsules. Flow cytometry is a widely used biophysical technology that can be used for a range of applications, primarily immunophenotyping, cell counting and cell sorting. The technique is based on suspending cells in a stream of sheath fluid, and passing the sample solution by a laser beam and an electronic detection apparatus. The detectors will record forward scatter (FSC, reflecting the size of the cells) and side scatter (SSC, reflecting the granularity and structural complexity inside the cell), as well as any fluorescence. Flow cytometry thus makes it possible to distinguish cell types from each other depending on their size and inner complexity, and the use of fluorochrome-labeled antibodies towards specific cellular markers allows further discrimination between cells of interest.

2.3.1 CD11b

In addition to being central in cell adhesion, integrins are also convenient cell-surface markers for distinguishing different cell types. In this study, fluorochrome-conjuagated antibody specific towards CD11b, the α-chain of the heterodimeric integrin receptor CR3, or CD11b/CD18, was used to detect the activation of monocytes and granulocytes. Monocytes and granulocytes express CD11b on their membranes in roughly equal amounts. Moreover, it is known that activation of leukocytes will lead to upregulation of CD11b/CD18 expression on their membranes, and a fully activated neutrophil may express over 200,000 CD11b/CD18 receptors on its membrane [109]. CD11b may thus function as an early activation marker of

leukocytes. In order to specifically gate for monocytes, fluorochrome-conjugated antibody towards CD14 was employed. CD14 is a membrane protein found predominantly on monocytes and macrophages, which functions as a coreceptor along with TLR4 and MD-2 for detection of lipopolysaccharide (LPS, endotoxin) [63].

Expression of CD11b was measured after one hours incubation of whole blood with capsules and other stimulants. Blood (50 µl) was taken out from the samples and fixed with paraformaldehyde (PFA, 1 %, 50 µl) for 4 minutes in 37 °C. Fixed blood (25 µl) was added an antibody mixture (1:1, 5 µl) containing anti CD11b-PE and anti CD14-FITC (both: BD Biosciences, USA – see tables 2.4-2.5) and incubated dark for 15 minutes. Samples were transferred to flow vials and incubated dark for 15 minutes with EasyLyse erythrocyte-lysis reagent (500 µl, Dako, Denmark) to remove red blood cells. CD11b expression on granulocytes and monocytes, and thus level of leukocyte activation, was measured on a flow cytometer (FACSCanto II, BD Biosciences, USA) by detecting $CD11b^+$ cells. $CD14^+$ cells generated FITC-fluorescence, allowing gating of $CD14^+CD11b^+$ monocytes.

2.4 ELISA

Enzyme-linked immunosorbent assay (ELISA) was performed on plasma from whole blood assays. ELISA is an immunological technique based on the use of mono- or polyclonal antibodies and an enzymatic color reaction. ELISA may be used for detection of antigens or antibodies. For the detection of an antigen in a sample, such as a certain cytokine, the use of a so-called sandwich ELISA can be employed. In this work, ELISA was used to detect the cytokines IL-8, TNF-a, as well as the complement component sTCC. Figure 2.1 illustrates the principle for the ELISAs used in this work.

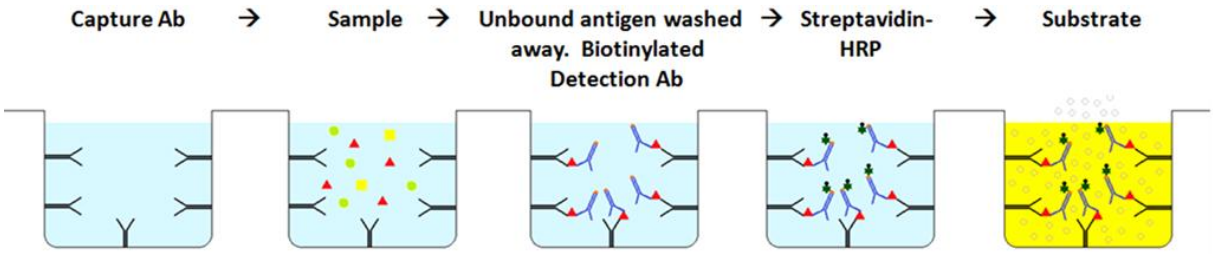

Figure 2.1. Principle for sandwich ELISA. Streptavidin-HRP is the employed enzyme, binding specifically to biotin in biotinylated secondary antibody. By addition of substrate, a color reaction facilitated by the enzymatic activity of Streptavidin-HRP takes place. The strength of color reflects the initial concentration of antigen present in the samples.

Antigen specific antibodies were allowed to attach to the plastic in specific ELISA multiwell plates. Unbound capture antibody was removed through washing the plates. Any nonspecific binding sites in the wells were blocked with BSA, a common blocking agent. The plates were washed before adding the plasma samples. Any antigen present in the sample would bind to the high affinity antibodies coating the plate. The plates were washed to remove unbound antigen. A biotin-labeled and highly specific secondary antibody, which recognizes a different epitope as compared to the capture antibody, was added to detect the bound antigen. The

plates were further washed to remove unbound detection antibody. Streptavidin-conjugated horse radish peroxidase (HRP) was then linked to the biotin-labeled antibody. Streptavidin binds to biotin with high affinity, and the conjugated HRP provides enzymatic activity for detection upon addition of the substrate 3,3',5,5'-tetramethylbenzidine (TMB). HRP will oxidize TMB into a deep blue-colored product. Stopping the reaction with acidic stop solution (H_2SO_4) yields a clear yellow color. Light absorbance (or optical density, OD) was detected by a spectrophotometer (in this study: VICTOR^3 microplate reader, Perkin Elmer, USA) at 450 nm, with a wavelength correction set to 570 nm. Absorbance was used to calculate the level of antigen initially present in the respective samples.

2.4.1 IL-8

IL-8 ELISA (Human IL-8 DuoSet ELISA Development kit, R&D Systems, Minneapolis, MN, USA) was performed strictly in accordance with the manufacturers manual. IL-8 specific capture antibody (4.0 µg/ml in PBS, 50 µl/well) was added to Nunc 96-well microplate and left to incubate over night in room temperature (RT). The plate was washed with wash buffer (300 µl PBS with Tween 20/well) three times, before blocking the wells with BSA (1% BSA in PBS, 200 µl/well, R&D Systems, Minneapolis, MN, USA) for one hour at RT. The washing step was repeated before loading the samples. Samples were diluted in reagent diluent (0.1% BSA and 0.05% Tween 20 in Tris-buffered saline). IL-8 standard was diluted to 2000 pg/ml in reagent diluent, and was further serially diluted 1:2 in order to create a standard curve. Samples were loaded in triplicates and incubated at RT for two hours. After washing the plate, IL-8 specific detection antibody (20 ng/ml in reagent diluent, 50 µl/well) was added. The plate was washed after two hours incubation, and streptavidin-HRP was added (diluted 1:200 in reagent diluent, 50 µl/well) and left dark for 20 min. After a final washing step, a 1:1 mixture of TMB substrate A and B (50 µl/well) added. The reaction was stopped after approximately 10 min with H_2SO_4 (2 M, 50 µl/well) and light absorbance was detected.

2.4.2 TNF-α

TNF-α ELISA (Human TNF-α DuoSet ELISA Development kit, R&D Systems, Minneapolis, MN, USA) was performed strictly in accordance with the manufacturers manual, similar to IL-8 ELISA. Samples were loaded in triplicates in order to achieve more precise results. The reaction was stopped after approximately 20 min, and the light absorbance was determined.

2.4.3 TCC

TCC ELISA was performed similarly to IL-8 and TNF-α, but with a specific streptavidin-HRP, EDTA added to the reagent diluent, and other incubation times. The assay has been described previously in detail [110] and performed according to a later modification [61]. TCC specific capture antibody (1 mg/ml, anti-complement component C5b-9 [human], BioPorto, Gentofte, Denmark) was diluted 1:1000 in PBS and added to a Nunc 96-well microplate (50 µl/well). The plate was incubated over night at 4°C. This monoclonal antibody, clone aE11, binds specifically to an epitope which is exposed on C9 when incorporated into the TCC, and may react with both membrane-bound and fluid-phase TCC [111]. The plate was washed (three times, 300 µl PBS with Tween 20/well) before added

blocking solution (0.1 % BSA in PBS, 200 µl/well). After one hour incubation at RT, plates were washed. Plasma samples were diluted in reagent diluent (0.2% Tween 20 and 10 mM EDTA in PBS), before loading (50 µl/well) in triplicates onto the plate. A 1:2 dilution series of standard (zymosan activated serum, 5 au/ml) was made for the standard curve. The plate was incubated for 1 hour in RT, followed by another washing step. Detection antibody was then added to the plate (diluted 1:5000 in PBS with 0.2% Tween, 50 µl/well, Biotin Conjugated Anti-human SC5b-9, Quidel, USA), and incubated 45 minutes in RT. The plate was washed and added streptavidin-HRP (diluted 1:1000 in PBS with 0.2% Tween, 50 µl/well, BioLegend, San Diego, CA, USA). The plate was left dark for 30 minutes at RT, followed by a final washing step of four washing cycles. TMB substrate A and B (1:1 mixture, 50 µl/well, R&D Systems, USA) was added. The reaction was stopped after approximately 15 minutes by adding stop solution (2M H_2SO_4, 50 µl/well).The results are given in arbitrary units (AU/ml), which is related to a standard of maximally activated serum defined to contain 1000 AU/ml.

2.5 Bio-plex

The Bio-Plex™ Pro Assay (Bio-Rad Laboratories, Inc., Hercules, California, USA) multiplex assay was employed to detect 12 different cytokines simultaneously. The assay is based on a principle not very different from a sandwich ELISA, but instead of employing an antibody-coated multiwall plate, it takes use of magnetic beads covered with antibodies specific for certain cytokines, as illustrated in figure 2.2.

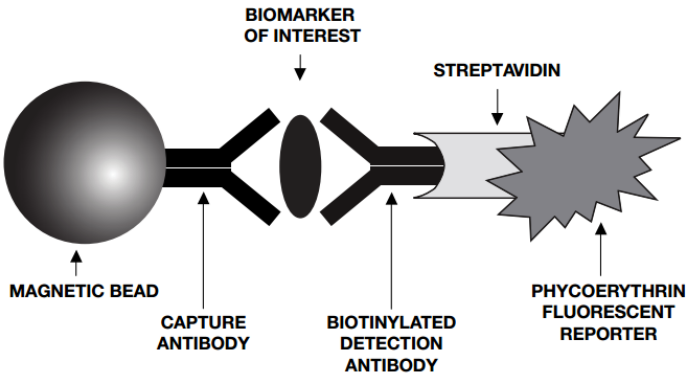

Figure 2.2. Bio-Plex sandwich immunoassay. Directly reproduced from [112].

The magnetic beads bind the cytokine of interest through the covalently attached capture antibodies. After washing to remove unbound protein, a biotinylated detection antibody is added to create a sandwich complex. Addition of a streptavidin-phycoerythrin (SA-PE) conjugate allows for detection and quantification of the cytokine concentration, as PE serves as a reporter. The magnetic beads each have a distinct color code which permits the direct identification of bound cytokine type. By using a two laser flow cytometer, it is thus possible to detect which bead is present, and then quantify the presence of cytokines bound to the bead surface by determining PE fluorescence. The fluorescent dyes within each bead are excited by a red (635 nm) laser to provide bead classification and thus assay identification. At the same time, a green (532 nm) laser excites PE to generate a reporter signal. The detected

fluorescence is interpreted into the concentration of different cytokines. The 12 different cytokines that were analyzed are shown in table 2.3

Table 2.3. Plasma cytokines analyzed through Bio-Plex assay after whole blood assays. PDGF-BB is the homodimer of PDGF consisting of two B-polypeptide subunits.

IL-1β	IL-10	TNF-α
IL-1RA	MCP-1	RANTES
IL-6	MIP-1α	PDGF-BB
IL-8	IFN-γ	VEGF

The Bio-Plex assay was performed strictly according to the manufacturers instruction manual [112], but using only half the amount of beads (25 µl per well). [112]. Plasma samples were diluted 1:4 in Bio-Plex sample diluent (20 µl plasma in 60 µl sample diluents). An automated magnetic bead washer (Bio-Plex Pro Wash Station, Bio-Rad, Hercules, CA, USA) was used for the washing steps. The fluorescence was detected by using the Bio-Plex 200 System, and as the concentration of cytokine bound to each bead is related to the median fluorescence intensity (MFI) of the reporter signal, the cytokine concentration (pg/ml) could be determined.

2.6 Protein adsorption assay

To get an understanding of the reactions taking place on alginate capsule surfaces, capsules were incubated in plasma and examined for protein adsorption. As previously mentioned, plasma contains immediate protein cascades including complement, coagulation, fibrinolysis and contact activation systems. To the present day, little is known about the mechanisms that initiate the host inflammatory processes directed towards biomaterials such as alginate. Insight into the surface adsorption of proteins may provide information on which innate mechanisms which are involved in host responses towards alginate microbeads and microcapsules, and also on interactions between different cascade systems.

Alginate capsules were incubated (37 °C) in pooled lepirudin plasma (300 µl unless otherwise specified). A protein adsorption study was also performed using fresh anti-coagulated whole blood incubated with compstatin analogue CP20 (25 µM, synthesized in the laboratory of Prof. John D. Lambris), control peptide (25 µM, Prof. John D. Lambris), soliris® (100 µg/ml, Alexion Pharmaceuticals, Cheshire, UK), PBS with Ca^{2+}/Mg^{2+} (equal volume as Soliris®, Sigma-Aldrich, MO, USA) or no additive. For the capsule samples with no additive, the normal amount of blood (500 µl) was used, whereas in the remaining samples a smaller amount of blood was added (250 µl). In this study, capsules were incubated 4 hours in anticoagulated whole blood before fixing of attached cells for 30 minutes with PFA (0.5%) prior to staining with fluorochrome-labeled antibodies.

After whole blood or plasma incubation, capsules were washed (0.9% NaCl, 3 x 1 ml) before incubation with fluorochrome-labeled antibody (50 µg/ml, 37 °C, 30 min). The antibodies used for protein adsorption assays are listed in table 2.4. Where appropriate, working dilutions of antibody were prepared in PBS. Unless otherwise stated, the employed PBS in this study is

generally without Ca^{2+}/Mg^{2+}. Capsules were washed (0.9% NaCl, 2 x 1 ml) after incubation with both primary (1°), and – where appropriate – secondary (2°) antibody. For the αTCC antibody, different incubation times and concentrations were attempted in order to optimize the protocol for TCC adsorption studies. Based on those results, capsules stained for TCC and its isotype control were incubated 60 minutes both with primary (1°) and secondary (°2) antibodies. After staining, samples were stored in wash solution (200 µl) and protected from light.

Table 2.4. Antibodies employed in the protein adsorption assays.

Antibody	Additional information	Catalogue number	Manufacturer
αC3c	FITC-labeled polyclonal rabbit anti-human C3c complement, 3.2 mg/ml	F0201	Dako Denmark A/S, Glostrup, Denmark
αC3c control & αTCC (control) 2° Ab	FITC-labeled polyclonal rabbit anti-mouse immunoglobulins, 1.9 mg/ml	F0261	Dako Denmark A/S, Glostrup, Denmark
αTCC 1° Ab	Anti-complement component C5b-9 [human], 1 mg/ml	DIA 011-01	BioPorto, Gentofte, Denmark
αTCC control 1° Ab	Isotype control, mouse IgG2aκ , 0.5 mg/ml	553454	BD Biosciences, USA
αFibrinogen	FITC-labeled polyclonal sheep anti-human fibrinogen, 8 mg/ml	AB7144F	Chemicon International (now Bioscience Research Reagents), Temecula, CA, USA
αFibrinogen control	FITC-labeled polyclonal sheep anti-rat IgG immunoglobulins, 1 mg/ml	25-783-76143	GenWay Biotech, Inc., San Diego, CA, USA

2.7 Cell adhesion studies

In order to explore capsule-cell-interactions at the alginate microcapsule surface, cell adhesion studies in whole blood were performed. Leukocytes present in blood may attach to alginate capsule surfaces to a greater or lesser extent, depending on the capsule surface properties. Cell adhesion studies may provide us with information about which cell types are present, and in what numbers, in addition to the overall level of cell adhesion on the capsule surfaces.

Alginate capsules were incubated (37 °C) in fresh whole blood (500 µl). Samples to be incubated for longer than 6 hours were placed in a CO_2-incubator (5%). After removing the blood, attached cells were fixed with PFA (0.5%, 0.5 ml, 20 minutes, unless otherwise specified). Capsules were washed carefully (0.15% PFA in PBS, 2 x 0.5 ml, unless otherwise specified). The capsules were now either directly studied in a light microscope, or further incubated with fluorochrome-labeled antibody (1,25 µg/ml, 37 °C, 60 min). In the studies

where AP-capsules were stained for αCD14, αTF and αCD11b, antibodies were prepared in PBS (100 µl) with BSA (1%), which was further added to the capsule samples. BSA was added in order to block nonspecific protein interactions. The antibodies used for cell adhesion studies are listed in table 2.5. Capsules incubated with antibody were further carefully washed (0.15% PFA in PBS, 2 x 0.5 ml) and stored in wash solution (200 µl) protected from light before confocal imaging.

Table 2.5. Antibodies employed in the cell adhesion studies.

Antibody	Additional information	Catalogue number	Manufacturer
αCD14-APC	Allophycocyanin-labeled mouse anti-human CD14 (Clone 134620), IgG1, 10 µg/ml	FAB3832A	R&D systems Minneapolis, MN, USA
Isotype APC control (to αCD14)	Allophycocyanin-labeled mouse IgG1, isotype control, 5 µg/ml	IC002A	R&D systems Minneapolis, MN, USA
αTF-FITC	FITC-labeled mouse anti-human tissue factor, IgG1, 100 µg/ml	4508CJ	American Diagnostica GmbH, Pfungstadt, Germany
Isotype FITC contorl (to αTF)	FITC-labeled mouse IgG1, isotype control, 50 µg/ml	345815	BD Biosciences, USA
αCD11b-PE	PE-labeled mouse anti-human CD11b, IgG2a, 50 µg/ml	333142	BD Biosciences, USA
Isotype PE control (to αCD11b)	PE-labeled mouse IgG2a, isotype control, 200 µg /ml	553457	BD Biosciences, USA
αCD14-FITC	FITC-labeled mouse anti-human CD14, IgG2b, 25µg/ml	345784	BD Biosciences, USA
Isotype FITC control (to αCD14)	FITC-labeled mouse IgG_{2b}, isotype control, 0.5 mg/ml	555057	BD Biosciences, USA
αCD14-PE	PE-labeled mouse anti-human CD14, IgG2bκ, 50 µg /ml	345785	BD Biosciences, USA
Isotype PE control (to αCD14)	PE-labeled mouse IgG2bκ, isotype control, 25 µg /ml	555743	BD Biosciences, USA

2.8 CLSM

After staining with fluorochrome-labeled antibody, confocal laser scanning microscopy (CLSM) was used to observe the capsules. CLSM allows optical sectioning and thereby reconstruction of three-dimensional (3D) images of the capsules. To excite the fluorochromes, a 543 nm laser was used for PE, a 633 nm laser for APC, and a 488 nm Argon laser was used for FITC-labeled antibodies. Pictures were taken as optical cross sections through the equator using both laser and differential interference contrast (DIC), as well as z-stack 3D projections of the capsules using only laser. The employed objective for imaging was C-Apochromat 10x/0.45W. Beamsplitters HFT UV/488/543/633 nm and HFT 458/514/633 nm were used, as well as filters BP 505-530, BP 565-615 IR, LP 615 and LP 650.

2.9 Statistics

The Wilcoxon signed-rank test was used to calculate significant differences in sTCC and cytokine responses between the different samples in the whole blood assays. The Wilcoxon signed-rank test is a non-parametric paired difference test which can be used when comparing two related samples to assess whether their population mean ranks differ. There are expected to be some biological differences between each blood donor in the whole blood assays. Due to the low number of donors (n=5), the data could not be assumed to be normally distributed, which is taken into account for in this statistical test. The software SPSS Statistics (v. 21, IBM) was used to carry out statistical calculations. Differences were considered significant at $P<0.05$.

3 RESULTS

3.1 Preliminary studies

3.1.1 Hydroxyapatite-containing and epimerized capsules

To get a first indication on the inflammatory potential of microbeads epimerized with mannuronan C5-epimerases and calcium phosphate mineralized microbeads, a whole blood assay was performed using one single blood donor. This gave a rough estimate of complement and leukocyte activation, cell adhesion and cytokine induction for the capsules in question. TAM and AP were included as a negative and positive control, respectively, as the inflammatory properties of these capsules have been elaborated in previous experiments [45, 61]. Results from the whole blood assay are shown in figures 3.1a-c, with full data included in the appendix. In general, capsules containing polycation are designated as microcapsules, and those without polycation as microbeads.

sTCC responses were generally low and at the level with or lower than saline control, with the exception of CaP and AP which induced 4-5 times the amount of sTCC compared to saline (figure 3.1a). Whereas Enz-CaP induced sTCC levels similar to that of saline control, the TAM, Ca-bead and epimerized microbeads induced sTCC levels lower than saline control. For comparing the effects of HA mineralization and epimerization, the Ca-beads constitute the most proper control capsule. Compared to the Ca-beads, the introduction of HA induced elevated sTCC. This was specifically apparent with the microbeads mineralized by counter-diffusion precipitation (CaP), but also those made by enzymatic mineralization (Enz-CaP) provoked some elevation of sTCC. The beads of epimerized alginate did not induce an elevated level of TCC. Comparing the RGD-grafted Epi-RGD microbeads with the non-functionalized Epi-microbead indicated that the introduction of RGD did not influence the level of sTCC produced.

IL-8 levels were generally low (figure 3.1b). The exception to this trend was the epimerized microbeads as well as the AP microcapsules, which induced approximately 4-5 times higher levels of cytokine release. Other microbeads generally induced IL-8 levels lower than saline control, but with CaP resulting in a response slightly higher than saline control. It appeared that introducing HA into the alginate system induced higher levels of cytokine as compared to the corresponding non-mineralized control Ca-bead. As for the sTCC response, this was specifically apparent with CaP, but Enz-CaP also evoked some IL-8. Comparing the epimerized Epi-RGD with Epi indicated that the introduction of RGD reduced the IL-8 levels.

TNF-α was induced in very large amounts by the epimerized microbeads which were approximately 30-40 times higher compared to the other samples (figure 3.1c). For the remaining capsule types, TNF-α levels were generally low and on the level with saline control. The exception to this was CaP, which induced a response slightly higher than saline control, and AP microcapsules which induced responses approximately 3 times higher than saline. The HA-microbeads mineralized by enzymatic control did not induce a TNF-α response, whereas those made through counter-diffusion precipitation induced a slight

elevation compared to the control Ca-bead. Also here, as for IL-8, the grafting of RGD to the epimerized alginate resulted in reduced cytokine levels.

Considering the significantly elevated cytokine responses (particularly seen for TNF-α) for the epimerized microbeads, it was suspected that these were endotoxin contaminated. This was confirmed through performing a LAL-assay, which showed that the LPS levels for the Epi and Epi-RGD alginates were significantly high: 5233 EU/g and 721 EU/g, respectively. Due to this, the subsequent studies takes use of commercial peptide-coupled alginates, as the detected LPS contamination is likely to be the reason for the demonstrated responses.

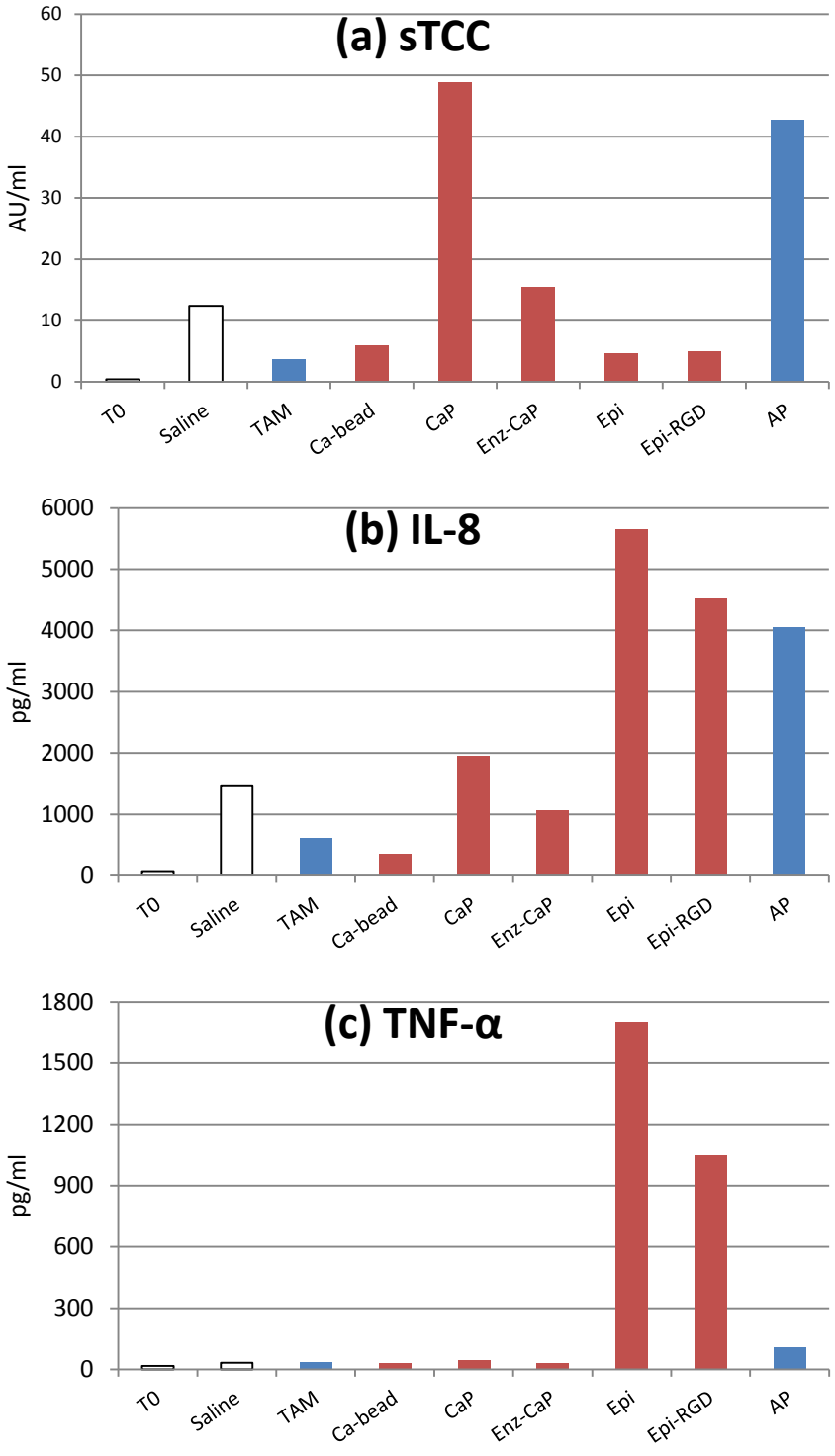

Figure 3.1a-c. sTCC, IL-8 and TNF-α levels for one donor after incubation of alginate microcapsules and microbeads with controls for 4 hours in fresh human whole blood. White bars are controls. Blue bars are control capsules. Red bars are HA-containing and epimerized microbeads with Ca-bead as a control. The zymosan values for sTCC, IL-8 and TNF-α are 218 AU/ml, 13163 pg/ml and 22046 pg/ml, respectively.

As previously mentioned, CD11b may function as an early activation marker of leukocytes. Results for the CD11b-expression induced by alginate microbeads and microcapsules are illustrated in figure 3.2. CD11b-levels were high for the epimerized microbeads, approximately twice as high as saline control, and higher than the positive control zymosan. Expression for the remaining capsules was generally low and at the level with or below saline control. Exceptions to this was CaP and AP, which induced some leukocyte activation. For comparing the effects of HA mineralization and epimerization, the Ca-beads constitute the most proper control capsule. Compared to the Ca-beads, the introduction of HA by counter-diffusion, but not enzymatic control, induced elevated CD11b-expression. Epimerization lead to a highly elevated level of leukocyte activation. Furthermore, grafting RGD to the epimerized alginate led to a reduction in leukocyte activation.

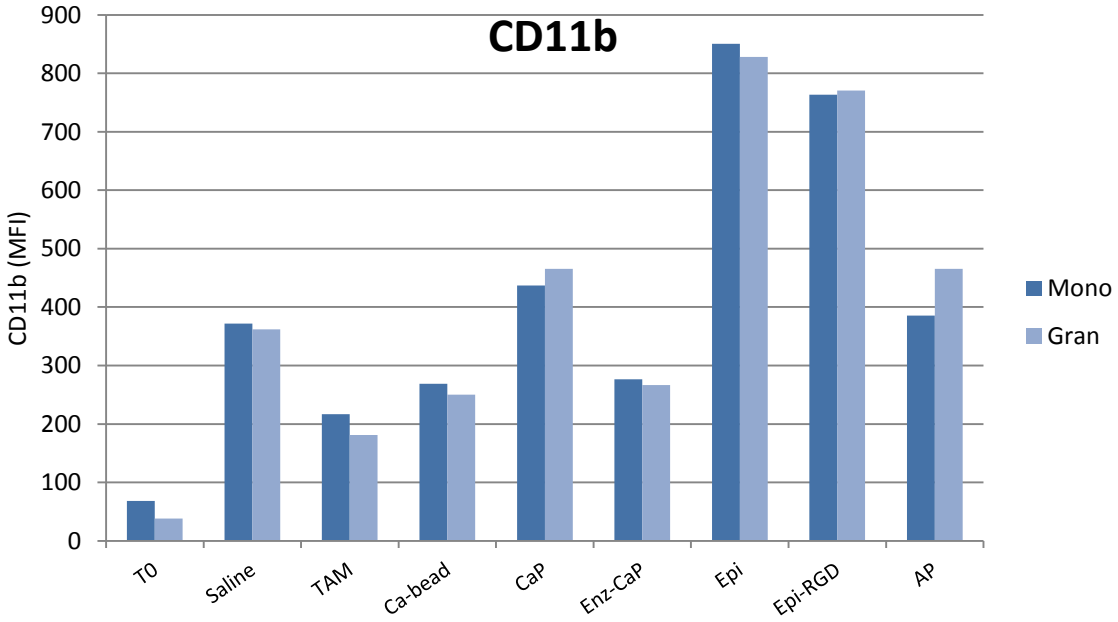

Figure 3.2. CD11b expression on leukocytes measured as median fluorescence intensity (MFI) for one donor after incubation of alginate microcapsules and microbeads with controls for 4 hours in fresh human whole blood. Mono=monocytes, gran=granulocytes. Ca-bead constitutes the control for the HA-containing microbeads (CaP and Enz-CaP) as well as the epimerized microbeads (Epi and Epi-RGD). TAM and AP are negative and positive control capsules, respectively. Zymosan values are 297 for monocytes and 491 for granulocytes.

Cell adhesion was studied on the same set of capsules after 3 hours incubation in whole blood. Attached cells were fixed in PFA (0,5%, 200 µl, 5 min). The results from the cell adhesion study are shown in figure 3.3. TAM and Ca-bead appeared inert, whereas AP appeared to induce cell adhesion, as was expected. The epimerized microbeads were mostly free of leukocyte adhesion, still, on some beads cells could be observed. Enz-CaP did not appear to induce cell adhesion, with the few leukocytes present seemingly located in cracks in the capsule surface. CaP-microbeads appeared to have rough textured surfaces, with relatively fair amounts of leukocyte adhesion. Although the presence of cells on CaP is not easily visible in figure 3.3, and might be mistaken for accumulations of HA, leukocyte adhesion on CaP was clearly detected during microscopy by scanning up and down through the microbead sample. The experiment also gave an indication on the mechanical stability of the microbeads.

CaP-microbeads appeared to have significantly better mechanical strength than the other mineralized microbeads as well as Ca-beads, which lost much of their integrity after rounds of washing and treatment with PFA.

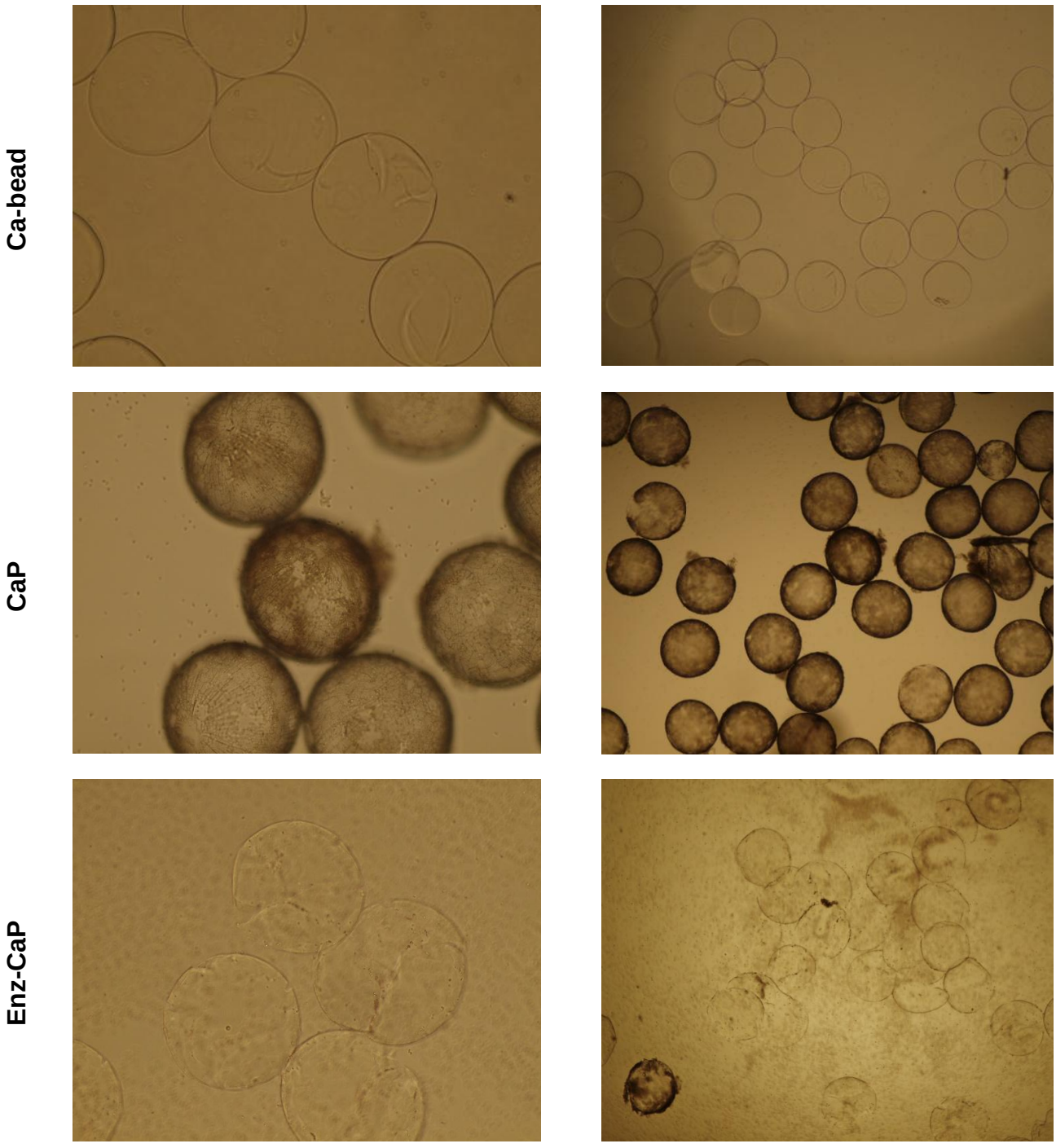

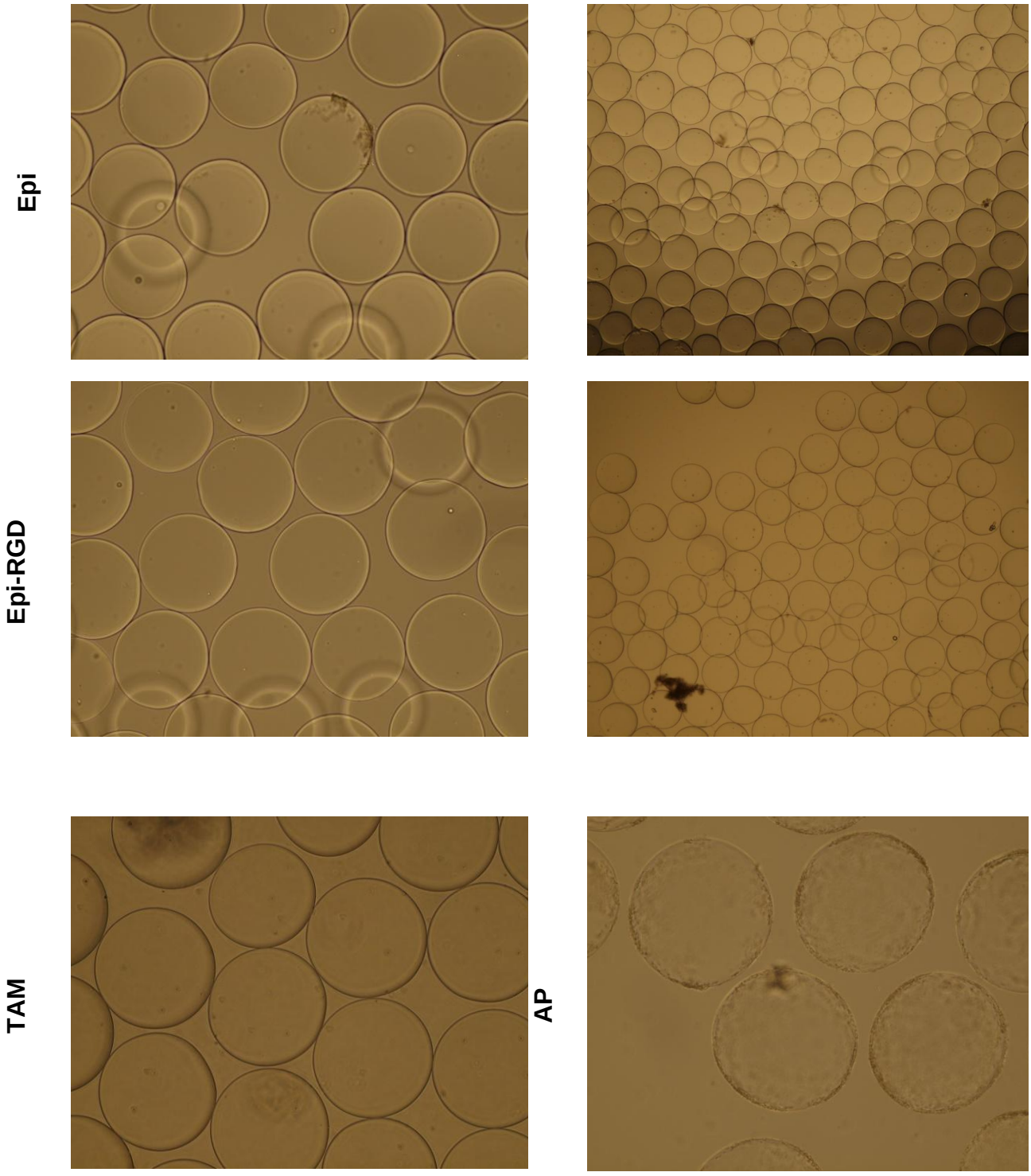

Figure 3.3. Cell adhesion on HA-containing and epimerized microbeads with control capsules after 3 hours incubation in whole blood. Ca-bead constitutes the control for HA- and epimerized microbeads. Pictures were taken with both 10x (left column) and 4x (right column) objective lens magnification. The control capsules AP and TAM are displayed only in 10x magnification.

3.3.1 C3 and fibrinogen deposition on AP and TAM

In order to get a first indication of the potential level of complement activation initiated by the capsule surfaces, alginate microcapsules and microbeads were stained for C3 deposition. C3 is abundant in plasma, and is a central component of the complement system, required for formation of both the classical/lectin and alternative C5 convertases (see figure 1.9). Moreover, cleavage of C3 by the C3 convertases is considered the central event of complement activation, as this reaction yields the anaphylatoxin C3a, which is important in initiating inflammation, as well as the central opsonin C3b. By staining for C3c, it is possible to detect capsule surface adsorption of either native C3, active C3 (C3b) and the C5 convertases, all in which the C3c fragment is present (see figure 4.1). AP-microcapsules and TAM-microbeads were incubated 21 hours in lepirudin plasma (500 µl). Figure 3.4 shows that C3 deposition was observed on AP microcapsules, whereas no C3 was detected on TAM microbeads. A time study of C3 deposition was subsequently conducted, in order to explore the rate at which C3 deposits on the capsule surfaces. The detected C3c on AP microcapsules increased steadily from 1 to 4 hours, and from 4 hours to 8 hours (figure 3.5). After 16 hours, the AP capsule surface appeared to be completely covered by C3c. In turn, the TAM microbeads did not appear to induce C3 deposition. After 4 and 8 hours incubation, minor levels of C3c appeared on TAM microbeads. However, after 16 hours incubation, TAM appeared to be completely free of C3 deposition. The staining was specific for C3 as demonstrated by the negative controls.

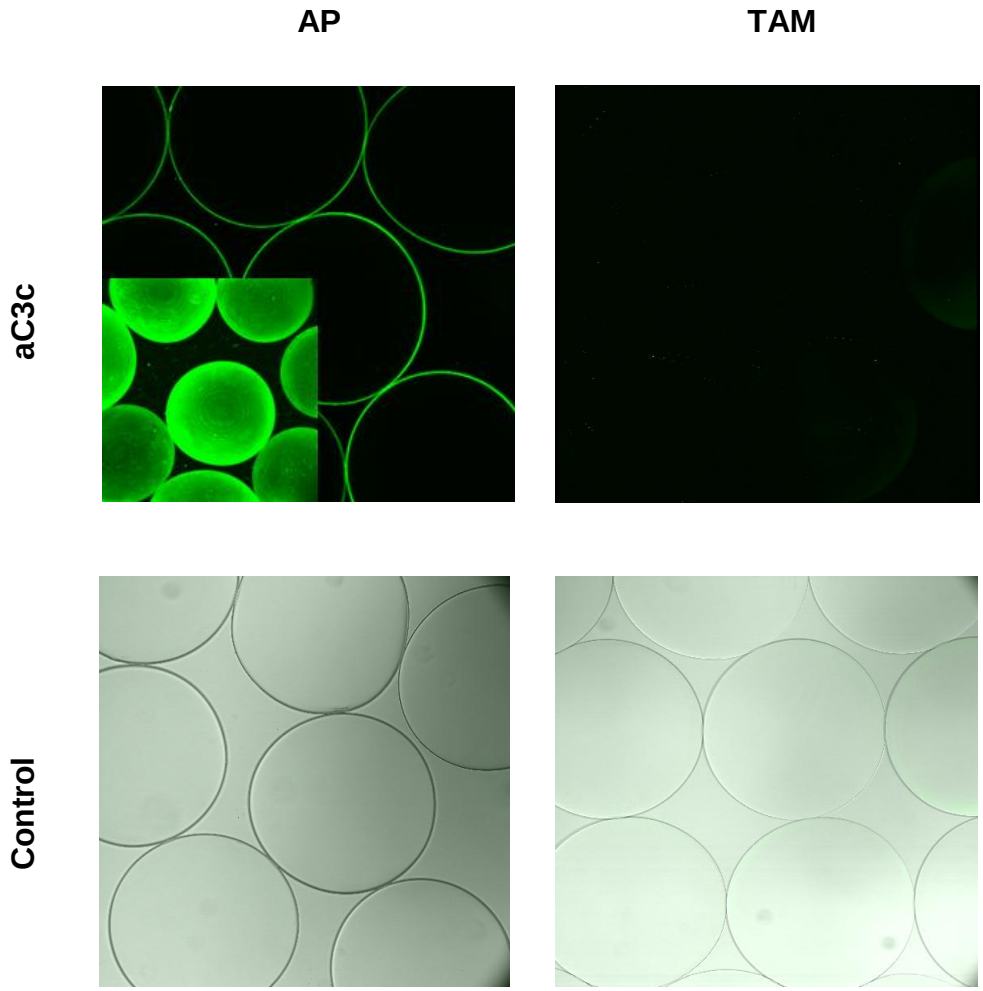

Figure 3.4. C3 deposition on AP microcapsules and TAM microbeads after 21h incubation in lepirudin plasma. Capsules are stained for αC3c and negative control antibodies. Capsules are displayed as equatorial sections through the capsules, and as 3D projections.

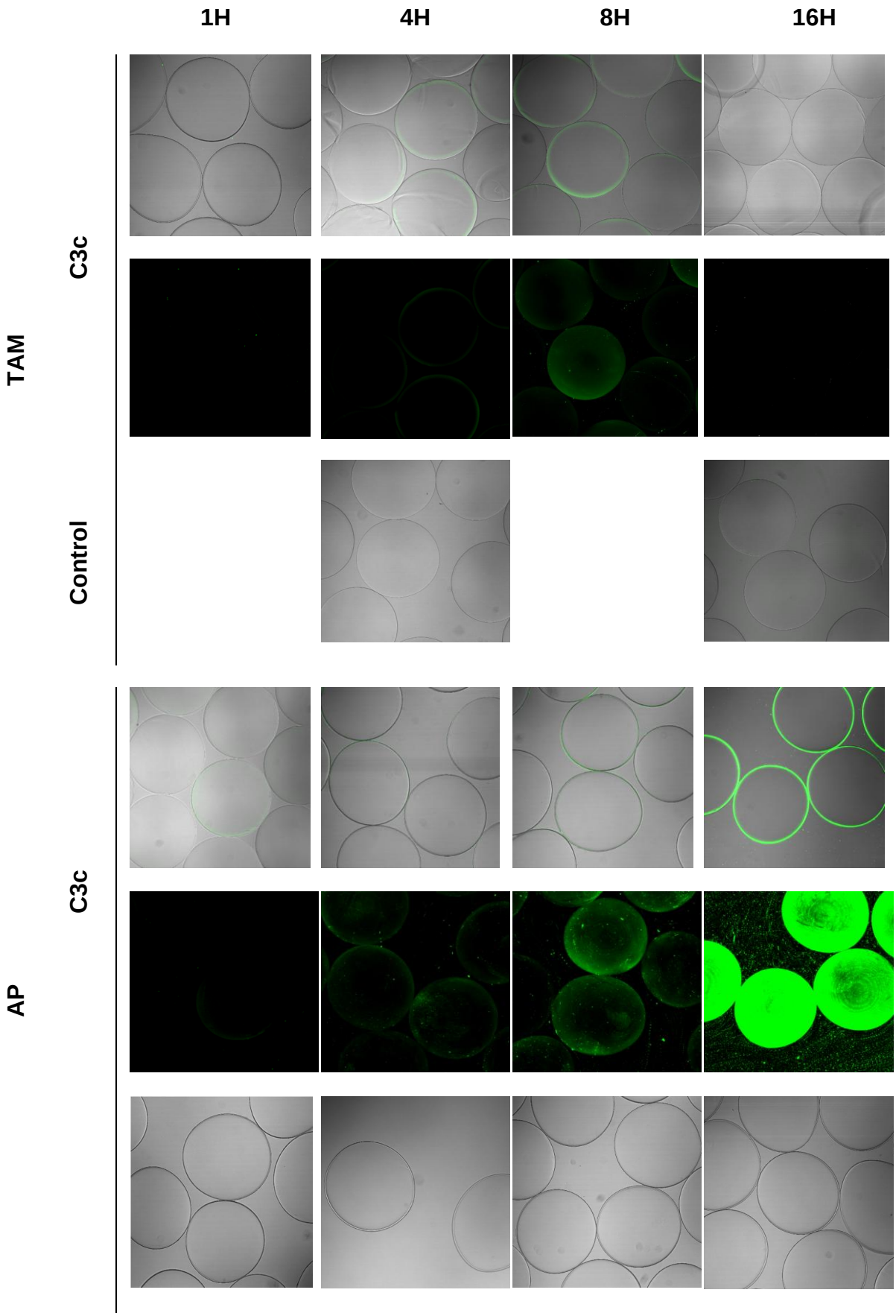

Figure 3.5. Time study of C3 deposition on AP microcapsules and TAM microbeads after incubation 1h, 4h, 8h and 16h in lepirudin plasma. Negative controls for TAM incubated for 1h and 8h are lost. Capsules are stained for αC3c and negative control antibodies. Capsules are displayed as equatorial sections through the capsules, and as 3D projections.

AP and TAM were also stained for fibrinogen deposition in order to see if fibrinogen could be adsorbed to the capsule surfaces. Upon adsorption, fibrinogen may potentially expose specific sequences for cell attachment. AP-microcapsules and TAM-microbeads were incubated over night for 8 and 16 hours in lepirudin plasma before staining. Results from the confocal imaging are shown in figure 3.6. No fibrinogen deposition was detected, neither on AP-microcapsules nor TAM-microbeads.

An attempt to study fibrinogen deposition on HA-containing and epimerized microbeads after incubation in whole blood was also conducted. However, the experiment produced unclear results due to considerable background fluorescence from the negative control antibody which could not be solved. Thus, data on fibrinogen deposition on HA-containing and epimerized microbeads were regarded as biased (included in the appendix, figure A1).

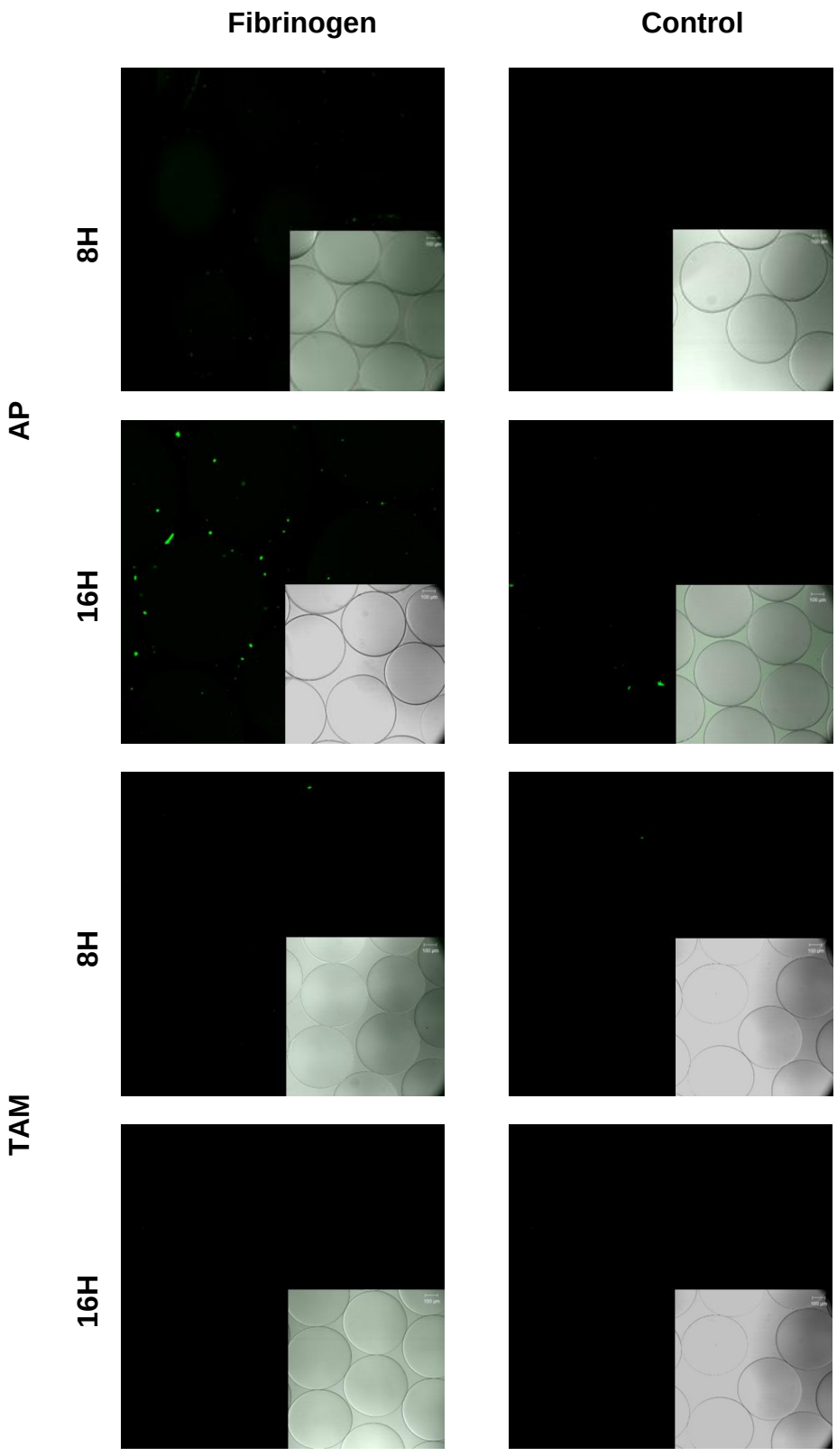

Figure 3.6. Fibrinogen deposition on AP microcapsules and TAM microbeads after 8h and 16 incubation in lepirudin plasma. Capsules are stained for αFibrinogen and negative control antibodies. Capsules are displayed as equatorial sections through the capsules, and as 3D projections.

3.2 Main study - Peptide-coupled and hydroxyapatite-containing capsules

The inflammatory potential of specialized biomaterials was explored for HA-containing microbeads and microbeads of commercially available peptide-coupled alginates using fresh anticoagulated whole blood from five individual donors. The specialized biomaterials include those intended for producing new ECM-like bioscaffolds – the peptide-coupled alginates, and those with potential in bone tissue engineering – the mineralized calcium microbeads.

For studying the effects of introducing specific properties into the alginate system, the different capsule types can be compared to respective control microbeads with best accordance to the alginate G/M ratio and the gelling conditions. For the HA-containing microbeads, the Ca-beads are the most proper controls. TAM microbeads constitute the most proper control for the high G peptide-coupled microbeads (G VAPG and G RGD), whereas the most suited control for high M peptide-coupled microbeads was considered to be the UP-MVM microbeads. Additional control microcapsules that were included were the polycation-containing AP, AP and PMCG microcapsules, which were previously demonstrated to evoke inflammatory responses through complement-mediated pathways, as well as the TAM microbeads previously demonstrated to be non-inflammatory [45, 61]. In the following charts, capsule types are grouped in different colors in order to more clearly illustrate which capsule should be compared.

3.2.1 Leukocyte activation and adhesion

CD11b-expression was measured after 1 hours incubation of the same set of alginate capsules in whole blood. The results are presented in figure 3.7. In general, CD11b-expression on both monocytes and granulocytes was low for saline control and most of the alginate microbeads, while elevated for the polycation-containing microcapsules. For the peptide-coupled capsules, one exception in stimulating potential was seen for the G VAPG microbeads. These beads induced significantly elevated CD11b-expression, higher than the positive control zymosan, which could be due to the elevated level of endotoxin within this sample. Of the remaining peptide-coupled microbeads, the G RGD microbead showed low stimulatory properties at the level of its control (TAM), and neither M REDV nor M RGD beads showed more stimulation than their control (UP-MVM). In contrast, a slight and significant elevated level of CD11b was detected for CaP compared to its control Ca-bead, while Enz-CaP was no more stimulating than its control bead. HA mineralization by counter-diffusion precipitation therefore appeared to have a slight stimulatory effect on the alginate beads. The polycation-containing microcapsules APA and PMCG induced significantly elevated CD11b expression compared to their control Ca-bead, whereas PMCG was also significant compared to saline control. It should be noted that AP most likely significantly induced CD11b too; however, since values from one donor were lost for this capsule type so that n=4, the employed statistics probably fails to show significance for these data.

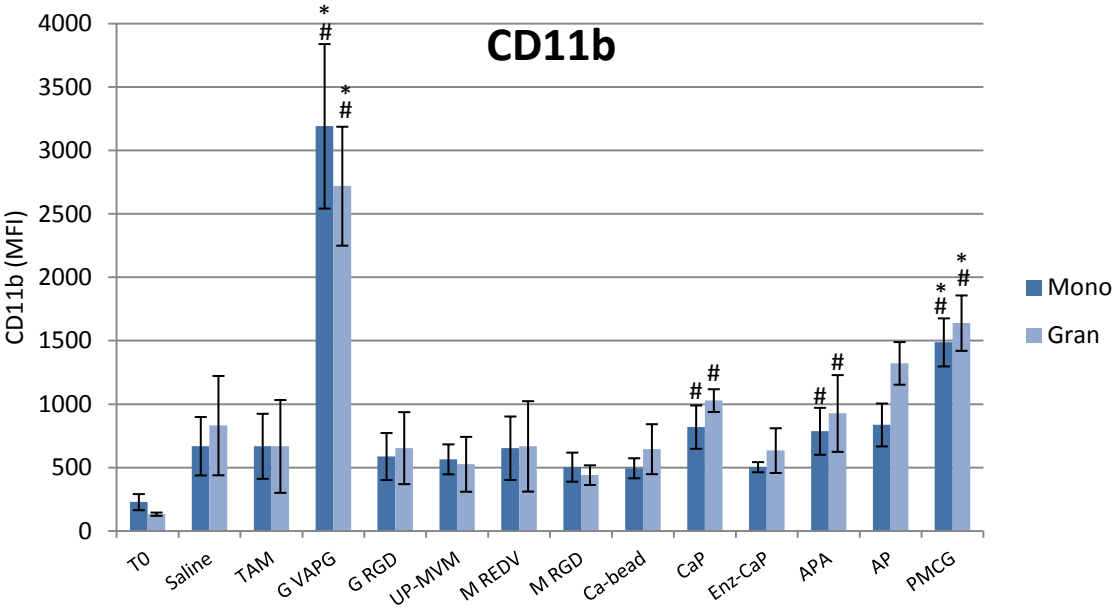

Figure 3.7. CD11b-levels measured as mean fluorescence intensity (MFI) after incubation of alginate capsules and controls for 4 hours in fresh human whole blood. Mono=monocytes, gran=granulocytes. TAM is the control microbead for high G peptide-coupled microbeads (G VAPG, G RGD), UP-MVM is the control for high M peptide-coupled microbeads (M REDV, M RGD). Ca-bead is the control for the HA-mineralized microbeads (CaP, Enz-CaP) and the polycation-microcapsules (APA, AP, PMCG). Data are expressed as the mean ± SEM (n=5). The zymosan value is 1713* ± 312 for monocytes and 3100* ± 367 for granulocytes. Significant values are given as $P < 0.05$ *compared to saline control #compared to the respective control capsules.

Leukocyte activation is normally associated with leukocyte adhesion. In order to get an indication of leukocyte adhesion on the peptide-coupled capsules, the respective microcapsules were incubated in whole blood for 3 hours before fixing of attached cells. TAM and APA were included as negative and positive controls, respectively. The high M microbeads (M REDV, M RGD and UP-MVM) appeared to suffer considerable osmotic swelling from this treatment. This led to bursting of the respective capsules, and no evaluation of cell-adhesion could be performed. The results for TAM, G VAPG, G RGD and APA are shown in figure 3.8. Neither G VAPG nor G RGD microbeads appeared to induce any leukocyte adhesion. In other words, neither the presence of peptides nor endotoxin appeared to have any effect on leukocyte adhesion, although leukocyte activation (in terms of CD11b-expression) was elevated. As was expected, polycation-containing APA microcapsules induced considerable amounts of cell adhesion, whereas the negative control microbeads TAM did not.

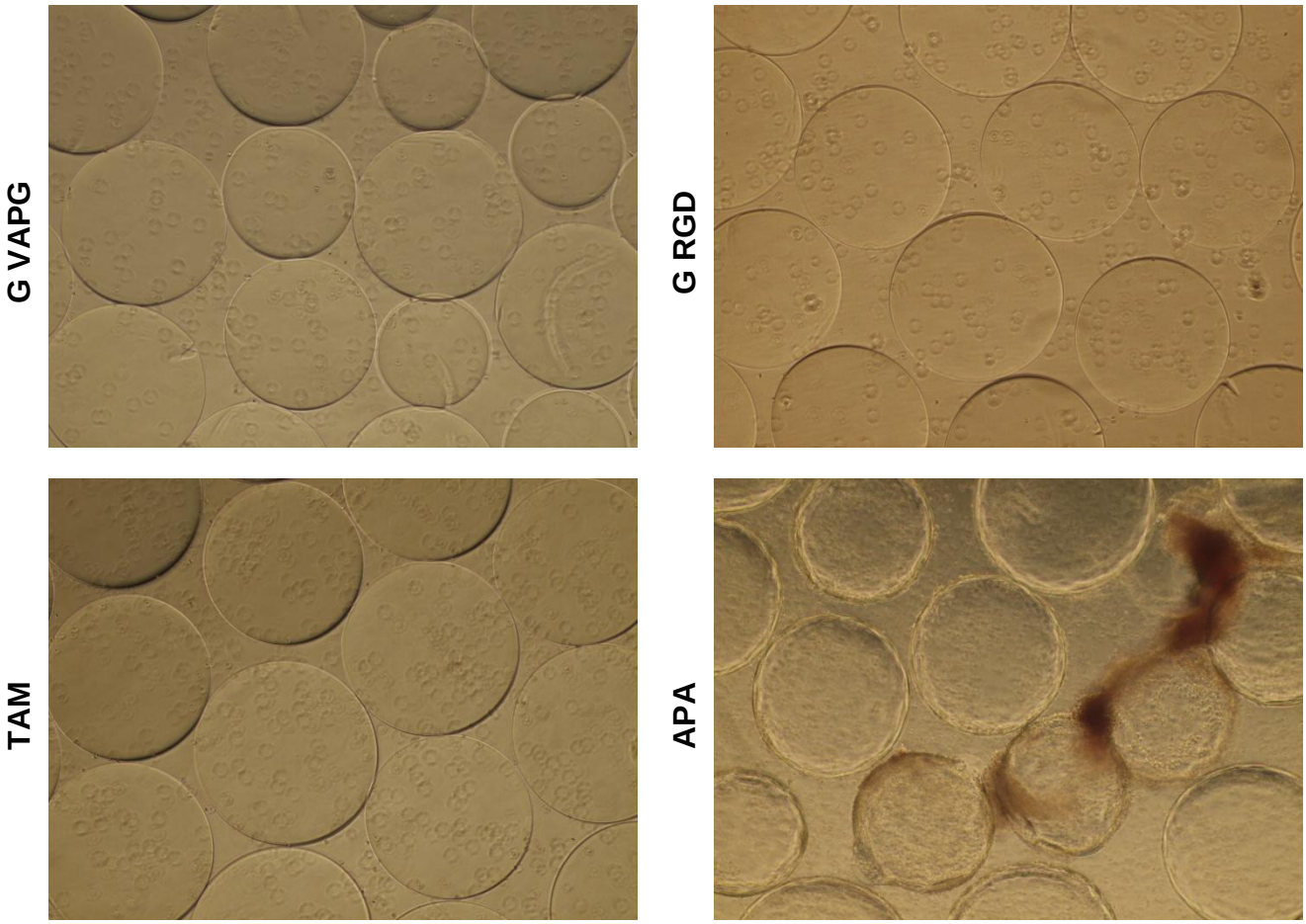

Figure 3.8. Cell adhesion on high G-containing peptide-coupled microbeads with control capsules after 3 hours incubation in whole blood. Pictures are taken with 10x objective lens magnification. G VAPG and G RGD can be compared to TAM as a negative control microbead. APA poses as a positive control.

Considering the significantly elevated CD11b expression and cytokine responses (figures 3.10-3.14) for the VAPG-coupled microcapsules, these capsules were suspected to be endotoxin contaminated. This was confirmed through performing a LAL-assay, showing that the endotoxin level was 320,4 EU/g for this alginate. As the presence of LPS significantly influences the inflammatory response, the data from the G VAPG capsules cannot be trusted to provide any significant information about the inflammatory potential of VAPG-coupled alginates.

3.2.1 Complement activation

sTCC is shown to be a sensitive indicator of complement activation. Figure 3.9 shows the amount of sTCC after incubation with various microcapsules. The sTCC amounts were generally low for most of the microbeads—with responses similar to or below saline. For the polycation-containing microcapsules (APA, AP, PMCG) the sTCC levels were 8-9 times higher than saline control. The mineralization of HA did evoke a significantly elevated sTCC response as compared to its control Ca-bead. This was specifically apparent with the microbeads mineralized by counter-diffusion precipitation (CaP), but also the microbeads made by enzymatic control (Enz-CaP) provoked some elevation of sTCC. Functionalizing alginates with peptides did not induce sTCC levels. G VAPG and G RGD microbeads showed low stimulatory properties at the level of their control (TAM), and neither M REDV nor M RGD beads showed more stimulation than their control (UP-MVM). Only the PMCG microcapsule was found to induce significantly elevated responses, but it should be noted that AP and APA most likely induced significantly higher levels of sTCC too. However, since values from one donor were lost for these capsule types so that n=4, the employed statistics probably fails to show significance for these data.

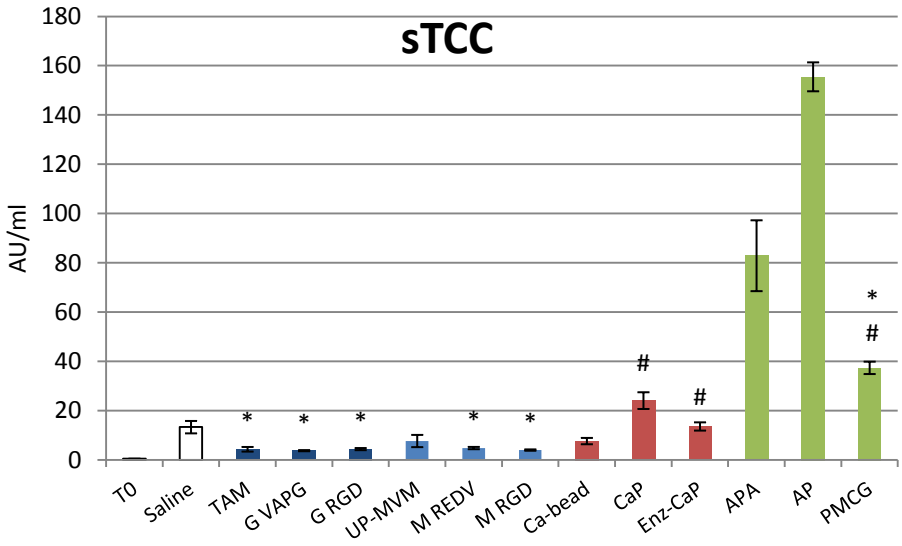

Figure 3.9. sTCC levels after incubation of alginate capsules and controls for 4 hours in fresh human whole blood. Data are expressed as the mean ± SEM (n=5 for all samples, except APA and AP where n=4). White bars are controls. Dark blue bars are high G peptide-coupled microbeads with TAM as a control capsule, light blue bars are high M peptide-coupled microbeads with UP-MVM as control capsule. Red bars are HA-containing microbeads with Ca-bead as control capsule, and green bars are polycation-containing capsules, with Ca-bead constituting their control capsule. The zymosan value is 154 * ± 8 AU/ml. Significant values are given as $P < 0.05$ *compared to saline control #compared to the respective control capsules.

3.2.2 Chemokines

The same set of capsules was also screened by use of a multiplex assay for 12 different cytokines, including chemokines, pro- and anti-inflammatory cytokines, growth factors and others. Chemokines are chemotactic cytokines, known to induce directed chemotaxis. The cytokine responses for the classical chemokines IL-8, MCP-1 and MIP-1α are shown in figures 3.10a-c. Responses were generally low for the various alginate microbeads, whereas the polycation-containing microcapsules induced some elevation.

The IL-8 secretion is shown in figure 3.10a. TAM and the functionalized alginate microbeads generally gave lower amounts of cytokine than saline control, with significant differences compared to saline – except for M RGD. The HA-mineralized capsules, including its control microbeads, induced responses slightly higher than saline control. The APA and AP microcapsules induced significantly higher amounts of IL-8 as compared to saline control, as well as the Ca-beads.

The MCP-1 levels induced by the various capsule types are shown in figure 3.10b. Responses were generally low for TAM and the functionalized alginate microbeads, with M REDV and M RGD inducing a very slight elevation. In terms of the HA-mineralized capsules and their control microbead, Enz-CaP and Ca-bead induced a slight increase of MCP-1, whereas CaP evoked a rather high response – approximately 2-3 times higher than saline, and above the polycation-containing capsules. The polycation-microcapsules induced MCP-1, with the most apparent elevation induced by AP, which was significant compared to the control Ca-bead.

The MIP-1α response is shown in figure 3.10c. TAM and the functionalized alginate microbeads generally gave low amounts, with values below (TAM, G RGD, UP-MVM) or slightly above (M RGD, M REDV) saline control. The HA-mineralized capsules and its control microbeads induced responses slightly higher than saline control, with Ca-bead being significantly higher than saline control and Enz-CaP being significantly lower than Ca-bead. The polycation-microcapsules induced elevated MIP-1α, which was most apparent for AP and PMCG microcapsules. AP was significantly higher than saline control, and PMCG was significantly elevated compared to saline control and the control Ca-bead.

Due to the LPS-contamination detected in the G VAPG alginate, these microbeads are not included in the charts in the following sections. Rather, the respective values for the G VAPG responses are included in the figure descriptions along with the positive zymosan control. The LPS-contaminated G VAPG induced a very high and significant MIP-1α response. This was not surprising, as MIP-1α is known to be produced by macrophages after stimulation with bacterial endotoxins. Furthermore, G VAPG was found to induce significantly elevated levels of IL-8 and MCP-1, which might also be due to the demonstrated LPS-contamination.

In general, the grafting of peptides to the alginates did not appear to affect cytokine induction, whereas for the HA-microbeads it appeared that alginates mineralized through counter-diffusion precipitation were slightly more stimulatory. The introduction of polycations into the alginate system generally induced elevated cytokine levels.

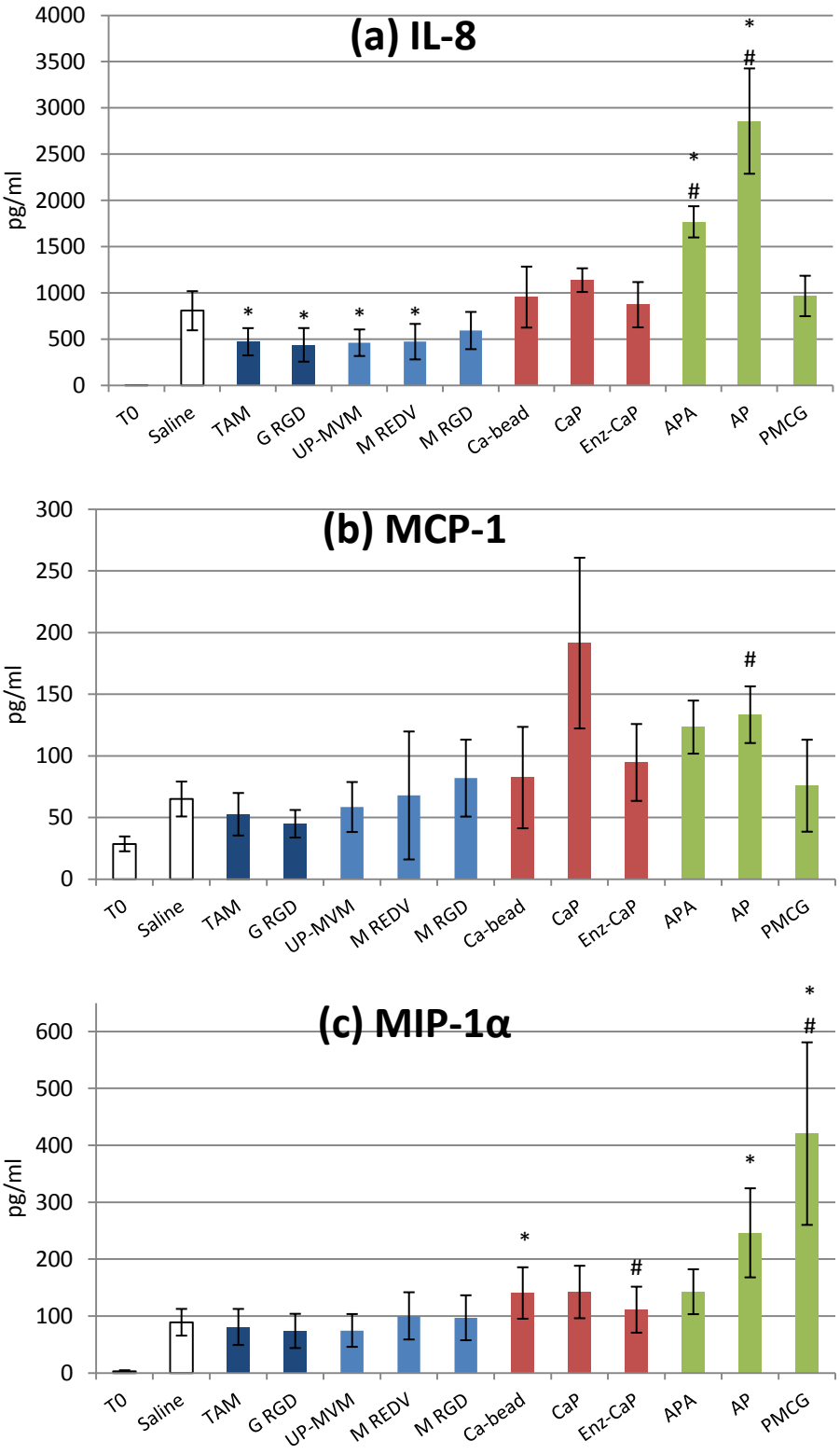

Figure 3.10a-c. Responses for the chemokines IL-8, MCP-1 and MIP-1α after incubation of alginate capsules and controls for 4 hours in fresh human whole blood. Data are expressed as the mean ± SEM (n=5). White bars are controls. Dark blue bars are high G peptide-coupled microbeads with TAM as a control capsule, light blue bars are high M peptide-coupled microbeads with UP-MVM as control capsule. Red bars are HA-containing microbeads with Ca-bead as control capsule, and green bars are polycation-containing capsules, with Ca-bead constituting their control capsule. The G VAPG and zymosan values are, respectively: 3934*# ± 907 pg/ml and 4770* ± 1309 pg/ml for IL-8; 233* ± 59 pg/ml and 360* ± 83 pg/ml for MCP-1; 2092*# ± 618 pg/ml and 984* ± 461 pg/ml for MIP-1α. Significant values are given as $P < 0.05$ *compared to saline control #compared to the respective control capsules.

3.2.3 Inflammatory cytokines

Inflammatory, or pro-inflammatory, cytokines, is a general description which includes cytokines that promote inflammation. Mediators typically regarded as pro-inflammatory cytokines are IL-1β, IL-6 and TNF-α. Figures 3.11a-c show the detected levels of these cytokines after incubation of different microcapsules in whole blood. In general, all microbeads showed low cytokine responses whereas the polycation-containing microcapsules – in particular PMCG – induced elevation.

The IL-1β secretion is shown in figure 3.11a. TAM and the functionalized alginate microbeads generally induced amounts similar to or below saline control, with M REDV and G RGD being significantly lower than saline. Of the HA-containing microbeads, Enz-CaP induced IL-1β, and also the control Ca-bead induced a slight response. All polycation-capsules gave significantly elevated IL-1β levels compared to Ca-bead and saline control, with the strongest response induced by PMCG microcapsules.

The IL-6 levels induced by the various capsule types are shown in figure 3.11b. TAM and the functionalized alginate microbeads generally gave low amounts of cytokine, with G RGD, UP-MVM and M REDV inducing significantly lower amounts of IL-6 compared to saline control. The HA-containing microbeads did not induce IL-6 secretion, while their control Ca-bead induced a very slight elevation. Also here, all polycation-capsules induced significantly elevated levels compared to Ca-bead and saline control, with PMCG inducing the most potent response – approximately 25 times higher than saline.

The TNF-α response is shown in figure 3.11c. Of the peptide-coupled alginate microbeads and their controls, two of the microbeads – TAM and M RGD – did not induce TNF-α secretion, while three microbeads did – G RGD, UP-MVM and M REDV. However, the data for these results are less reliable due to biological differences between individual blood donors, as illustrated by the large standard deviances seen in figure 3.11c. Of the HA-containing capsules, Enz-CaP induced TNF-α, and also the control Ca-bead induced cytokine secretion. CaP was slightly below saline control. The polycation-microcapsules – APA, AP and PMCG – all stimulated TNF-α secretion. PMCG induced the strongest response, which was 17 times higher than saline, and significant compared to saline control and Ca-bead.

As seen from the figure 3.11a-c description, the LPS-contaminated G VAPG microbeads induced very high responses for all pro-inflammatory cytokines, which were significant compared to TAM and saline control.

Overall, the peptide-coupled microbeads were generally seen to have minimal stimulatory properties in terms of pro-inflammatory cytokine induction. The introduction of HA did not appear to have significant effects on pro-inflammatory cytokine production; however, HA-mineralization through enzymatic mineralization appeared to be the most stimulatory of the two mineralization methods. Moreover, the introduction of polycations was seen to significantly influence the stimulatory potential of the alginate microcapsules.

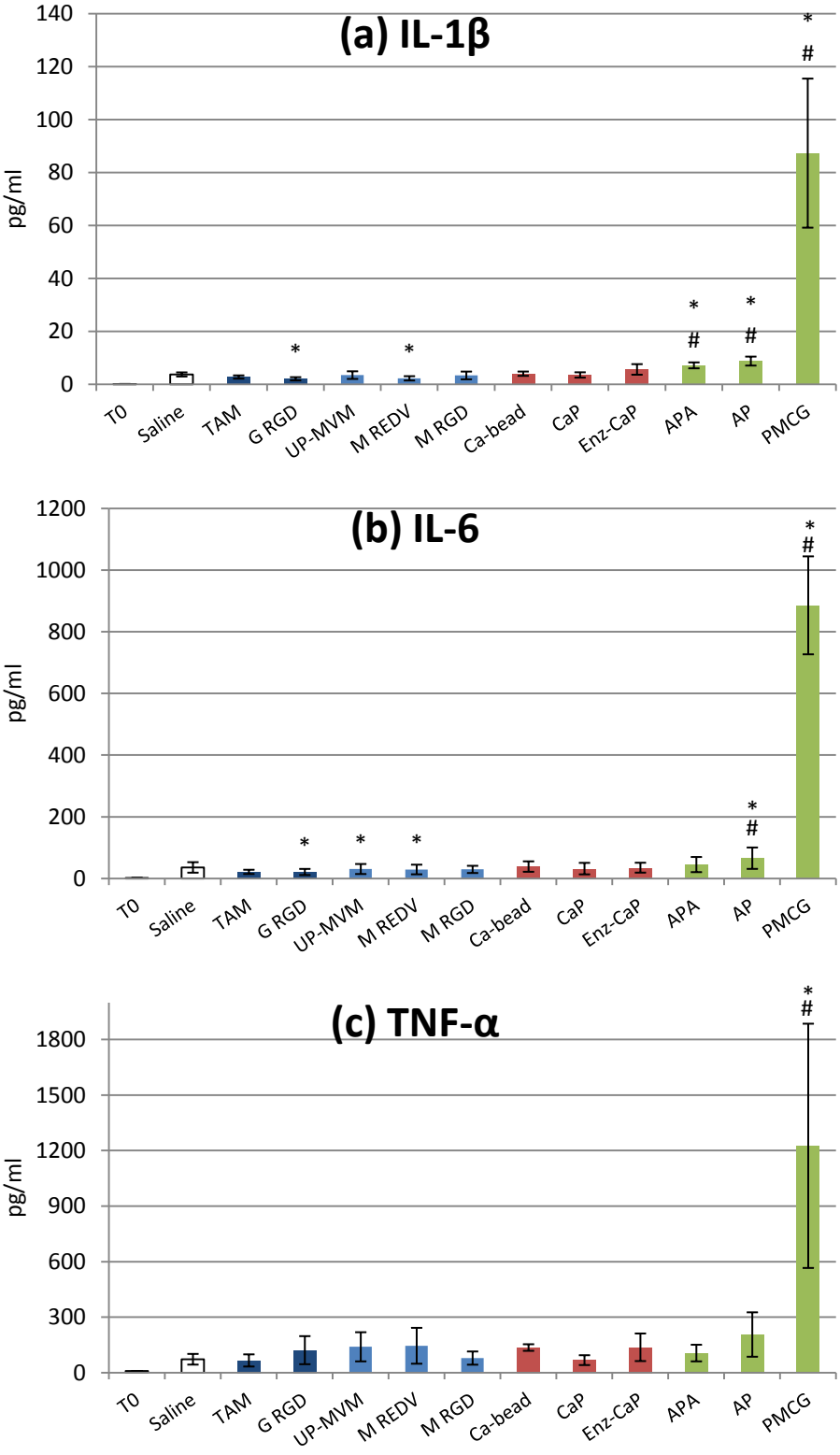

Figure 3.11a-c. Responses for the pro-inflammatory cytokines IL-1β, IL-6 and TNF-α after incubation of alginate capsules and controls for 4 hours in fresh human whole blood. Data are expressed as the mean ± SEM (n=5). White bars are controls. Dark blue bars are high G peptide-coupled microbeads with TAM as a control capsule, light blue bars are high M peptide-coupled microbeads with UP-MVM as control capsule. Red bars are HA-containing microbeads with Ca-bead as control capsule, and green bars are polycation-containing capsules, with Ca-bead constituting their control capsule. The G VAPG and zymosan values are, respectively: 1434*# ± 643 pg/ml and 74* ± 36 pg/ml.for IL-1β; 10716*# ± 1302 pg/ml and 1214* ± 671 pg/ml for IL-6; 11373*# ± 2973 pg/ml and 597* ± 274 pg/ml for TNF-α. Significant values are given as $P < 0.05$ *compared to saline control #compared to the respective control capsules.

3.2.4 Anti-inflammatory cytokines:

Anti-inflammatory cytokines regulate the pro-inflammatory cytokine response, and the delicate balance between pro- and anti-inflammatory cytokines influence the net effect of the inflammatory response. IL-10 and IL-1 receptor antagonist (IL-1ra) are well recognized as anti-inflammatory mediators. Cytokine levels for IL-10 and IL-1ra after incubation with alginate microcapsules are shown in figure 3.12a-b. Responses were generally slightly above saline control, with PMCG inducing the strongest cytokine release.

Figure 3.12a shows the IL-10 values after incubation with various capsules. In general, the IL-10 values were low with a slight elevation above saline control. Only M REDV and AP capsules induced significant elevation compared to saline control, and no capsule types were significantly different from their respective control capsules.

The response for IL-1ra secretion is shown in figure 3.12b. Generally, the responses were low with values comparable to the saline control. Moreover, for the specialized capsules (HA-mineralized and peptide-coupled microbeads) there were no markable differences in cytokine response compared to their respective control capsules. The PMCG microcapsule was the only capsule type that gave significant elevation of IL-1ra.

Furthermore, G VAPG induced a high response for IL-10, as well as a significantly elevated IL-1ra response compared to TAM and saline control (see figure 3.12a-b description). This could be due to the presence of endotoxin in these microbeads.

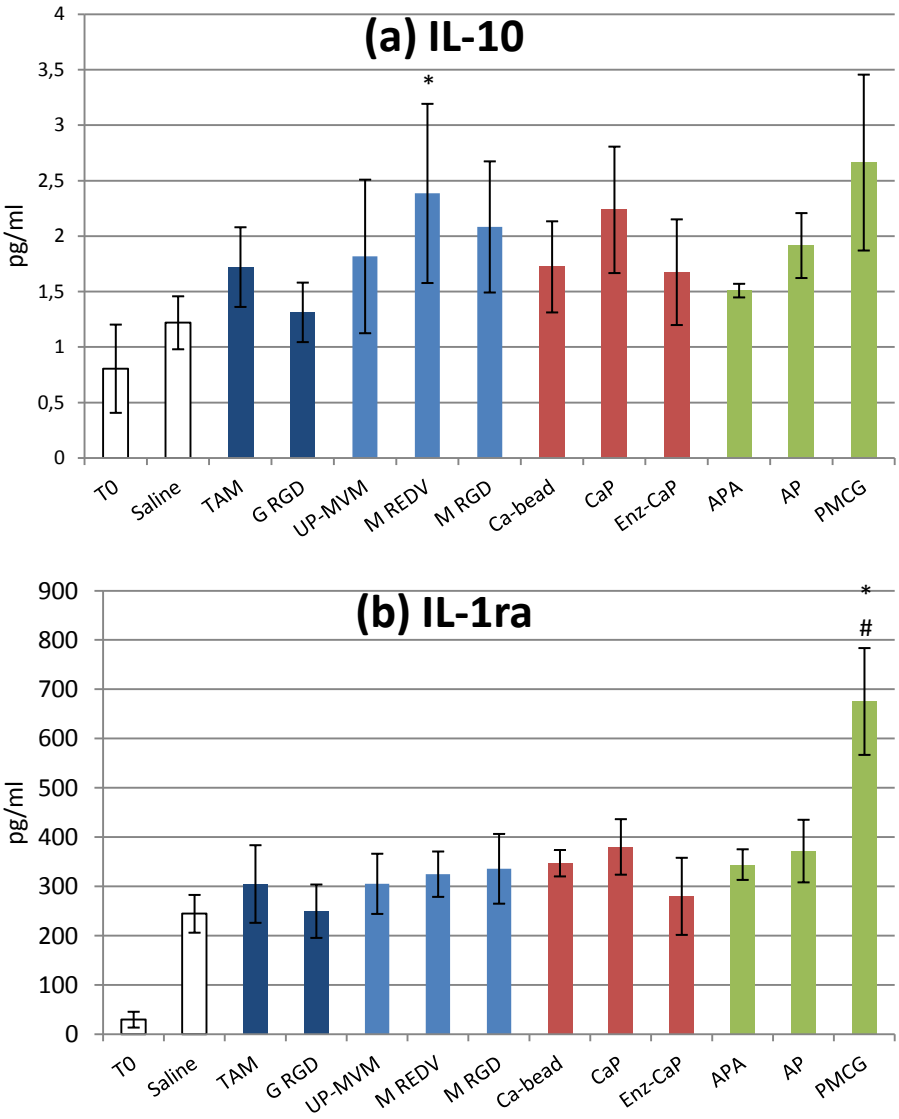

Figure 3.12a-b. Responses for the anti-inflammatory cytokines IL-10 and IL-1ra after incubation of alginate capsules and controls for 4 hours in fresh human whole blood. Data are expressed as the mean ± SEM (n=5). White bars are controls. Dark blue bars are high G peptide-coupled microbeads with TAM as a control capsule, light blue bars are high M peptide-coupled microbeads with UP-MVM as control capsule. Red bars are HA-containing microbeads with Ca-bead as control capsule, and green bars are polycation-containing capsules, with Ca-bead constituting their control capsule. The G VAPG and zymosan values are, respectively: 4,9 ± 0,6 pg/ml and 2,5* ± 0,4 pg/ml for IL-10; 1464*# ± 349 pg/ml and 350* ± 25 pg/ml for IL-1ra. Significant values are given as $P < 0.05$ *compared to saline control #compared to the respective control capsules.

3.2.5 Growth factors

Growth factors regulate cell growth and division, and may be involved in stimulating processes such as angiogenesis. Two growth factors were assessed in this study: the platelet-derived growth factor composed of two B-glycoprotein chains (PDGF-BB) and vascular endothelial growth factor (VEGF). The results from the analysis are shown in figure 3.13a-b. Overall, any obvious trends were difficult to identify for the growth factor induction. However, the peptide-coupled microbeads were generally seen to induce low responses, while the HA-mineralized microbeads induced slight cytokine secretion. The polycation-containing microcapsules appeared to be the most stimulatory.

Figure 3.13a shows the PDGF-BB secretion after incubation with different capsules. In general, the PDGF-BB response was only slightly above the saline control. Clear-cut trends were difficult to identify due to substantial variance between the individual donors, as illustrated by the large standard deviations. The capsules that induced the strongest responses were TAM, APA and AP, although non-significant compared to the saline control. The only significant difference was found between TAM and G RGD, with the latter inducing significant lower levels of PDGF-BB as compared to TAM.

Figure 3.13b shows the VEGF amounts induced by the various capsules. The peptide-coupled microbeads as well as their control microbeads showed lower amounts of cytokine compared to saline control. M REDV was found to induce significantly lower levels as compared to saline. A slightly higher amount, although non-significant from saline control, was detected for the mineralized microbeads and its control Ca-bead. Enz-CaP was significantly lower than Ca-bead. Furthermore, compared to saline control and the Ca-bead, the polycation-containing microcapsules showed elevated amounts of VEGF. Significant differences were seen for AP and PMCG microcapsules.

The endotoxin-contaminated G VAPG was not found to induce significantly elevated levels of the two growth factors. In fact, both G VAPG-induced responses were on the level with TAM (see figure 3.13a-b description).

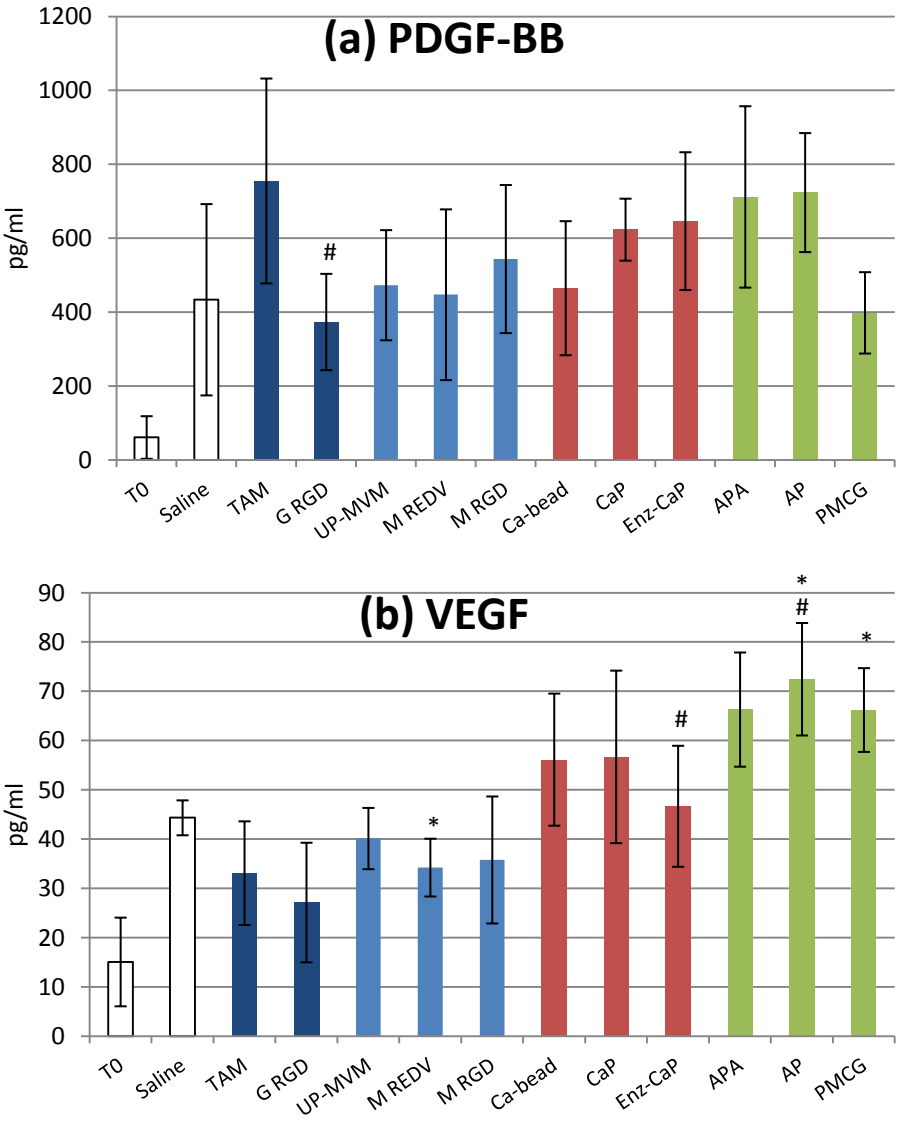

Figure 3.13a-b. Responses for growth factors PDGF-BB and VEGF after incubation of alginate capsules and controls for 4 hours in fresh human whole blood. Data are expressed as the mean ± SEM (n=5). White bars are controls. Dark blue bars are high G peptide-coupled microbeads with TAM as a control capsule, light blue bars are high M peptide-coupled microbeads with UP-MVM as control capsule. Red bars are HA-containing microbeads with Ca-bead as control capsule, and green bars are polycation-containing capsules, with Ca-bead constituting their control capsule. The G VAPG and zymosan values are, respectively: 710 ± 247 pg/ml and 681 ± 365 pg/ml for PDGF-BB; 29 ± 9 pg/ml and 57 ± 23 pg/ml. for VEGF. Significant values are given as $P < 0.05$ *compared to saline control #compared to the respective control capsules.

3.2.6 Other cytokines

Cytokine responses for RANTES and IFN-γ are shown in figure 3.14a-b. The results generally showed large standard deviances and variation between the donors. None of the capsules were found to induce significant cytokine responses compared to their respective control beads. This makes it harder to clearly identify potential effects of functionalizing the alginates in question.

Figure 3.14a shows the RANTES secretion after incubation with different capsules. It generally appears that the presence of microcapsules and microbeads in the samples induced cytokine elevation as compared with saline control. Responses for the peptide-coupled microbeads and their controls were generally low and close to saline control, with M RGD inducing a slightly higher cytokine amount. The HA-mineralized microbeads induced a slight but non-significant response compared to their control Ca-bead. The only response that was significantly higher than saline control was induced by AP.

In addition, the baseline value T0 was found to be relatively high for RANTES compared to other cytokines, with an average value well above 500 pg/ml. A potential reason for this may be due to the release of RANTES-containing α-granules from platelets, activated upon the exposure to low temperature (see section 2.2.1).

The IFN-γ responses are shown in figure 3.14b, and were generally low. The peptide-coupled microbeads and their control capsules were found to be similar to or below saline control, with the exception of M REDV which induced a response significantly higher than saline. The HA-mineralized microbeads induced a slight but non-significant cytokine response compared to their control Ca-bead. Furthermore, the polycation-containing microcapsules were seen to induce cytokine levels lower than the saline control.

The G VAPG microbeads (as indicted in the description of figure 3.14a-b) induced significantly elevated cytokine levels compared to saline control. This may be due to the detected LPS contamination of this alginate.

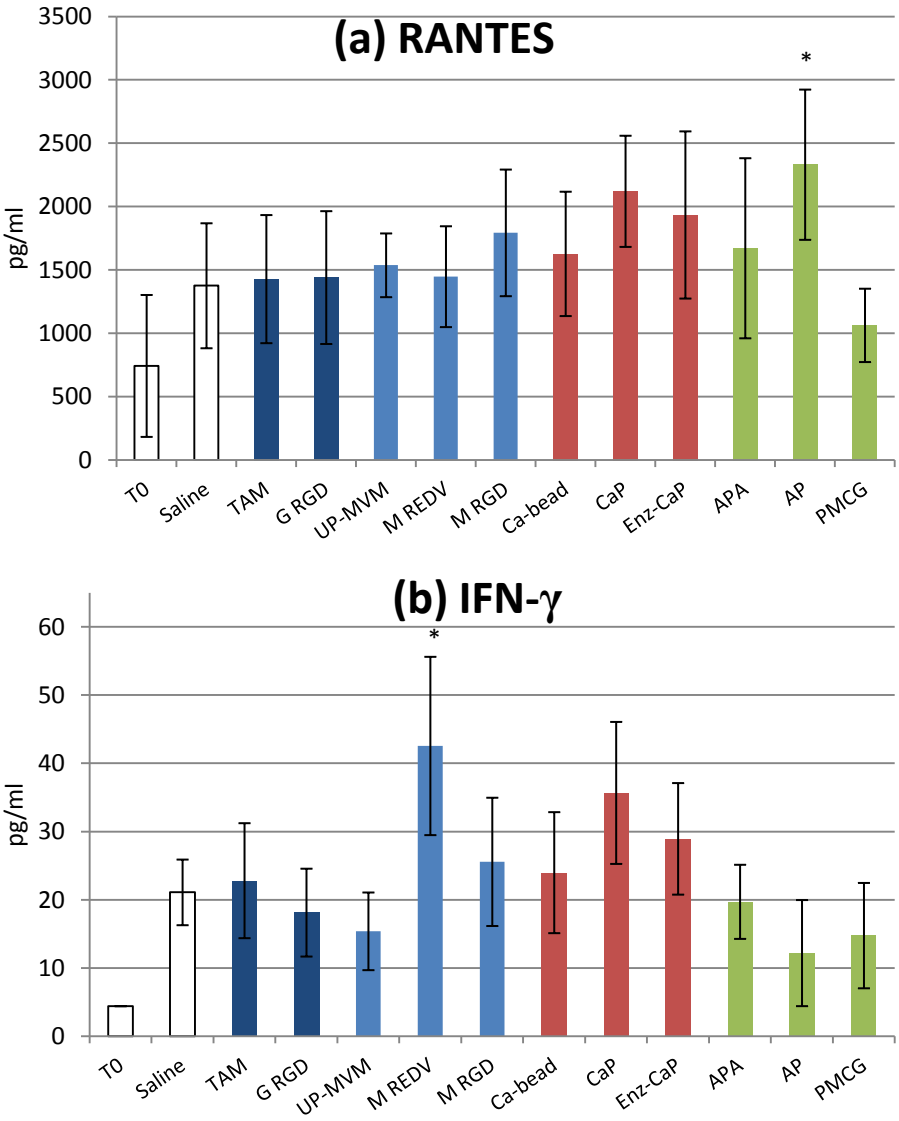

Figure 3.14a-b. Responses for the cytokines RANTES and IFN-γ after incubation of alginate capsules and controls for 4 hours in fresh human whole blood. Data are expressed as the mean ± SEM (n=5). White bars are controls. Dark blue bars are high G peptide-coupled microbeads with TAM as a control capsule, light blue bars are high M peptide-coupled microbeads with UP-MVM as control capsule. Red bars are HA-containing microbeads with Ca-bead as control capsule, and green bars are polycation-containing capsules, with Ca-bead constituting their control capsule. The G VAPG and zymosan values are, respectively: 3076* ± 936 pg/ml and 2480 ± 1019 pg/ml for RANTES; 55* ± 7 pg/ml and 28 ± 12 pg/ml for IFN-γ. Significant values are given as $P < 0.05$ *compared to saline control #compared to the respective control capsules.

3.3 Mechanism studies of capsule-induced inflammatory events

Further studies were conducted on polycation-containing microcapsules in order to elucidate the mechanisms leading to inflammatory events, as well as to unmask potential differences in activation between different types of microcapsules. The following studies employ cell adhesion and protein adsorption assays, as well as leukocyte and complement inhibitors, in order to obtain a better understanding of the mechanisms leading to complement activation and cytokine production. Furthermore, additional studies were performed to explore leukocyte receptor expression and capsule-cell-interactions at the microcapsule surface. These results were variable, and are included in the appendix (section A.3).

3.3.1 C3 and TCC deposition – Hollow versus solid capsules

In order to explore potential differences in complement activation between capsules with a liquefied core as opposed to those with a solid core, capsules were stained for C3 and TCC adsorption. The results for these studies are shown in figures 3.15-16. The capsules studied in the following experiments are PLO Hollow (high M hollow core, 0.14% PLO, high M outer coat), PLL Hollow (high M hollow core, 0.14% PLL, high M outer coat) and PLL Solid (high M solid core, 0.14% PLL, high M outer coat). PLL Hollow may be directly compared to PLL Solid. PLL Hollow may further be compared with PLO Hollow, in which the employed polycation is poly-$_L$-ornithine (PLO) instead of poly-$_L$-lysine (PLL). It should however be mentioned that the stoichiometry is not entirely correct between the PLO and PLL employed in the hollow microcapsules. The amount of polycation in the PLO Hollow microcapsules (0.14%) actually corresponds to 0.10% PLL mole-wise, instead of the 0.14% PLL that is employed in PLL Hollow, due to the presence of bromide as counterions for PLO instead of chloride ions as for PLL. Furthermore, APA microcapsules (high G solid core, 0.1% PLL, high M outer coat) were also included to observe any potential effects of high G vs. high M content, and for the TCC deposition study TAM microbeads were included as a negative control. A cell adhesion study was also performed on hollow versus solid microcapsules (see section A.2 in the appendix). Hollow microcapsules were generally seen to have lesser amounts of attached leukocytes compared to solid capsules, which induced a fair degree of cell adhesion. However, some of the hollow microcapsules burst and appeared to contain large amounts of cells inside. In general, it did appear that the hollow microcapsules were more susceptible to osmotic swelling as compared to solid microcapsules.

Figure 3.15 shows the C3 deposition on the various capsules. C3 deposition generally appeared to increase from 6 hours to 24 hours. The C3 deposition was clearly higher on solid microcapsules compared to hollow ones. Furthermore, a slower C3 deposition was seen on the PLO Hollow microcapsules compared to PLL Hollow. In terms of the high G-containing APA microcapsules, the C3 deposition after 6 hours appeared more unevenly distributed compared to the high M microcapsules. After 24 hours, both solid microcapsules were completely covered by C3. The staining was specific for C3 as demonstrated by the negative controls.

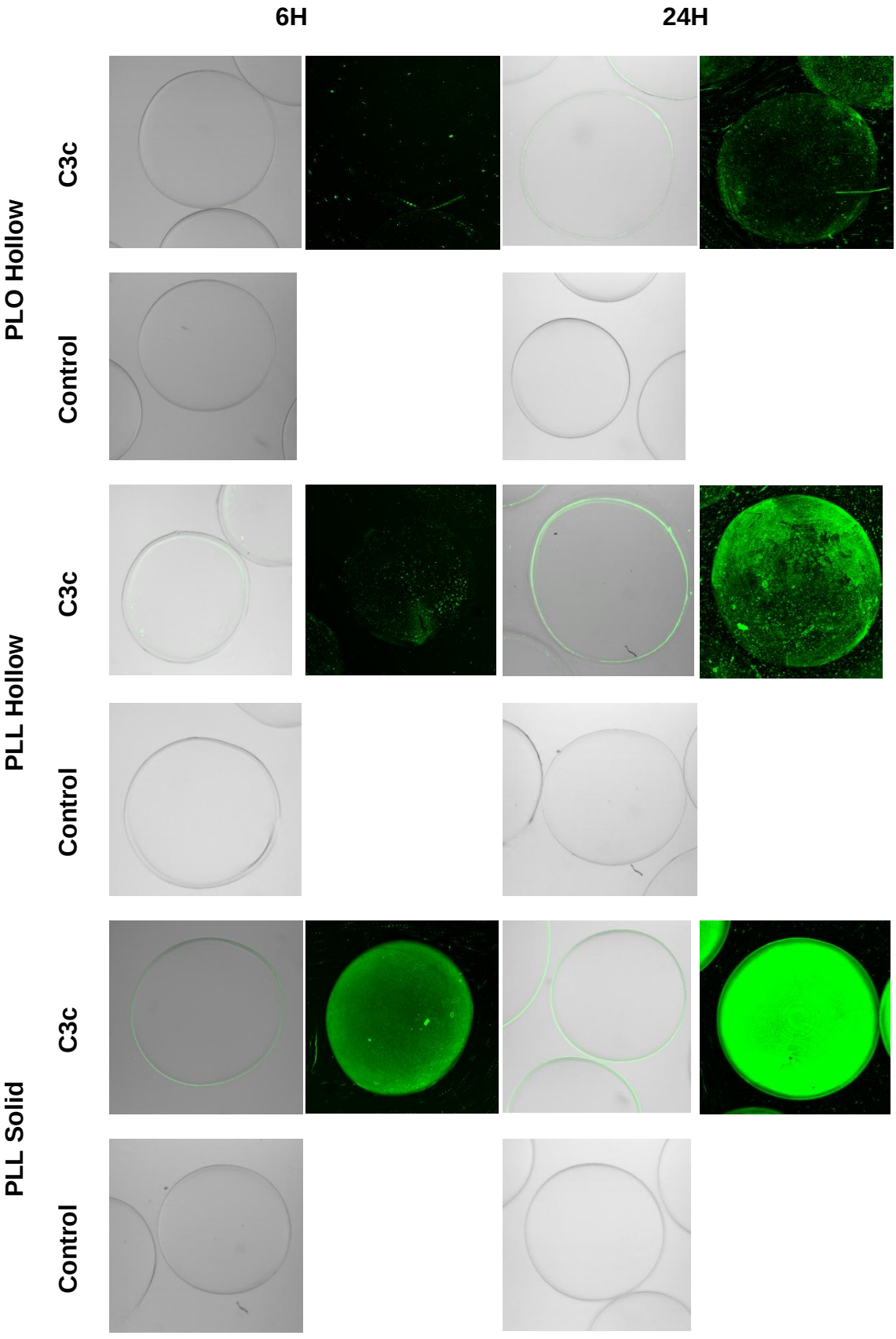
6H
24H
PLO Hollow
PLL Hollow
PLL Solid
C3c
Control
C3c
Control
C3c
Control

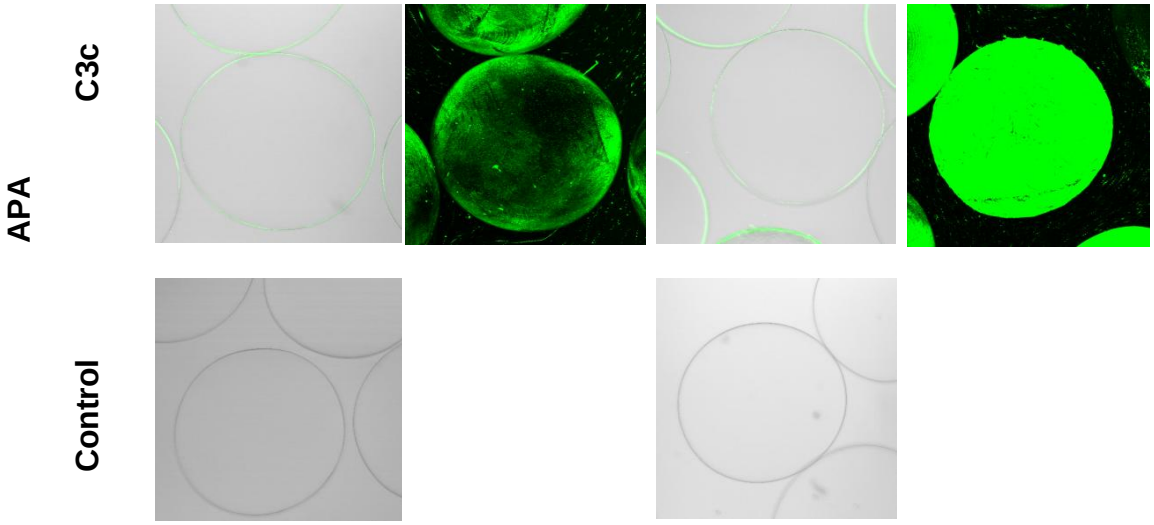

Figure 3.15. C3 deposition on hollow versus solid capsules. Capsules are incubated 6h and 24h in lepirudin plasma and stained for αC3c and negative control antibodies. Capsules are displayed as optical sections through the equator and as 3D projections.

Figure 3.16 shows the TCC deposition on the various capsules. TCC deposition appeared to be only slightly higher on solid microcapsules compared to hollow microcapsules. PLL Hollow appeared to induce more TCC deposition on its surface than PLO Hollow. APA microcapsules with a high G content seemed to induce slightly more TCC deposition than did those with a high M content. It also appeared that the high M-containing microcapsules had swelled up a bit, as compared with the high G-containing APA and TAM. TAM did not show any TCC deposition. It could appear as if there was some variation within some of the individual samples in terms of protein adsorption, perhaps especially for PLO Hollow. When comparing some of the 3D pictures in figure 3.16 to their respective equatorial sections with transmitted light, it appeared that some capsules were subjected to a lot of TCC deposition, whereas others within the same sample showed little or no protein adsorption at all. The staining was specific for TCC as demonstrated by the negative controls

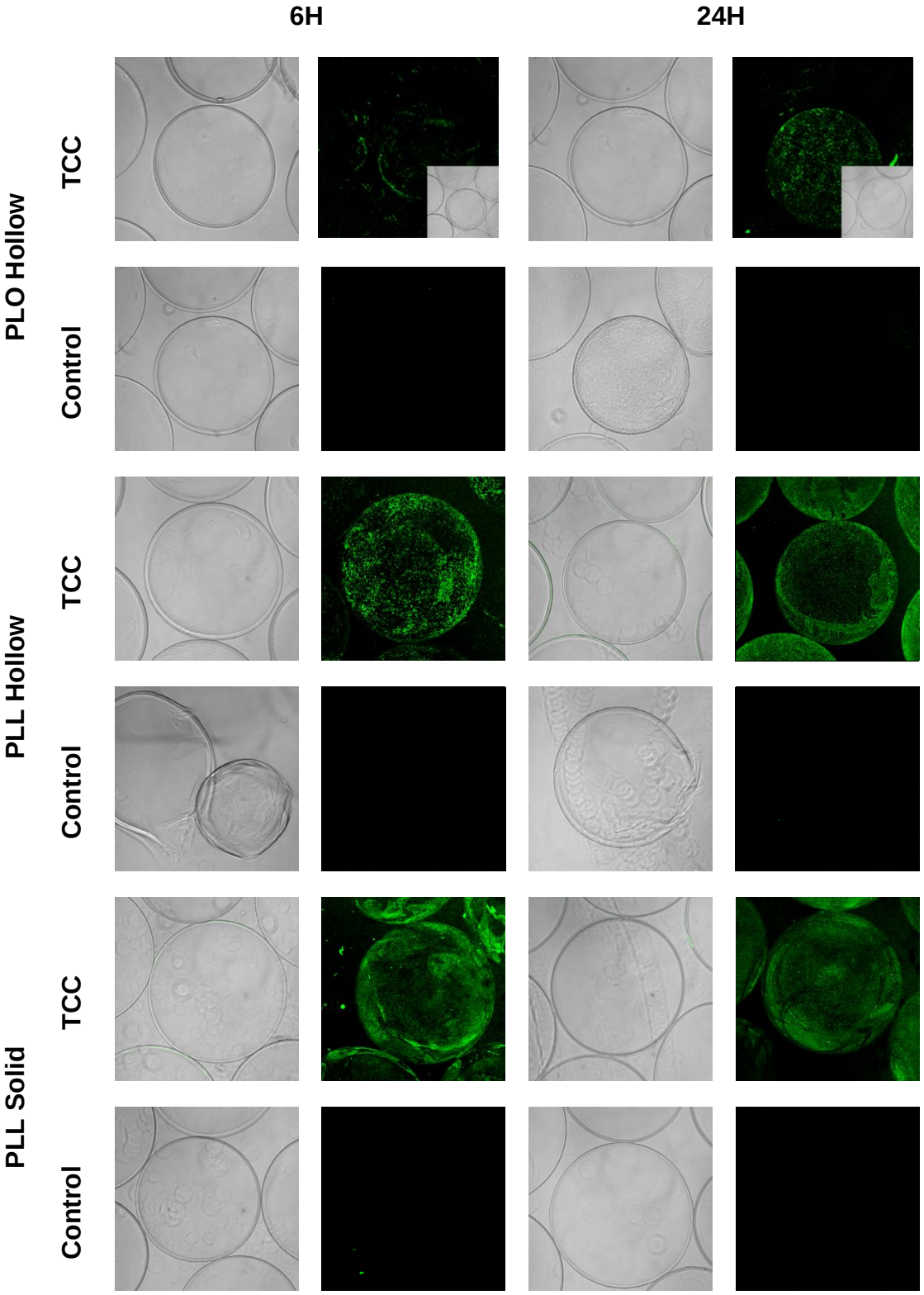
6H
24H
PLO Hollow
PLL Hollow
PLL Solid
TCC
Control
TCC
Control
TCC
Control

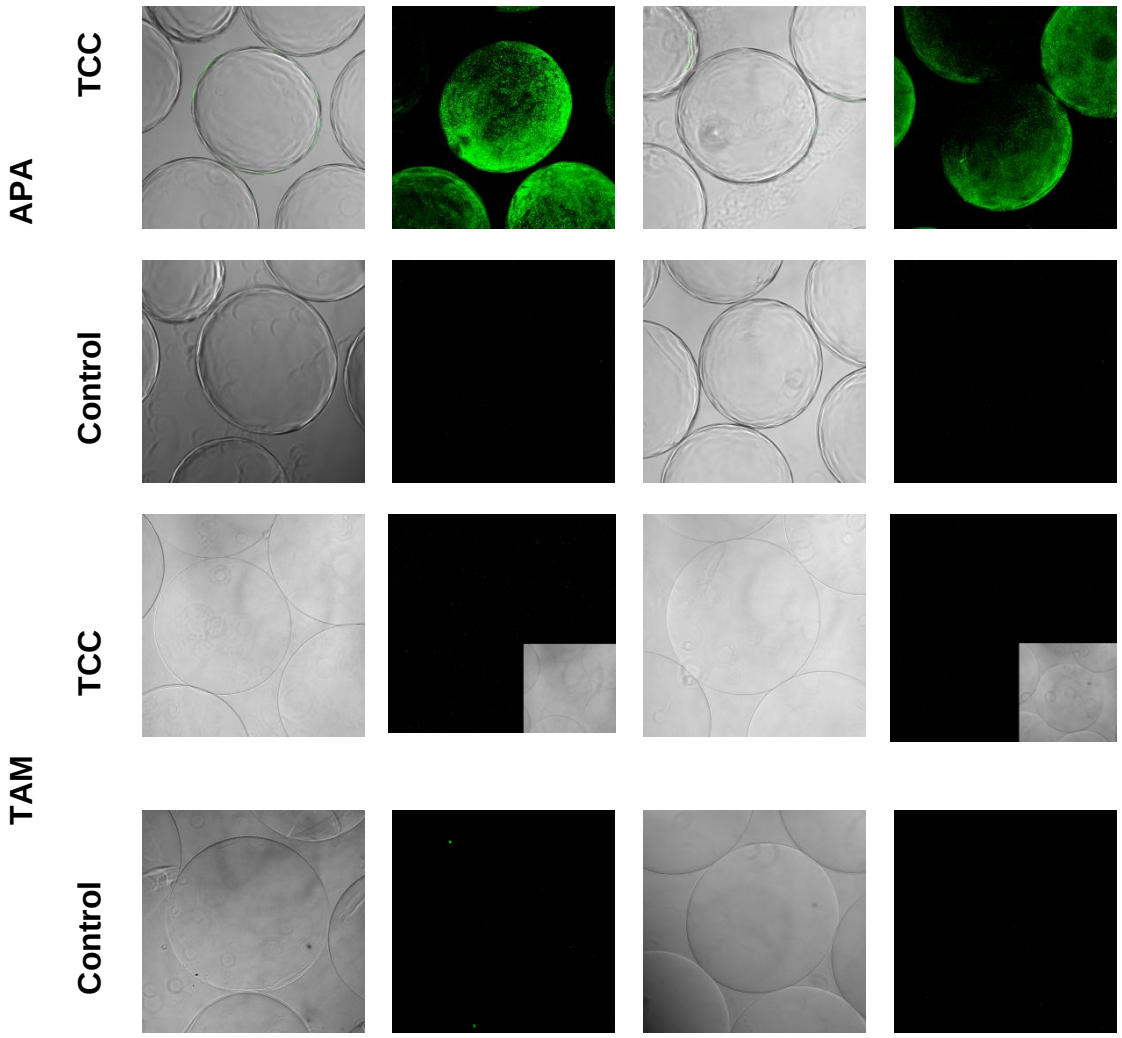

Figure 3.16. TCC deposition on hollow versus solid capsules. Capsules are incubated 6h and 24h in lepirudin plasma and stained for αTCC and negative control antibodies. Capsules are displayed as optical sections through the equator and as 3D projections.

3.3.2 Complement inhibition and cytokine induction - Hollow versus solid capsules

The results from the previous section imply that the hollow microcapsules induce lower levels of C3 and TCC deposition on their surface compared to solid microcapsules. In contrast, it has been shown that hollow microcapsules induce significantly higher levels of sTCC, with the IL-8 levels not correspondingly elevated [106]. It could therefore be questioned whether or not the elevated TCC-level seen for the hollow microcapsules was caused by complement activation. To explore this, inhibition studies with the C3-specific complement inhibitor compstatin were performed.

Figure 3.17a shows the sTCC amounts produced by spontaneous activation (no additive) by PLL Hollow, PLO Hollow and PLL Solid, and the following addition of the C3-inhibitory peptide compstatin or its control peptide. The samples with no additive produced sTCC amounts that were considerably higher for PLL Hollow than the other capsule types. The addition of compstatin substantially inhibited the complement activation. The presence of the control peptide did not appear to affect sTCC formation. Two distinct values (listed in table C3 in the appendix) for the PLL Solid samples for one particular blood donor have been removed in the presentation of the sTCC results. The respective values were substantially higher than those of the two other donors, and did not correspond to neither expectations nor general trends observed in previous studies [106] and for the other donors.

Figure 3.17b shows the IL-8 patterns from the inhibition experiments using compstatin. The spontaneous activation of IL-8 was more prominent for the solid PLL microcapsules as compared to the hollow microcapsules containing either PLL or PLO. The same trends were also seen upon addition of control peptide, with a slight elevation of the values. By adding compstatin, the IL-8 secretion was reduced. This was most prominent for the solid microcapsules. Regardless, the IL-8 responses showed substantial variation between the individual blood donors, making it harder to identify clear-cut trends in the data.

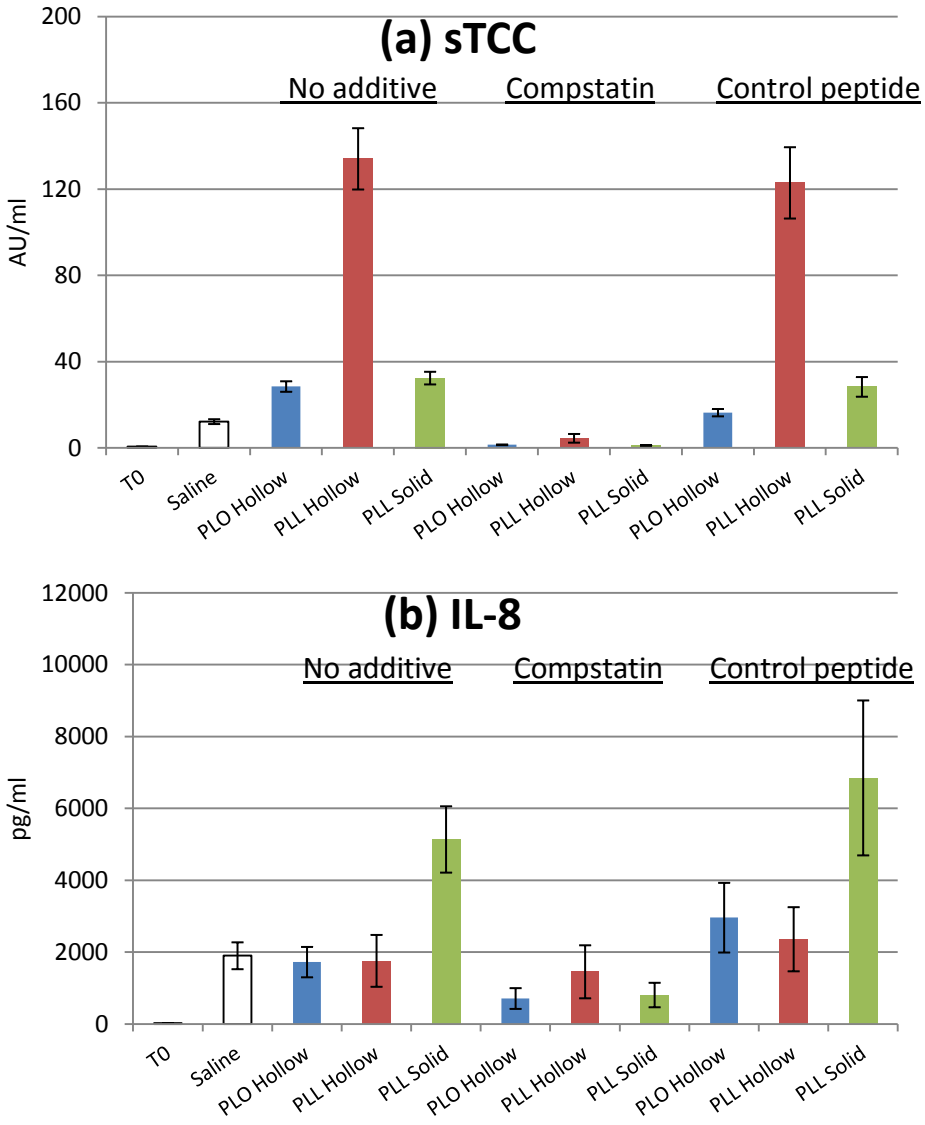

Figure 3.17a-b. sTCC and IL-8 levels after incubation of alginate capsules and controls for 4 hours in fresh human whole blood with compstatin, control peptide or no additive. Data are expressed as the mean ± SEM (n=3, except for PLL Solid with no additive and control peptide for sTCC, where n=2). White bars are controls. Blue bars are PLO Hollow, red bars are PLL Hollow, green bars are PLL Solid capsules. The zymosan values for sTCC and IL-8, respectively, are 132 ± 29 AU/ml and 8183 ± 894 pg/ml.

3.3.3 Complement inhibition - C3 deposition and cell adhesion on solid capsules

AP microcapsules were incubated in whole blood with the complement inhibitors Soliris® or compstatin, and stained for C3-deposition. This was done in order to explore the effects these inhibitors on complement activation, as well as the effects of complement activation on leukocyte adhesion. Figure 3.18 shows the C3 deposition on the microcapsules. The control for the compstatin samples was a control peptide. As no appropriate control protein for Soliris® was available, PBS (Ca^{2+}/Mg^{2+}) represents the control for these samples. Furthermore, the samples with no additive constitutes a positive control for both the compstatin and the Soliris® samples. The staining was specific for C3c, as demonstrated by microcapsules stained with negative control antibody.

Figure 3.18 shows that the microcapsules with no complement inhibitors (control peptide, PBS and no additive) had significant levels of leukocyte adhesion as well as C3 deposition. No C3 deposition was found on capsules incubated in compstatin-blood. This indicates that compstatin was effective in inhibiting the activity of complement component C3. Furthermore, compstatin-capsules were completely free of attached leukocytes. The control peptide did not appear to affect C3 deposition and leukocyte adhesion. Microcapsules incubated with Soliris® showed C3 deposition and some cell adhesion, but in seemingly lesser amounts than microcapsules with no inhibitor added. The control with PBS appeared to induce similar amounts of C3 deposition and cell adhesion compared to Soliris® samples.

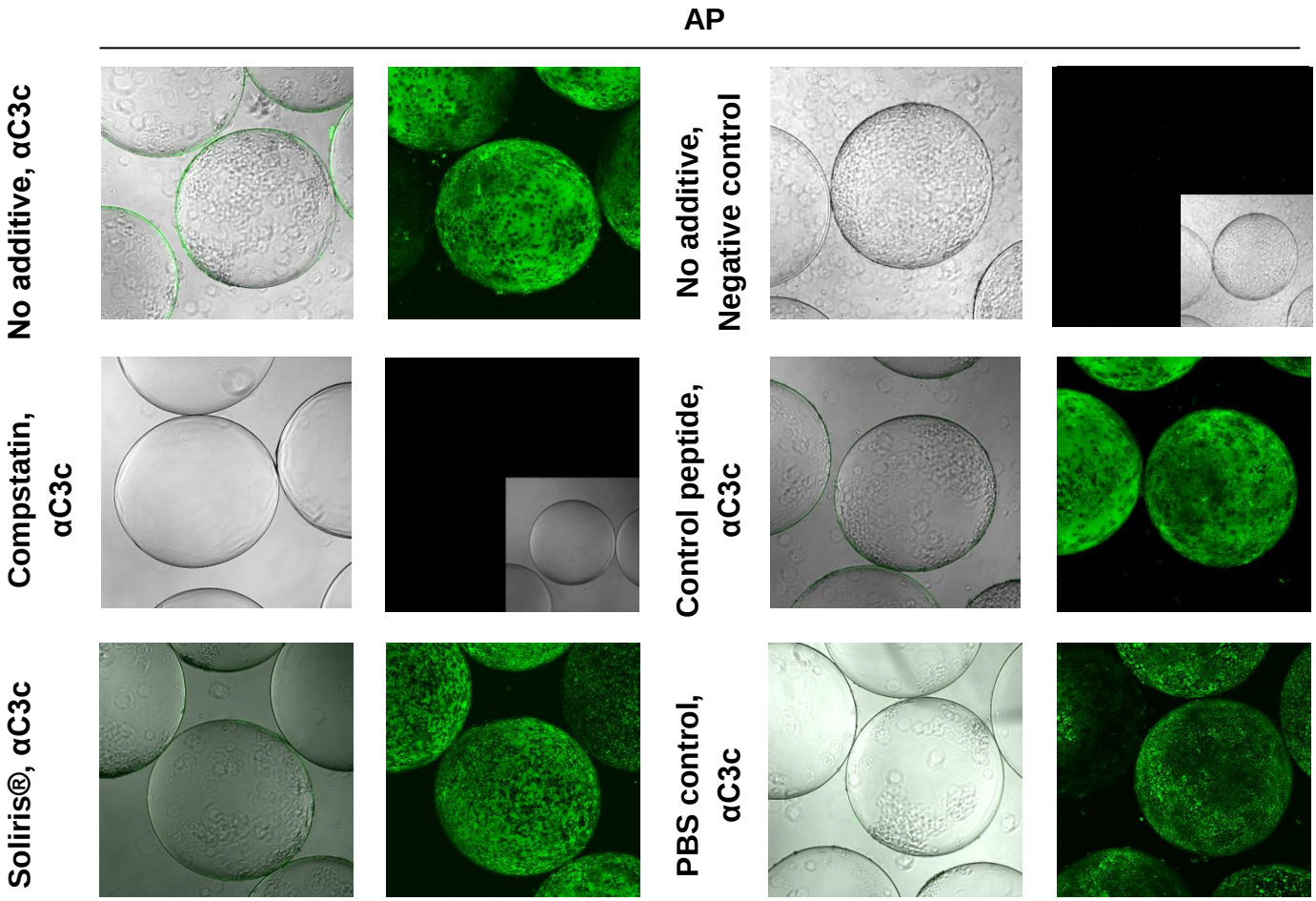

Figure 3.18. AP microcapsules incubated 4 hours in whole blood containing Soliris®, compstatin analogue CP20, control peptide, PBS w/$Ca^{2+}Mg^{2+}$, or no additive. Capsules are stained for αC3c and negative control Capsules are displayed as equatorial section through the capsules, and as 3D projections.

3.3.4 *Leukocyte inhibition studies - Cell adhesion and cytokines*

The previous results imply that TCC in solution is low for solid capsules, whereas cytokine responses in terms of IL-8 are high. It was therefore speculated that the mechanisms leading to the cytokine production induced from solid capsules take place predominantly on the capsule surfaces, and not in the solution. The aim of this study was therefore to explore mechanisms leading to cytokine secretion. We aimed to assess the importance of CD11b, or CD11b/CD18 (CR3), in terms of leukocyte adhesion and cytokine induction, as well as the role of phagocytosis and cell spreading in cytokine induction. To do this, APA microcapsules were added αCD11b antibody, cytochalasin D or control additives (ethanol or BSA). The αCD11b antibody has an inhibitory effect on the CD11b-subunit of complement receptor CD11b/CD18, while cytochalasin D inhibits phagocytosis.

Results for the cell adhesion study with CD11b-inhibitor are shown in figure 3.19. The anti-CD11b antibody clearly inhibited the adhesion of leukocytes. While only a few cells were seen on the capsules treated with CD11b-inhibitor, substantial amounts of leukocytes were found on APA microcapsules with no anti-CD11b present.

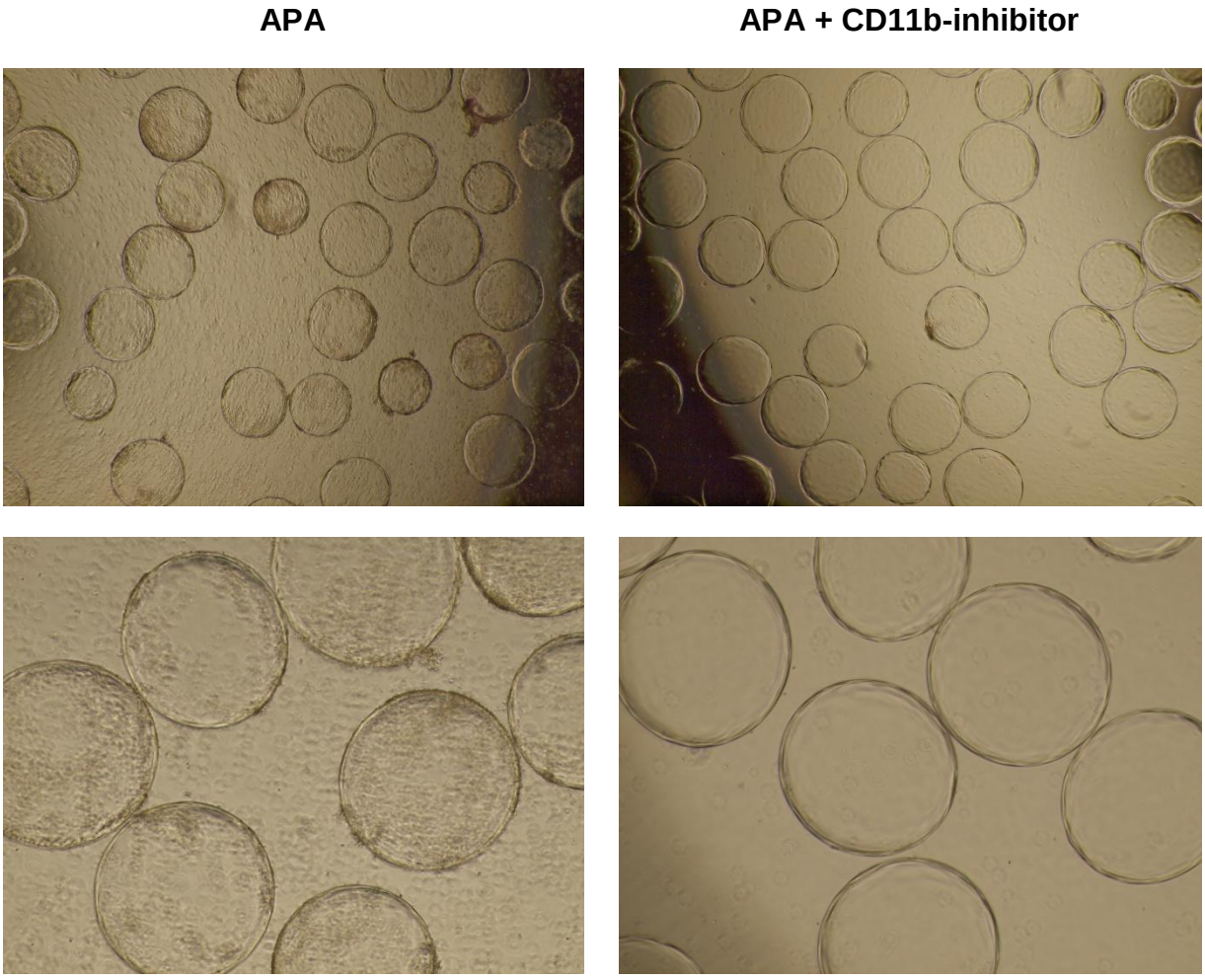

Figure 3.19. Cell adhesion on APA microcapsules with and without the addition of CD11b-inhibitor after incubation 4 hours in whole blood. Pictures were taken with 4x (top row) and 10x (bottom row) objective lens magnification.

Results for the IL-8 response for three individual donors are shown in figure 3.20. Generally, the cytokine values were highly variable between the donors, and probably reflects some of the pilot character of the present study. The CD11b-inhibition did not seem to steer the IL-8 secretion in one particular direction, as this response was found to vary between the donors. Since a proper control antibody was not available, it could not be deduced whether the αCD11b-antibody itself had some stimulatory effect. The IL-8 responses for donor A were significantly higher than those for donor B and C. This is likely due to the fact that the capsule/blood ratio was higher for donor A, since the same amount of microcapsules were incubated in a smaller amount of blood (125 µl) than for the two other donors in order to reduce the use of expensive materials (cytochalasin D and CD11b-inhibitory antibody). The addition of cytochalasin D appeared to reduce the IL-8 response as compared to its controls with no inhibitor added (figure 3.20); however, as cytochalasin D was solubilized in ethanol, a more correct control would contain ethanol. Furthermore, we could not exclude that that the cytochalasin itself could impact the toxicity of ethanol. Controls with ethanol or ethanol + BSA as a control protein were therefore included. The BSA and ethanol controls showed lower IL-8 induction than samples with no additive, implicating that the ethanol itself might have negatively affected the IL-8 secretion. A slight effect by the cytochalasin could be seen compared to some of the controls, however, the data was not consistent enough to draw any conclusions on the relationship of cytokine production with CD11b and phagocytosis. Reasons for this assumption are discussed in section 4.6.

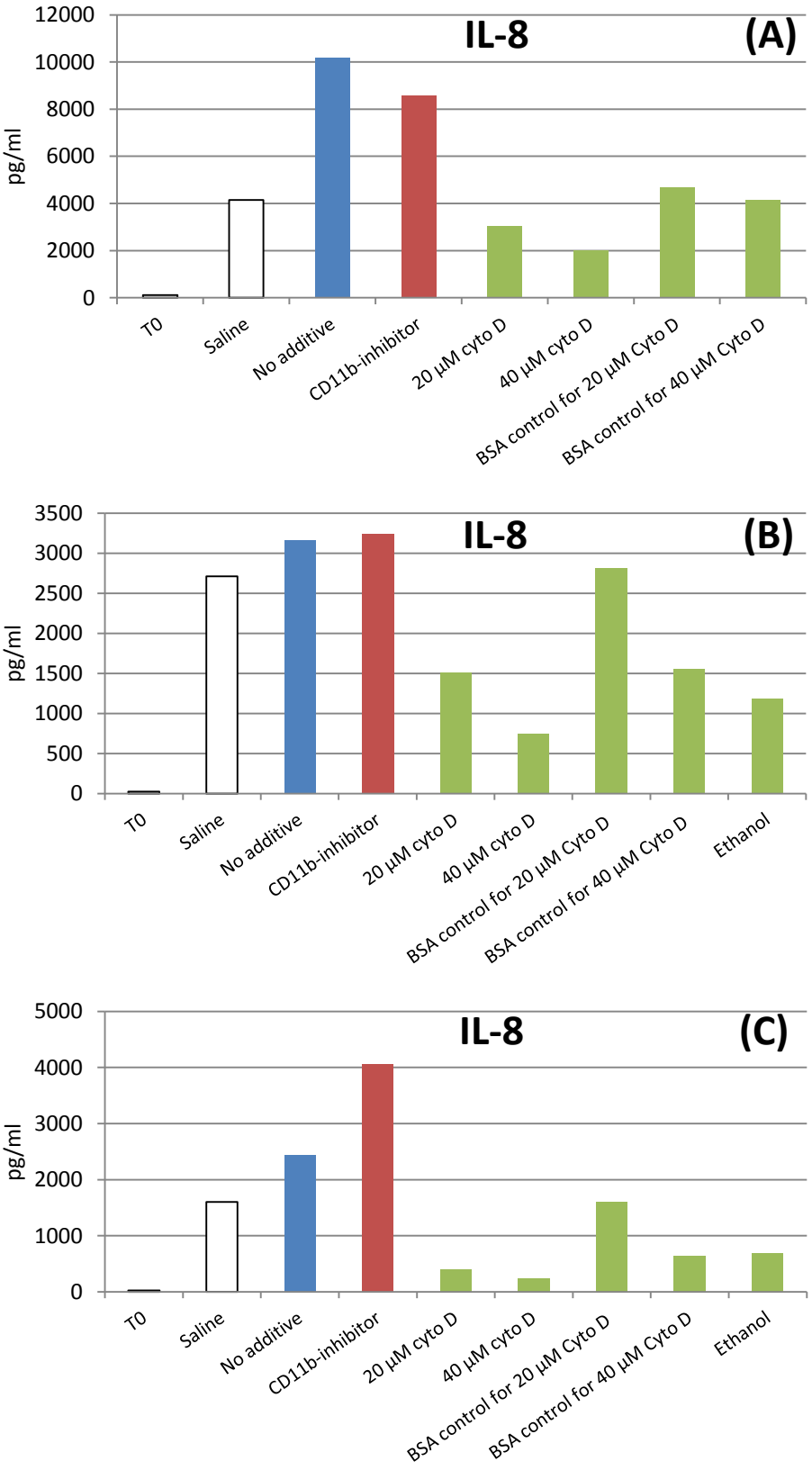

Figure 3.20. IL-8 levels for three individual donors (A, B and C) after incubation of APA microcapsules and controls for 4 hours in fresh human whole blood with CD11b-inhibitor, cytochalasin D (Cyto D), BSA or ethanol controls, or no additive. For donor A, the volume of blood is reduced (125 µl). White bars are controls with no capsules, blue bars are capsules with no additive, red bars are capsules added 60 µg/ml CD11b-inhibitor. Green bars represent capsules added cytochalasin D as well as BSA and ethanol controls for cytochalasin D. The zymosan value is 10036 pg/ml, 9063 pg/ml and 4216 pg/ml for donor A, B and C, respectively.

4 DISCUSSION

The aim of this work was to explore the inflammatory potential of a set of different alginate microcapsules *in vitro*. This was done in order to increase our knowledge of the inflammatory mechanisms potentially involved upon implanting alginate capsules *in vivo*. To do this, the present study takes use of several experimental setups. Some of these, such as the whole blood model, are well-established methods known to produce reliable results. Others, however, are newer, less-established methods that have largely been developed based on trial and error. The following sections will therefore include some methodical discussion as well as debate around the actual results from the present work.

4.1 Hydroxyapatite-containing capsules

The hydroxyapatite (HA) containing capsules include those formed through counter-diffusion (CaP) and alkaline phosphatase-mediated (Enz-CaP) HA-mineralization. HA is generally regarded as biocompatible as it exists in substantial amounts in the body, and this mineral form has been used to coat metal parts in order to improve their biocompatibility [113]. A few experiments have assessed the inflammatory properties of HA in different settings (e.g. nanosized HA particles and HA-covered titanium surfaces) [113-116]. These findings generally report that HA does not appear to be immunostimulatory, however, release of TNF-α from macrophages has been repeatedly found [113-116]. Based on observations from the present study, the introduction of HA into the alginate system—as seen when comparing to Ca-bead—did appear to have a slight stimulatory effect, which was most apparent for the microbeads made through counter-diffusion precipitation. This was true in terms of complement and leukocyte activation, as well as cytokine induction. Microscopy revealed that CaP microbeads had a rough textured surface. As rough surfaces have been implicated to induce greater degrees of protein deposition (see section 1.9.1), this may potentially explain the rather fair amount of leukocyte adhesion on these capsules. On the other hand, the microbeads mineralized through enzymatic control generally induced very little or no leukocyte adhesion. The few leukocytes that were present on Enz-CaP seemed to be located in cracks in the capsule surface. The reason for this is unknown, but a higher degree of protein deposition on these localizations may be a possible explanation. Furthermore, these observations were reflected in the leukocyte activation, for which CaP induced significantly elevated levels of CD11b-expression, whereas Enz-CaP did not induce CD11b upregulation. The slightly stimulatory effect – although non-significant in all cases – that was seen for cytokine induction was perhaps most apparent for chemokines and least apparent for the pro-inflammatory cytokines. For certain cytokines (e.g. MCP-1, IL-10 and IFN-γ) CaP actually induced responses higher than the polycation-containing microcapsules, which are generally regarded to have substantial immunostimulatory potential and have previously been demonstrated to induce a potent secretion of these same cytokines [61]. Furthermore, as previously mentioned it has been observed that TNF-α is induced by HA in different settings [113-116]. In this experiment, CaP did not induce TNF-α, whereas Enz-CaP did. This was in contrast to the expectations, as the TNF-α induction is generally seen to reflect the sTCC

induction, for which CaP was found to induce a more potent response than Enz-CaP. One might thus speculate whether the ALP-enzymes used for mineralizing Enz-CaP could contain endotoxins, however, this does not reflect the overall performance of these microbeads. It is unknown whether the difference in TNF-α induction in the present work is related to the HA content of CaP and Enz-CaP.

Overall, the advantage to counter-diffusion is that mechanically stable capsules may be made in one single step, whereas disadvantages include some degree of immunostimulation and the use of high calcium concentrations, which is negative for the viability of enclosed cells. Although the capsules mineralized through enzymatic control generally appeared inert, these were also found to induce complement activation as well as certain cytokines (e.g. PDGF-BB and IL-1β). Advantages to this method is a seemingly low inflammatory potential and better control of the mineralization process, whereas a significant drawback is poor mechanical strength.

4.2 Peptide-coupled capsules

The alginates studied in this work have been covalently grafted with specific peptides to create a microenvironment that mimics the ECM, with the aim to stimulate cell adhesion, cell proliferation and improve tissue repair. The design of these alginates is based on knowledge about specific ligand-recepor interactions; the peptide sequences REDV and VAPG are known to bind preferentially to endothelial cells [54] and smooth muscle cells [53], respectively, and RGD is found in many ECM proteins and is known to facilitate binding to a range of cells [51]. It was in our interest to explore how the grafting of peptides to alginates affected the inflammatory response.

Overall, the peptide-coupled microbeads were found to be non-stimulatory, and generally induced low inflammatory responses – in many cases lower than saline control. The introduction of the specific peptides into the alginate system did not appear to induce complement or leukocyte activation, nor any apparent cell adhesion. Some level of cell adhesion might be expected as the RGD-peptide facilitates cell binding, and it has been shown that RGD may induce macrophage adhesion [117, 118]. However, the amount of RGD coupled to the alginate might not be high enough for the effect of RGD on cell adhesion to be visible in a light microscope. Furthermore, the high M microbeads were seen to possess poor mechanical stability compared to the high G microbeads. This is in accordance with previous observations that alginate gel stability is affected by the G/M ratio [119]. Indeed, Morch et al. demonstrated that the leakage of divalent ions (e.g Ba^{2+}) was significantly higher from high M than high G alginates, leading to a less stable gel system for high M-containing alginates [119]. Furthermore, the peptide-coupled microbeads generally appeared to be non-inflammatory regarding cytokine induction. In only a few cases some of the peptide-coupled microbeads – mostly high M beads – stimulated a minor elevation of certain cytokines. This was particularly apparent for M REDV, which induced significantly elevated responses for IFN-γ and IL-10. Based on these observations, it might seem as the high M capsules possessed a slightly more stimulatory effect than did the high G peptide-coupled capsules.

This is in accordance with previous findings, which have demonstrated that high M alginates induce a more potent cytokine secretion compared with those with a high G content [120, 121].

As mentioned in section 3.2, G VAPG-capsules were found to contain substantial levels of endotoxin, which is well known to significantly affect the inflammatory properties of alginate [19]. LPS is a pathogen-associated molecular pattern (PAMP) which will stimulate Toll-like receptors (mainly TLR4) and evoke inflammatory reactions, predominantly via activation of the NF-κB signaling pathway [122]. For these reasons, the data from the G VAPG capsules cannot be trusted to provide significant information about the inflammatory potential of VAPG-coupled alginates. Indeed, the G VAPG capsules were generally found to induce significantly high levels of leukocyte activation and cytokine induction. G VAPG did not, however, appear to induce growth factors (PDGF-BB and VEGF), indicating that endotoxin is not involved in stimulation of these mediators. Furthermore, G VAPG capsules did not appear to induce complement activation in terms of sTCC, nor apparent leukocyte adhesion.

4.3 Epimerized alginates

The alginates used to make the epimerized microbeads studied in this work had been treated with C-5 epimerases in order to make Ca-alginate beads with a high stability and intermediate flexibility [23, 25]. Furthermore, to produce the Epi-RGD capsule, RGD-containing peptides were grafted onto the alginate. This grafting was performed by using carbodiimide chemistry, and the amount of RGDs coupled to the alginate was ultimately found to be very low (~0.1%) [24], which might reflect the seemingly low levels of cell adhesion on the Epi-RGD microbeads. The results from the present study indicated that grafting RGD to the alginate did not have a stimulatory effect compared to the non-grafted epimerized capsules. In fact, this functionalization of the alginate rather appeared to lead to reduced responses. This observation may be linked to a study in which RGD-containing peptides were demonstrated to inhibit platelet aggregation and arterial thrombosis [111]. Furthermore, the alginates used for making both Epi and Epi-RGD were demonstrated to contain high levels of endotoxin. The presence of LPS is likely to be derived from the C-5 epimerases used in making these epimerized alginates, as these enzymes were produced in *Escherichia coli*. Due to the endotoxin contamination (see section 4.2), these alginates were not studied further in this work, and commercially available RGD-grafted alginates were chosen for studying peptide-coupled alginates.

4.4 Polycation-containing capsules

As mentioned in section 1.3.2, polycation-containing microcapsules exhibit excellent mechanical properties and have been frequently studied in animal models with the purpose of cell immunoprotection upon transplantation. Some researchers suggest that the addition of a permselective polycation layer such as PLL is necessary in larger animals to prevent the entrance of cytokines, Ig and complement [123]. However, the use of a polycation layer has often come to be regarded as the main contributor of the bioincompatibility observed for

these microcapsules *in vivo*. Main reasons for this effect may be the potential release of stimulating components from the material, or the exposure of polycation on the microcapsule surface. Indeed, the exposure of immunogenic PLL to the surrounding milieu may further give rise to adverse inflammatory responses, as has been demonstrated in a range of studies [33-36]. To sum up the following section, the polycation-containing microcapsules appeared to hold potent pro-inflammatory properties, and were generally found to induce substantial levels of a range of different cytokines known to be involved in inflammation directed towards biomaterials. Hence, the introduction of polycations into the alginate system generally appeared to have an adverse effect on the stimulatory potential of the microcapsules, which may be observed by comparing to non-polycation containing Ca-microbeads.

Overall, the responses observed in the present work were largely consistent with those demonstrated in similar experiments by Rokstad et al. [45, 61].The polycation-containing microcapsules induced high levels of cell adhesion, which was reflected in the high induction of leukocyte activation in terms of CD11b-upregulation. Leukocyte adhesion on PMCG was not explored in the present work; however, a recent study performed in a similar setting demonstrated that PMCG microcapsules induced considerable amounts of cell adhesion, seemingly with granulocytes constituting the majority of the adherent cells [45]. The high levels of protein deposition (C3, TCC) observed on AP and APA was in accordance with the high levels of leukocyte adhesion and activation observed for these microcapsules. As previously mentioned, monocytes and granulocytes express the CD11b/CD18 complement receptor, which binds specifically to iC3b (manifested by C3 deposition) on biomaterial surfaces. This general chain of events can be simplified as follows: Protein deposition (iC3b etc.) → Leukocyte adhesion (e.g. via CD11b/CD18 receptor) → Activated leukocytes (CD11b upregulation) → Cytokine secretion (see figure 4.1). Indeed, the potent induction of complement (sTCC) and cytokines observed for the polycation-containing microcapsules is in accordance with the substantial level of leukocyte adhesion and activation. The majority of cytokines screened for in this study were noticeably elevated by the polycation-microcapsules, including chemokines, pro- and anti-inflammatory cytokines as well as growth factors. For some cytokines, the PLL-containing microcapsules induced the highest response, e.g. the growth factors PDGF-BB and VEGF as well as the chemokines IL-8 and MCP-1. In general, APA was seen to be slightly less immunostimulatory than AP capsules. This indicates that some of the immunogenic effects of PLL are neutralized by the outer alginate coat. On the other hand, PMCG microcapsules induced significant and highly potent responses for pro- and anti-inflammatory cytokines. It has been speculated whether PMCG is able to release some mediator to the surroundings which holds a toxic effect [46]. A study has also demonstrated that PMCG-microcapsules induce a potent and highly rapid coagulation activation, which is likely to occur prior to complement activation and may potentially affect subsequent complement activity [46]. Nevertheless, although PMCG induction was observed to be low for a few cytokines in the present work (e.g. PDGF-BB, RANTES and IFN-γ), the PMCG microcapsules were generally regarded as immunostimulatory.

4.5 TAM microbeads

The Trondheim Alginate Microcapsule (TAM) has produced promising results in terms of *in vivo* trials as well as the whole blood model, and has generally been observed to be non-inflammatory [30, 31, 45, 61, 106]. For this reason, TAM is thought to constitute a proper control bead for certain capsule types in the present study. The results observed for TAM in this work are generally consistent with previous findings by Rokstad et al. from similar studies using the whole blood model, which indicate that TAM is inert [45, 61]. TAM is made by adding a small amount of barium to the calcium-containing gelling solution, which confers considerable stability and strength to the alginate matrix consisting of a high G alginate. Indeed, when compared to Ca-bead (made without Ba^{2+} in the gelling solution) TAM appeared to have much better mechanical strength. In some cases the addition of barium also appeared to decrease the immunostimulatory properties of the alginate, e.g. in terms of lower chemokine induction by TAM than Ca-bead. In general, TAM was found not to induce leukocyte activation or adhesion, complement activation or elevated cytokine secretion. This was reflected by the protein deposition studies, in which no C3or TCC deposition was detected on TAM microbeads. Actually, in most cases TAM was observed to induce lower responses than saline control. In a previous study by Ørning it was debated whether this could be due to adsorption of complement regulatory proteins (e.g. factor H and vitronectin) to the microbead surface, that prevented the onset of the complement cascade [106]. However, this was disproved through protein deposition studies, which showed that it was in fact APA capsules that displayed the greatest inhibitory effects, as could be seen from heavy factor H and vitronectin adsorption on the APA capsules [106]. Regardless, although TAM generally appeared inert, these microbeads were found to induce an increased level of PDGF-BB, which is in contrast to the findings by Rokstad et al. [61]. Furthermore, TAM induced a slight increase of the anti-inflammatory cytokines IL-10 and IL-1ra. In fact, the mere presence of alginate microcapsules and microbeads itself appeared to stimulate more or less elevation of these anti-inflammatory cytokines, as compared with saline control (figures 3.12a-b). Nevertheless, the induction of specific cytokines need not necessarily be negative, as the outcome of inflammation is determined by a delicate balance between different inflammatory mediators. In certain settings inflammation may even be favorable, e.g. in a wound healing process.

4.6 Mechanism studies

As described in section 1.9.1, the nature of the proteins adsorbed to a biomaterial surface will influence host cell interactions and adhesion, and subsequent inflammatory responses. AP microcapsules induced significant amounts of C3 deposition on its surfaces, while TAM on the other hand did not. This was consistent with the findings in a recent study by Rokstad et al. [61]. Furthermore, as C3 deposition is required for TCC deposition, TAM microbeads accordingly did not induce TCC deposition whereas polycation-containing APA microcapsules did. The time study indicated that it took quite some time for large amounts of C3 to deposit onto the microcapsule surface. This was in contrast to a previous study in which

C3 deposition on microcapsules occurred rapidly; however, this study made use of whole blood for capsule incubation instead of plasma [45]. Potentially, the presence of cells might further stimulate C3deposition, as it has been demonstrated that monocytes are able to produce C3 [124]. This is consistent with the observations for the protein adsorption study with compstatin and Soliris® (figure 3.18), in which microcapsules were incubated in whole blood before αC3c-staining. After the same incubation time (4 hours) noticeably more C3 deposition was detected on these microcapsules as opposed to those incubated in plasma (figure 3.5). Moreover, in terms of the time study, there appeared to be a minor deposition of C3 on TAM microbeads after 4 and 8 hours, however, this response was absent after 16 hours. Given the low TCC responses, it is likely that the C3 detected on TAM may be C3 in its native form, absorbed in the permeable alginate matrix, as suggested in a study by Rokstad et al. [45]. This inactive C3 might potentially have loosened from the microbeads after some time, as seen after 16 hours incubation. Furthermore, we also aimed to explore fibrinogen adsorption on TAM and AP. Fibrinogen – which is involved in the coagulation cascade – is abundant in plasma and contains the common cell adhesion motif RGD. Potentially, fibrinogen adsorbed to biomaterial surfaces may expose binding sites for cells, and might thereby play a role in facilitating leukocyte adhesion [73]. Regardless, in the present study neither AP microcapsules nor TAM microbeads were found to have fibrinogen deposition, which is consistent with previous observations [106]. Based on the observations in the present study, it generally appears that complement is the most central initiator of subsequent inflammatory events induced by alginate microcapsules.

In order to visualize potential effects of complement inhibition, AP microcapsules were incubated in whole blood with the complement inhibitors Soliris® and compstatin. Capsules incubated with Soliris® showed C3 deposition and some cell adhesion. Soliris® is a humanized antibody that binds C5 and prevents the cleavage of C5 into C5b and the potent anaphylatoxin C5a, while not affecting C3. Therefore, C3 is still able to react with the microcapsule surface. Furthermore, the results implied that the employed compstatin analogue (CP20) was highly effective in inhibiting complement component C3, as no C3 deposition was found on capsules incubated in compstatin-blood as compared to the control-peptide samples. Compstatin-microcapsules were also completely free of attached leukocytes. This is likely due to the absence of iC3b (inactivated C3b) on the microcapsule surface, since compstatin will inhibit the cleavage of C3 into C3a and C3b. As previously mentioned, iC3b is a major opsonin for leukocytes, which can specifically bind to this ligand through the CD11b/CD18 receptor. This facilitates cell adhesion, with subsequent activation of the attached leukocytes. One might speculate in whether this specific receptor/ligand-interaction between iC3b and CD11b/CD18 is required for inducing cytokine release. This idea was further explored by adding CD11b-inhibitory antibody to APA microcapsules. The importance of the CD11b/CD18 for leukocyte adhesion was clearly visualized by microscopy, as the CD11b-inhibitor substantially inhibited cell adhesion (figure 3.19). We would therefore expect that cytokine responses, e.g. in terms of IL-8, would accordingly be reduced. However the IL-8 response in two of the three donors was actually found to increase in the presence of CD11b-inhibitor (figure 3.20). A reason for this might be that something in the CD11b-

inhibitory antibody solution has an immunostimulatory effect in whole blood, whether it be aggregates of the antibody itself or other components present in the solution.

Furthermore, there was some speculation whether the level of cytokine secretion depended on the cell spreading on the microcapsule surface, and the attempt of leukocytes to phagocytize the microcapsule (frustrated phagocytosis). In order to explore this hypothesis, APA-capsules were added cytochalasin D, which is an inhibitor of phagocytosis (see section 2.2.3). Indeed, a previous study demonstrated that cytochalasin D was effective in inhibiting phagocytosis of carbon nanofibres, and thereby abolishing the increase of pro-inflammatory IL-1β [125]. Figure 4.1 illustrates the hypothesized effects of the different inhibitors employed in the present work – cytochalasin D, CD11b-inhibitor, and compstatin.

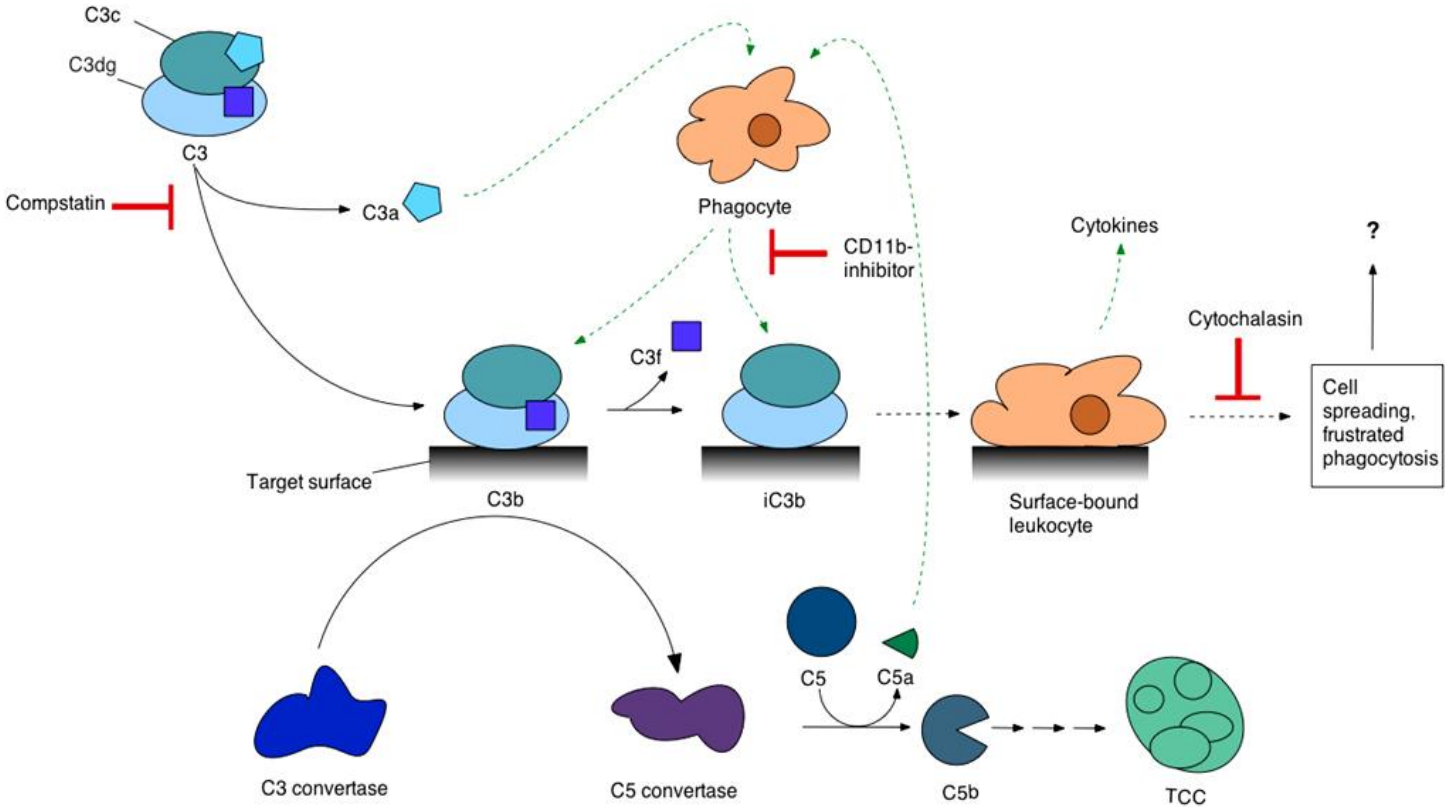

Figure 4.1. Simplified overview of hypothesized events leading to cytokine secretion, and the effects of the leukocyte inhibitors CD11b-inhibitor and cytochalasin D, as well as complement inhibitor compstatin. Complement proteins including (i)C3b deposit on the microcapsule surface unless C3 cleavage is inhibited by compstatin. Leukocytes bind complement proteins adsorbed on the capsule surface via surface receptors – e.g. the CD11b/CD18 complement receptor which is specific for iC3b – leading to their subsequent activation and cytokine secretion. Further cytokine release potentially induced by cell spreading and the attempt of leukocytes to phagocytose the biomaterial is inhibited by cytochalasin D.

The results from the inhibition studies with cytochalasin D indicates that the IL-8 levels were reduced with the addition of cytochalasin D compared to microcapsule controls with no additive. However, the experiment is not thought to produce reliable results. As cytochalasin D was dissolved in ethanol, controls containing ethanol was included. This was done to see whether the observed effects on IL-8 induction came from cytochalasin itself, or from the ethanol in which it was dissolved. Indeed, it appeared that the ethanol had a toxic effect which

negatively affected the IL-8 secretion, since cytokine levels were low for all samples added cytochalasin or ethanol-containing controls. Therefore, the reduction in IL-8 seen when increasing the cytochalasin concentration might as well be due to the accompanying increased ethanol volume. In conclusion, whether the inhibition of phagocytosis did or did not affect cytokine production could not be determined by the experimental protocol employed in this work.

4.7 Hollow versus solid microcapsules

As outlined in the previous section, solid microcapsules have been implied to induce cytokine secretion mainly via complement-dependent mechanisms associated with the microcapsule surface. However, the observed patterns of inflammatory events is somewhat altered when the microcapsule core is liquefied. The aim of liquefying the capsule core is to reverse the gelation process and create a less static microenvironment inside the microcapsules [126]. A recent study by Ørning demonstrated that microcapsules with a liquefied core induced high levels of sTCC, but low levels of IL-8 [106]. This was in contrast to the picture commonly seen for solid microcapsules, which generally induce high levels of IL-8 by a complement-dependent mechanism, as suggested by Rokstad et al. [61]. We wished to further expand the studies done by Ørning and to explore the mechanisms induced by hollow microcapsules containing PLL and PLO, respectively, compared with solid microcapsules.

The complement protein deposition studies in figures 3.15-3.16 demonstrated that the hollow microcapsules induced noticeably lower levels of C3 and TCC. This was especially apparent for the C3 deposition, but also TCC was detected in lower amounts on hollow microcapsules compared to solid ones. The solid microcapsules therefore seemed to have a surface that promoted C3 deposition and formation of the C3 and C5 convertases. This was in contrast to the hollow microcapsules, that seemed to secrete some complement-stimulating component into the solution, but failed to induce cytokines due to less building of convertases on their surface.

It generally appeared that PLO Hollow was less immunostimulatory than PLL Hollow. In contrast to PLL Hollow, the PLO Hollow microcapsules induced low responses for both complement and cytokine induction (figure 3.17a-b). Moreover, PLO Hollow appeared to have noticeably lower amounts of protein deposition on their surfaces as compared with PLL Hollow. This may be due to a lower exposure of free amino groups for PLO, which are generally prone to activate complement via C3b-binding [68, 127]. A study by Darrabie et al., demonstrated that PLO binds more efficiently to the alginate membrane than PLL does, resulting in a better complexation of alginate/PLO than alginate/PLL [126]. In a study by Tam et al. it was demonstrated less overgrowth and better biocompatibility of PLO-containing microcapsules compared to those with PLL [34], which is in accordance with the findings by Ørning [106] as well as the present study. However, at least one other study using similar methods showed the opposite results, with poorer biocompatibility for PLO-containing microcapsules as opposed to PLL-microcapsules [38]. Nevertheless, the present study showed

more promising properties for PLO-containing microcapsules than the PLL-containing microcapsules.

The observed responses in terms of C3 and TCC deposition on hollow microcapsules were not reflected by the sTCC response (figure 3.17a). Indeed, the sTCC response for the PLL Hollow microcapsules was observed to be substantially elevated compared to solid microcapsules. However, the hollow microcapsules induced lower amounts of cytokine release in terms of IL-8 compared to solid microcapsules (figure 3.17b). These observations are consistent with previous findings by Ørning [106]. The relatively low levels of cytokine secretion induced by PLO Hollow and PLL Hollow may be linked to the low degree of C3 and TCC deposition observed for these microcapsules. As previously described, the adsorption of activated complement proteins may facilitate binding of leukocytes via the CD11b/CD18 receptor. A lower amount of protein deposition will thus lead to a lower level of leukocyte adhesion (as seen in figure A2 in the appendix) and subsequent activation, with an accompanying reduced level of cytokine secretion. These events are illustrated in figure 4.2.

In order to explore if the cytokine induction by hollow microcapsules was complement-dependent, the complement inhibitor compstatin was added the microcapsule samples (figure 3.17a-b). Compstatin clearly knocked down the sTCC response as well as the IL-8 response for both hollow and solid microcapsules compared with control peptide- or no additive-samples. This implies that the IL-8 secretion for hollow microcapsules is also heavily dependent on complement activity, as suggested for the solid microcapsules.

In terms of the sTCC responses, the following hypothesis has been developed based on the described outcomes. We suggest that some soluble component might leak out from the PLL Hollow microcapsule and into the solution, stimulating formation of the high levels of sTCC observed for these microcapsules. The rationale behind this is that relatively low amounts of C3 and TCC were found on the hollow microcapsule surfaces. This implies that the potent sTCC induction seen for PLL Hollow is not associated with events on the microcapsules' surface. The described hypothesis is illustrated in figure 4.2. The potent sTCC induction seen for PLL Hollow may potentially be further involved in cytokine induction, as sTCC complexes have previously been demonstrated to interact with and activate platelets, which may further facilitate inflammatory reactions [105]. One might speculate in whether the soluble component leaking out from the PLL Solid capsules could be the polycation PLL itself, as PLO Hollow capsules did not induce the same response. However, previous experiments have shown that PMCG microcapsules – which also have a citrate-treated liquefied core – induce similar responses as PLL Hollow [61], implying that the soluble component may not be PLL. Moreover, PLO has been demonstrated to have lower permeability for higher molecular weight components compared with PLL [38], which might potentially restrict the leakage of the hypothesized soluble trigger of sTCC. In order to further elucidate this issue, it could be interesting to study the leakage of polycation from various hollow microcapsules.

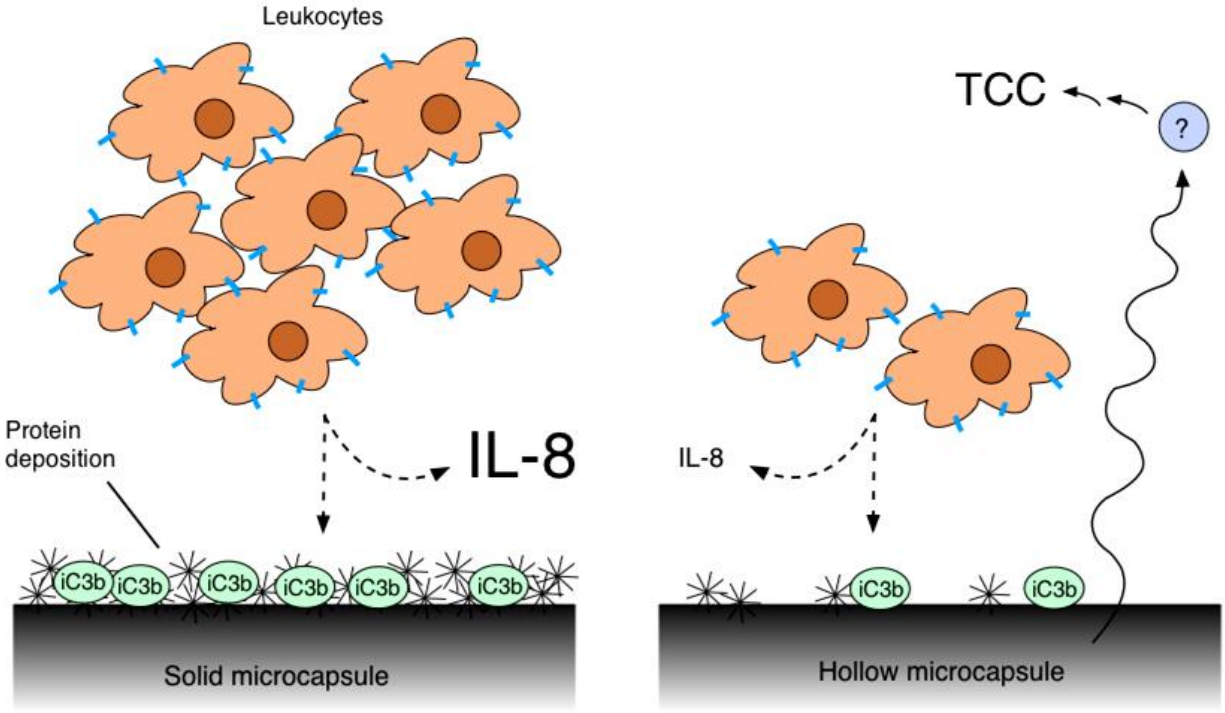

Figure 4.2. Hypothesized complement-associated events induced by microcapsules containing a solid and a hollow core, respectively. Substantial amounts of proteins, e.g. C3b/iC3b and TCC, deposit on the solid microcapsules. It is reasonable to believe that a large amount of the deposited proteins is iC3b (as illustrated), since inhibiting the CD11b/CD18 receptor – for which iC3b is a ligand – substantially reduced cell adhesion on the solid microcapsules. High levels of iC3b deposition leads to large amounts of leukocyte attachment via the CD11b/CD18 receptor (shown in blue). The subsequent activation of a large amount of cells on the solid microcapsules leads to an accompanying substantial cytokine secretion, e.g. IL-8. The hollow microcapsules induce only low levels of protein deposition on their surfaces, thus facilitating less cell adhesion and an accompanying low level of cytokine secretion from attached leukocytes. The TCC formation observed for hollow microcapsules is not associated with events on the microcapsules' surface, but is potentially evoked by a soluble molecule (designated as "?") leaking out from the capsule and stimulating TCC formation in the solution.

To sum up, it appeared that liquefying the capsule core influenced the microcapsules' inflammatory potential. Hollow microcapsules were generally observed to be less immunostimulating than solid microcapsules in terms of complement protein deposition and cytokine induction. PLL-containing hollow microcapsules did, however, induce a potent complement activation in the solution (sTCC). Potentially, this response is evoked by some stimulatory soluble molecule or component leaking out from the PLL Hollow microcapsules. The IL-8 induction was observed to be substantially reduced by the addition of the complement inhibitor compstatin, indicating that cytokine secretion for hollow microcapsules occurs via a complement-dependent mechanism. An apparent advantage to hollow microcapsules is thus their lower immunostimulatory properties; however, a drawback is their relatively poor mechanical strength. Their susceptibility to osmotic swelling means that some microcapsules may burst and release their contents – including encapsulated cells – to the surrounding environment, potentially evoking potent inflammatory reactions. Moreover, PLO appears to be the better choice for the polycation as compared to PLL, in terms of a lower complement activation.

4.8 Implications for *in vivo* applications

The observations made in the present work gives an indication of how different alginate capsules would perform in an *in vivo* setting. Based on the findings in this study, alginates grafted with certain ECM-associated peptides are not likely to induce substantial overgrowth *in vivo*, thus retaining the therapeutic function of the capsule. This implication is important since the biofunctionalization of alginates may create a much more stimulating environment for encapsulated cells and thus a better function of the graft, e.g. in relation to pancreatic islet encapsulation for treatment of type 1 diabetes mellitus. The same implication can be made for TAM-microbeads, which have indeed showed promising results *in vivo* [30, 31]. HA-mineralized alginates made through counter-diffusion precipitation and enzymatic mineralization intended for use in bone tissue engineering may potentially induce a slight level of inflammation and some overgrowth. This may have adverse effects on encapsulated cells (e.g. osteoblasts) and may impair the bone graft. Furthermore, the HA-mineralized microbeads formed by enzymatic control may potentially not be able to withstand the considerable mechanical stress accounted for by a surgical procedure as well as after implantation. Polycation-containing alginate microcapsules appeared immunostimulatory and would be expected to induce substantial overgrowth *in vivo*, which has indeed been repeatedly observed [33, 34, 36]. These microcapsules stimulated cytokine induction as well as a potent complement activation, which has indeed been shown to affect fibroblast activation, extracellular matrix protein deposition and macrophage influx in a renal fibrosis model using C5 deficient mice [128]. Hollow polycation-microcapsules with a liquefied core – and in particular those containing PLO – may induce less overgrowth, but may not be able to withstand the considerable mechanical stress to which they will be exposed *in vivo*.

It should be noted that the whole blood model has an important limitation in studying capsule-induced inflammatory events, which is the use of relatively short incubation times. Indeed, the whole blood model is not optimal for studying long-term effects, as cell viability will be limited under the conditions in the assay. The use of short incubation times only allows for exploring the most immediate immune responses. As alginate capsules implanted *in vivo* are intended to remain and exert their function over extended periods of time, it would also be a great advantage to be able to study inflammatory events after longer time periods. Furthermore, even though the whole blood model provides important information about the upregulation of individual cytokines *in vitro*, the collective effect of the different inflammatory mediators *in vivo* should not be underscored. Indeed, different cytokines might in combination have other effects than each cytokine alone.

4.9 Future perspectives

In order to optimize the biocompatibility of alginate microbeads and microcapsules, it is necessary to obtain further knowledge about their properties in relation to inflammatory events. In terms of continuing some of the trials attempted in this work, it could be desirable to explore the inflammatory properties of ultrapure VAPG-coupled alginates. Moreover, a

better protocol should be established for examining tissue factor expression patterns on monocytes, as the upregulation of tissue factor might help trigger the extrinsic pathway of coagulation. The protein adsorption assays could be performed with longer incubation lengths in order to see if this was the limiting factor (e.g. for fibrinogen), or they could be expanded to include screening for coagulation factors (e.g. kallikrein and factor XII) as well as activated plasma cascade proteins as opposed to their inactive counterparts (e.g. fibrin instead of fibrinogen). Furthermore, it could be interesting to screen for deposition of properdin – a positive regulator of complement activation that stabilizes the alternative pathway convertases – as well as complement components associated with the classical activation pathway, e.g. antibodies (IgA/IgM/IgG) and C1q. A study of coagulation activation in whole blood could also provide much information. For instance, is it complement or coagulation that is the primary inductor of capsule-induced inflammatory events? Indeed, it has been demonstrated that PMCG microcapsules induce a potent coagulation activation [46]. Since the complement and coagulation cascades are highly interconnected, coagulation might potentially be the primary initiator of PMCG-induced stimulation. A potential marker in screening for coagulation activation is prothrombin fragments 1+2 (PF1+2), which are not subjected to inhibition by lepirudin [129]. Furthermore, studies with isolated monocytes – and potentially fibroblasts – could be performed in order to observe how the cells attach and spread on the capsule surfaces. Long incubation periods should be used for these studies, in which the cell-associated events on the capsules could be observed on a daily basis. After some time, frustrated phagocytosis and fusion of macrophages into foreign body giant cells might potentially be observed. In the described settings, it could further be interesting to study the effect of phagocytosis inhibition, e.g. with cytochalasin D, on the release of inflammatory mediators. This requires that an optimal protocol for studying the effect of cytochalasin D is established. Furthermore, the importance of cell binding via complement receptors, e.g. CD11b/CD18, on cytokine release should be further assessed. By employing a humanized inhibitory antibody towards CD11b and/or CD18, the antibody itself should not elicit inflammatory reactions. Although CD11b- humanized antibodies do not exist yet [130], there has been developed CD18-selective humanized antibodies [131] as well as humanized antibodies towards the entire CD11b/CD18 receptor [132].

5 CONCLUSION

The present study has demonstrated the inflammatory potential of a set of different alginate microbeads and microcapsules by use of the whole blood assay. The following conclusions are based on observations of protein deposition, complement and leukocyte activation, cell adhesion and cytokine secretion.

TAM microbeads as well as microbeads made from alginates coupled with the peptides REDV and RGD were generally non-inflammatory, with the only exception that REDV-coupled microbeads induced significant cytokine secretion in terms of IFN-γ and IL-10. In general, the covalent grafting with these peptides to alginates for the purpose of functionalization was not regarded to affect the immunostimulatory properties of the alginates. No significant information about the inflammatory potential of VAPG-coupled alginates could be obtained due to endotoxin contamination.

Hydroxyapatite-mineralized microbeads intended for use in bone tissue engineering were observed to elicit a slight stimulation of inflammatory responses, and triggered significant complement and leukocyte activation. Microbeads made from alginates mineralized through counter-diffusion precipitation appeared more stimulatory than those mineralized through enzymatic control. Compared with non-HA-containing controls, the introduction of HA into the alginate system did appear to affect the inflammatory potential of the alginate.

Polycation-containing microcapsules induced potent inflammatory responses in terms of significant levels of leukocyte and complement activation as well as cytokine secretion, including chemokines (IL-8, MCP-1, MIP-1α), inflammatory cytokines (IL-1β, IL-6, TNF-α), anti-inflammatory cytokines (IL-1ra) as well as growth factors (VEGF).

Hollow PLL-containing microcapsules were less stimulatory than solid PLL-containing microcapsules in terms of a reduced complement protein deposition, cell adhesion and IL-8 secretion. In contrast, a more potent TCC induction was detected for these hollow PLL-containing microcapsules, potentially due to some soluble component leaking out and triggering fluid-phase TCC formation. The relatively low IL-8 secretion induced by hollow microcapsules was further demonstrated to rely on complement-dependent mechanisms. Moreover, hollow microcapsules containing PLO as a polycation generally showed more promising properties for *in vivo* applications in terms of a lower complement activation compared with PLL-containing hollow microcapsules.

The peptide-coupled and TAM microbeads generally appeared to have the lowest inflammatory potential of the capsules analyzed in the present work, and thus appear the most promising capsules for *in vivo* applications. Nevertheless, further studies should be performed in order to explore potential overgrowth on the microbeads and the mechanisms leading up to it. In addition, further information on microbeads as well as microcapsules could be obtained through continued protein deposition studies and screening for coagulation activation.

References

1. Stucker, F. and D. Ackermann, *[Immunosuppressive drugs - how they work, their side effects and interactions]*. Ther Umsch, 2011. **68**(12): p. 679-86.
2. Vaithilingam, V. and B.E. Tuch, *Islet transplantation and encapsulation: an update on recent developments.* Rev Diabet Stud, 2011. **8**(1): p. 51-67.
3. Lim, F. and A.M. Sun, *Microencapsulated islets as bioartificial endocrine pancreas.* Science (Washington, D. C.), 1980. **210**(4472): p. 908-10.
4. Reach, G., *Bioartificial Pancreas.* Diabetic Medicine, 1993. **10**(2): p. 105-109.
5. de Vos, P., et al., *Alginate-based microcapsules for immunoisolation of pancreatic islets.* Biomaterials, 2006. **27**(32): p. 5603-5617.
6. Hardouin, P., et al., *Tissue engineering and skeletal diseases.* Joint Bone Spine, 2000. **67**(5): p. 419-24.
7. Blitterswijk, C.v., et al., *Tissue Engineering*. 2008, London, UK: Elsvier Inc.
8. Santos, E., et al., *Biomaterials in cell microencapsulation.* Adv. Exp. Med. Biol., 2010. **670**(Therapeutic Applications of Cell Microencapsulation): p. 5-21.
9. Ratner, B.D., *The biocompatibility manifesto: biocompatibility for the twenty-first century.* J Cardiovasc Transl Res, 2011. **4**(5): p. 523-7.
10. Williams, D.F., *On the mechanisms of biocompatibility.* Biomaterials, 2008. **29**(20): p. 2941-53.
11. Bryers, J.D., C.M. Giachelli, and B.D. Ratner, *Engineering biomaterials to integrate and heal: the biocompatibility paradigm shifts.* Biotechnol Bioeng, 2012. **109**(8): p. 1898-911.
12. Anderson, J.M., A. Rodriguez, and D.T. Chang, *Foreign body reaction to biomaterials.* Semin Immunol, 2008. **20**(2): p. 86-100.
13. Jones, J.A., *Biomaterials and the Foreign Body Reaction: Surface Chemistry Dependent Macrophage Adhesion, Fusion, Apoptosis, and Cytokine Production*, 2007, Case Western Reserve University.
14. Xia, Z. and J.T. Triffitt, *A review on macrophage responses to biomaterials.* Biomed Mater, 2006. **1**(1): p. R1-9.
15. Onuki, Y., et al., *A review of the biocompatibility of implantable devices: current challenges to overcome foreign body response.* J Diabetes Sci Technol, 2008. **2**(6): p. 1003-15.
16. de Vos, P., et al., *Long-term biocompatibility, chemistry, and function of microencapsulated pancreatic islets.* Biomaterials, 2003. **24**(2): p. 305-312.
17. Soon-Shiong, P., et al., *An immunologic basis for the fibrotic reaction to implanted microcapsules.* Transplant Proc, 1991. **23**(1 Pt 1): p. 758-9.
18. Ma, P.X. *Alginate for tissue engineering*. 2006. CRC Press LLC.
19. Rokstad, A.M., *Alginate Capsules as Bioreactors for Cell Therapy*, in *Department of Cancer Research and Molecular Medicine*2006, NTNU: Trondheim.
20. Arlov, Ø., *Heparin analogs created by sulfation of alginates using a chemoenzymatic strategy*, in *Department of Biotechnology*2012, Norwegian University of Science and Technology: Trondheim.
21. Augst, A.D., H.J. Kong, and D.J. Mooney, *Alginate hydrogels as biomaterials.* Macromol Biosci, 2006. **6**(8): p. 623-33.
22. Ertesvag, H., et al., *Mannuronan C-5-epimerases and their application for in vitro and in vivo design of new alginates useful in biotechnology.* Metab Eng, 1999. **1**(3): p. 262-9.

23. Morch, Y.A., et al., *Molecular engineering as an approach to design new functional properties of alginate.* Biomacromolecules, 2007. **8**(9): p. 2809-14.
24. Karstensen, K., *Novel alginate matrix for tissue engineering: selective substitution ofmannuronic acid residues in alginate with bioactive peptides and the use of these polymers as scaffolds for cells*, in *Department of Biotechnology*2010, NTNU: Trondheim.
25. Morch, Y.A., et al., *Mechanical properties of C-5 epimerized alginates.* Biomacromolecules, 2008. **9**(9): p. 2360-8.
26. Donati, I., et al., *New Hypothesis on the Role of Alternating Sequences in Calcium−Alginate Gels.* Biomacromolecules, 2005. **6**(2): p. 1031-1040.
27. Ibáñez, J.P. and Y. Umetsu, *Potential of protonated alginate beads for heavy metals uptake.* Hydrometallurgy, 2002. **64**(2): p. 89-99.
28. Strand, B.L., et al., *Visualization of alginate-poly-L-lysine-alginate microcapsules by confocal laser scanning microscopy.* Biotechnol. Bioeng., 2003. **82**(4): p. 386-394.
29. Morch, Y.A., et al., *Effect of Ca2+, Ba2+, and Sr2+ on alginate microbeads.* Biomacromolecules, 2006. **7**(5): p. 1471-80.
30. Qi, M., et al., *Survival of human islets in microbeads containing high guluronic acid alginate crosslinked with Ca2+ and Ba2+.* Xenotransplantation, 2012. **19**(6): p. 355-64.
31. Qi, M., et al., *Encapsulation of Human Islets in Novel Inhomogeneous Alginate-Ca2+/Ba2+ Microbeads: In Vitro and In Vivo Function.* Artif. Cells, Blood Substitutes, Biotechnol., 2008. **36**(5): p. 403-420.
32. Strand, B.L., et al., *Alginate-polylysine-alginate microcapsules: effect of size reduction on capsule properties.* J Microencapsul, 2002. **19**(5): p. 615-30.
33. Safley, S.A., et al., *Biocompatibility and immune acceptance of adult porcine islets transplanted intraperitoneally in diabetic NOD mice in calcium alginate poly-L-lysine microcapsules versus barium alginate microcapsules without poly-L-lysine.* J Diabetes Sci Technol, 2008. **2**(5): p. 760-7.
34. Tam, S.K., et al., *Biocompatibility and physicochemical characteristics of alginate-polycation microcapsules.* Acta Biomater, 2011. **7**(4): p. 1683-92.
35. De Vos, P., B. De Haan, and R. Van Schilfgaarde, *Effect of the alginate composition on the biocompatibility of alginate-polylysine microcapsules.* Biomaterials, 1997. **18**(3): p. 273-8.
36. Strand, B.L., et al., *Poly-L-Lysine induces fibrosis on alginate microcapsules via the induction of cytokines.* Cell Transplant, 2001. **10**(3): p. 263-75.
37. De, C.M., et al., *Comparative study of microcapsules elaborated with three polycations (PLL, PDL, PLO) for cell immobilization.* J. Microencapsulation, 2005. **22**(3): p. 303-315.
38. Ponce, S., et al., *Chemistry and the biological response against immunoisolating alginate-polycation capsules of different composition.* Biomaterials, 2006. **27**(28): p. 4831-4839.
39. Wang, T., et al., *An encapsulation system for the immunoisolation of pancreatic islets.* Nat Biotechnol, 1997. **15**(4): p. 358-62.
40. Powers, A.C., et al., *Permeability assessment of capsules for islet transplantation.* Ann N Y Acad Sci, 1997. **831**: p. 208-16.
41. Lacik, I., et al., *New capsule with tailored properties for the encapsulation of living cells.* J Biomed Mater Res, 1998. **39**(1): p. 52-60.
42. Renken, A. and D. Hunkeler, *Polymethylene-co-guanidine based capsules: a mechanistic study of the formation using alginate and cellulose sulphate.* J Microencapsul, 2007. **24**(1): p. 20-39.

43. Wang, T., et al., *Successful allotransplantation of encapsulated islets in pancreatectomized canines for diabetic management without the use of immunosuppression.* Transplantation, 2008. **85**(3): p. 331-7.
44. Qi, M., et al., *A recommended laparoscopic procedure for implantation of microcapsules in the peritoneal cavity of non-human primates.* J Surg Res, 2011. **168**(1): p. e117-23.
45. Rokstad, A.M., et al., *Alginate microbeads are complement compatible, in contrast to polycation containing microcapsules, as revealed in a human whole blood model.* Acta Biomater., 2011. **7**(6): p. 2566-2578.
46. Rokstad, A.M., *Personal communication*.
47. Tuch, B.E., et al., *Safety and viability of microencapsulated human islets transplanted into diabetic humans.* Diabetes Care, 2009. **32**(10): p. 1887-9.
48. Andersen, T., et al., *Alginates as biomaterials in tissue engineering.* Carbohydrate Chemistry, 2012. **37**: p. 227-258.
49. Calafiore, R., et al., *Microencapsulated pancreatic islet allografts into nonimmunosuppressed patients with type 1 diabetes: first two cases.* Diabetes Care, 2006. **29**(1): p. 137-8.
50. Fonseca, K.B., et al., *Molecularly designed alginate hydrogels susceptible to local proteolysis as three-dimensional cellular microenvironments.* Acta Biomater, 2011. **7**(4): p. 1674-82.
51. Rowley, J.A., G. Madlambayan, and D.J. Mooney, *Alginate hydrogels as synthetic extracellular matrix materials.* Biomaterials, 1999. **20**(1): p. 45-53.
52. Bidarra, S.J., et al., *Injectable in situ crosslinkable RGD-modified alginate matrix for endothelial cells delivery.* Biomaterials, 2011. **32**(31): p. 7897-904.
53. Gobin, A.S. and J.L. West, *Val-ala-pro-gly, an elastin-derived non-integrin ligand: smooth muscle cell adhesion and specificity.* J Biomed Mater Res A, 2003. **67**(1): p. 255-9.
54. Heilshorn, S.C., et al., *Endothelial cell adhesion to the fibronectin CS5 domain in artificial extracellular matrix proteins.* Biomaterials, 2003. **24**(23): p. 4245-52.
55. Humphries, M.J., et al., *Identification of an alternatively spliced site in human plasma fibronectin that mediates cell type-specific adhesion.* J Cell Biol, 1986. **103**(6 Pt 2): p. 2637-47.
56. Xie, M., et al., *Biocomposites prepared by alkaline phosphatase mediated mineralization of alginate microbeads.* RSC Advances, 2012. **2**(4): p. 1457-1465.
57. Bernhardt, A., et al., *Proliferation and osteogenic differentiation of human bone marrow stromal cells on alginate-gelatine-hydroxyapatite scaffolds with anisotropic pore structure.* J Tissue Eng Regen Med, 2009. **3**(1): p. 54-62.
58. Dittrich, R., et al., *Scaffolds for hard tissue engineering by ionotropic gelation of alginate–influence of selected preparation parameters.* Journal of the American Ceramic Society, 2007. **90**(6): p. 1703-1708.
59. Xie, M., et al., *Alginate-controlled formation of nanoscale calcium carbonate and hydroxyapatite mineral phase within hydrogel networks.* Acta Biomater, 2010. **6**(9): p. 3665-75.
60. Lappegard, K.T., et al., *Artificial surface-induced cytokine synthesis: Effect of heparin coating and complement inhibition.* Annals of Thoracic Surgery, 2004. **78**(1): p. 38-45.
61. Rokstad, A.M., et al., *The induction of cytokines by polycation containing microspheres by a complement dependent mechanism.* Biomaterials, 2013. **34**(3): p. 621-30.

62. Mollnes, T.E., et al., *Essential role of the C5a receptor in E coli-induced oxidative burst and phagocytosis revealed by a novel lepirudin-based human whole blood model of inflammation.* Blood, 2002. **100**(5): p. 1869-77.
63. Murphy, K., P. Travers, and M. Walport, *Janeway's immunobiology, 8th edition*. 2012, New York, USA: Garland Science.
64. Kindt, T.J., R.A. Goldsby, and B.A. Osborne, *Kuby Immunology 6th edition*. 2007, New York, NY 10010: W. H. Freeman and Company.
65. Rinder, C.S., et al., *BLOCKADE OF C5A AND C5B-9 GENERATION INHIBITS LEUKOCYTE AND PLATELET ACTIVATION DURING EXTRACORPOREAL-CIRCULATION.* Journal of Clinical Investigation, 1995. **96**(3): p. 1564-1572.
66. Rinder, C.S., et al., *Leukocyte effects of C5a-receptor blockade during simulated extracorporeal circulation.* Annals of Thoracic Surgery, 2007. **83**(1): p. 146-152.
67. Andersson, J., et al., *Binding of C3 fragments on top of adsorbed plasma proteins during complement activation on a model biomaterial surface.* Biomaterials, 2005. **26**(13): p. 1477-85.
68. Toda, M., et al., *Complement activation on surfaces carrying amino groups.* Biomaterials, 2008. **29**(4): p. 407-17.
69. Pan, Z.K., *Anaphylatoxins C5a and C3a induce nuclear factor kappaB activation in human peripheral blood monocytes.* Biochim Biophys Acta, 1998. **1443**(1-2): p. 90-8.
70. Ahamed, J., et al., *C3a enhances nerve growth factor-induced NFAT activation and chemokine production in a human mast cell line, HMC-1.* J Immunol, 2004. **172**(11): p. 6961-8.
71. Monsinjon, T., et al., *Regulation by complement C3a and C5a anaphylatoxins of cytokine production in human umbilical vein endothelial cells.* FASEB J, 2003. **17**(9): p. 1003-14.
72. Monsinjon, T., et al., *C3A binds to the seven transmembrane anaphylatoxin receptor expressed by epithelial cells and triggers the production of IL-8.* FEBS Lett, 2001. **487**(3): p. 339-46.
73. Nilsson, B., et al., *The role of complement in biomaterial-induced inflammation.* Molecular Immunology, 2007. **44**(1-3): p. 82-94.
74. Tegla, C.A., et al., *Membrane attack by complement: the assembly and biology of terminal complement complexes.* Immunol Res, 2011. **51**(1): p. 45-60.
75. Schrezenmeier, H. and B. Höchsmann, *Drugs that inhibit complement.* Transfusion and Apheresis Science, 2012. **46**(1): p. 87-92.
76. Hakim, R.M., *Chapter 18 Complement activation by biomaterials.* Cardiovascular Pathology, 1993. **2**(3, Supplement): p. 187-197.
77. Gorbet, M.B. and M.V. Sefton, *Biomaterial-associated thrombosis: roles of coagulation factors, complement, platelets and leukocytes.* Biomaterials, 2004. **25**(26): p. 5681-5703.
78. Andersson, J., *Complement Activation Triggered by Biomaterial Surfaces*, in *Department of Oncology, Radiology and Clinical Immunology*2003, Uppsala University: Uppsala.
79. Bexborn, F., et al., *The tick-over theory revisited: formation and regulation of the soluble alternative complement C3 convertase (C3(H2O)Bb).* Mol Immunol, 2008. **45**(8): p. 2370-9.
80. Agarwal, S., et al., *An evaluation of the role of properdin in alternative pathway activation on Neisseria meningitidis and Neisseria gonorrhoeae.* J Immunol, 2010. **185**(1): p. 507-16.
81. Kemper, C., J.P. Atkinson, and D.E. Hourcade, *Properdin: emerging roles of a pattern-recognition molecule.* Annu Rev Immunol, 2010. **28**: p. 131-55.

82. Ricklin, D. and J.D. Lambris, *Compstatin: a complement inhibitor on its way to clinical application.* Current Topics in Complement II, 2008: p. 262-281.
83. Ember, J.A., et al., *Induction of interleukin-8 synthesis from monocytes by human C5a anaphylatoxin.* The American journal of pathology, 1994. **144**(2): p. 393.
84. Qu, H., et al., *New analogs of the clinical complement inhibitor compstatin with subnanomolar affinity and enhanced pharmacokinetic properties.* Immunobiology, 2012.
85. Oikonomopoulou, K., et al., *Interactions between coagulation and complement—their role in inflammation.* Seminars in Immunopathology, 2012. **34**(1): p. 151-165.
86. Mackman, N., R.E. Tilley, and N.S. Key, *Role of the extrinsic pathway of blood coagulation in hemostasis and thrombosis.* Arterioscler Thromb Vasc Biol, 2007. **27**(8): p. 1687-93.
87. Leatham, E.W., et al., *Increased monocyte tissue factor expression in coronary disease.* Br Heart J, 1995. **73**(1): p. 10-3.
88. Celi, A., et al., *P-selectin induces the expression of tissue factor on monocytes.* Proceedings of the National Academy of Sciences, 1994. **91**(19): p. 8767-8771.
89. Ohtsuka, H., et al., *Thrombin generates monocyte chemotactic activity from complement factor H.* Immunology, 1993. **80**(1): p. 140-5.
90. Sorensen, I., et al., *Fibrinogen, acting as a mitogen for tubulointerstitial fibroblasts, promotes renal fibrosis.* Kidney Int, 2011. **80**(10): p. 1035-44.
91. Knesek, D., T.C. Peterson, and D.C. Markel, *Thromboembolic Prophylaxis in Total Joint Arthroplasty.* Thrombosis, 2012. **2012**: p. 8.
92. Weiler, J.M., et al., *Heparin and modified heparin inhibit complement activation in vivo.* J Immunol, 1992. **148**(10): p. 3210-5.
93. Kirschfink, M. and T. Borsos, *Binding and activation of C4 and C3 on the red cell surface by non-complement enzymes.* Mol Immunol, 1988. **25**(5): p. 505-12.
94. Engberg, A.E., *Biomaterials and Hemocompatibility*, in *School of Natural Sciences*2010, Linnaeus University: Kalmar, Växjö.
95. Sperling, C., et al., *Blood coagulation on biomaterials requires the combination of distinct activation processes.* Biomaterials, 2009. **30**(27): p. 4447-4456.
96. Ekdahl, K.N., et al., *Innate immunity activation on biomaterial surfaces: A mechanistic model and coping strategies.* Advanced Drug Delivery Reviews, 2011. **63**(12): p. 1042-1050.
97. Arima, Y., M. Toda, and H. Iwata, *Surface plasmon resonance in monitoring of complement activation on biomaterials.* Advanced Drug Delivery Reviews, 2011. **63**(12): p. 988-999.
98. Arima, Y., et al., *Complement activation by polymers carrying hydroxyl groups.* ACS Appl Mater Interfaces, 2009. **1**(10): p. 2400-7.
99. Ferraz, N., et al., *Nanoporesize affects complement activation.* J Biomed Mater Res A, 2008. **87**(3): p. 575-81.
100. Xie, H., et al., *Basic properties of alginate/chitosan microcapsule surfaces and their interaction with proteins.* J Control Release, 2011. **152 Suppl 1**: p. e246-8.
101. Bacakova, L., et al., *Modulation of cell adhesion, proliferation and differentiation on materials designed for body implants.* Biotechnol Adv, 2011. **29**(6): p. 739-67.
102. Muhlfelder, T.W., et al., *C5 chemotactic fragment induces leukocyte production of tissue factor activity: a link between complement and coagulation.* J Clin Invest, 1979. **63**(1): p. 147-50.
103. Markiewski, M.M., et al., *Complement and coagulation: strangers or partners in crime?* Trends Immunol, 2007. **28**(4): p. 184-92.

104. Nilsson, B., et al., *Can cells and biomaterials in therapeutic medicine be shielded from innate immune recognition?* Trends Immunol, 2010. **31**(1): p. 32-8.
105. Polley, M.J. and R.L. Nachman, *Human complement in thrombin-mediated platelet function: uptake of the C5b-9 complex.* J Exp Med, 1979. **150**(3): p. 633-45.
106. Ørning, M.P.A., *Alginate Microcapsules for Cell Therapy: Effect of capsule composition on complement activation, cytokine secretion, and protein adsorption in a whole blood model*, in *Department of Biotechnology*2012, NTNU: Trondheim.
107. Westhrin, M., *Encapsulation of human mesenchymal stem cells in phosphate mineralized alginate beads*, in *Department of Physics*2011, NTNU: Trondheim, Norway.
108. Haberzettl, P., et al., *Actin plays a crucial role in the phagocytosis and biological response to respirable quartz particles in macrophages.* Arch Toxicol, 2007. **81**(7): p. 459-70.
109. Todd, R.F., 3rd, *The continuing saga of complement receptor type 3 (CR3).* J Clin Invest, 1996. **98**(1): p. 1-2.
110. Mollnes, T.E., T. Lea, and M. Harboe, *Detection and quantification of the terminal C5b-9 complex of human complement by a sensitive enzyme-linked immunosorbent assay.* Scand J Immunol, 1984. **20**(2): p. 157-66.
111. Bennett, J.S., *Platelet-fibrinogen interactions.* Ann N Y Acad Sci, 2001. **936**: p. 340-54.
112. Bio-Rad Laboratories, I. *Bio-Plex Pro™ Assays - Diabetes Instruction Manual*. Available from: http://www.bio-rad.com/webroot/web/pdf/lsr/literature/10010747.pdf.
113. Grandjean-Laquerriere, A., et al., *Involvement of toll-like receptor 4 in the inflammatory reaction induced by hydroxyapatite particles.* Biomaterials, 2007. **28**(3): p. 400-4.
114. Morimoto, S., et al., *Comparative study on in vitro biocompatibility of synthetic octacalcium phosphate and calcium phosphate ceramics used clinically.* Biomed Mater, 2012. **7**(4): p. 045020.
115. Scislowska-Czarnecka, A., et al., *Ceramic modifications of porous titanium: effects on macrophage activation.* Tissue Cell, 2012. **44**(6): p. 391-400.
116. Zhao, X., et al., *Cytotoxicity of hydroxyapatite nanoparticles is shape and cell dependent.* Arch Toxicol, 2012.
117. Kao, W.J., et al., *Fibronectin modulates macrophage adhesion and FBGC formation: the role of RGD, PHSRN, and PRRARV domains.* J Biomed Mater Res, 2001. **55**(1): p. 79-88.
118. Phillips, J.M. and W.J. Kao, *Macrophage adhesion on gelatin-based interpenetrating networks grafted with PEGylated RGD.* Tissue Eng, 2005. **11**(5-6): p. 964-73.
119. Morch, Y.A., et al., *Binding and leakage of barium in alginate microbeads.* J Biomed Mater Res A, 2012. **100**(11): p. 2939-47.
120. Otterlei, M., et al., *Induction of cytokine production from human monocytes stimulated with alginate.* J Immunother (1991), 1991. **10**(4): p. 286-91.
121. Espevik, T., et al. *Mechanisms of the host immune response to alginate microcapsules*. 2009. Transworld Research Network.
122. Diya, Z., et al., *Lipopolysaccharide (LPS) of Porphyromonas gingivalis induces IL-1beta, TNF-alpha and IL-6 production by THP-1 cells in a way different from that of Escherichia coli LPS.* Innate Immun, 2008. **14**(2): p. 99-107.
123. O'Sullivan, E.S., et al., *Islets transplanted in immunoisolation devices: a review of the progress and the challenges that remain.* Endocr Rev, 2011. **32**(6): p. 827-44.

124. Strunk, R.C., K.S. Kunke, and P.C. Giclas, *Human peripheral blood monocyte-derived macrophages produce haemolytically active C3 in vitro.* Immunology, 1983. **49**(1): p. 169-74.
125. Murphy, F.A., et al., *The mechanism of pleural inflammation by long carbon nanotubes: interaction of long fibres with macrophages stimulates them to amplify pro-inflammatory responses in mesothelial cells.* Part Fibre Toxicol, 2012. **9**: p. 8.
126. Darrabie, M.D., W.F. Kendall, Jr., and E.C. Opara, *Characteristics of Poly-L-Ornithine-coated alginate microcapsules.* Biomaterials, 2005. **26**(34): p. 6846-52.
127. Tam, S.K., et al., *Physicochemical model of alginate-poly-L-lysine microcapsules defined at the micrometric/nanometric scale using ATR-FTIR, XPS, and ToF-SIMS.* Biomaterials, 2005. **26**(34): p. 6950-61.
128. Boor, P., et al., *Complement C5 mediates experimental tubulointerstitial fibrosis.* J Am Soc Nephrol, 2007. **18**(5): p. 1508-15.
129. Rabiet, M.J., et al., *Prothrombin fragment 1 X 2 X 3, a major product of prothrombin activation in human plasma.* J Biol Chem, 1986. **261**(28): p. 13210-5.
130. Kuonen, F., C. Secondini, and C. Ruegg, *Molecular pathways: emerging pathways mediating growth, invasion, and metastasis of tumors progressing in an irradiated microenvironment.* Clin Cancer Res, 2012. **18**(19): p. 5196-202.
131. Rhee, P., et al., *Recombinant humanized monoclonal antibody against CD18 (rhuMAb CD18) in traumatic hemorrhagic shock: results of a phase II clinical trial. Traumatic Shock Group.* J Trauma, 2000. **49**(4): p. 611-9; discussion 619-20.
132. Jones, R., *Rovelizumab (ICOS Corp).* IDrugs, 2000. **3**(4): p. 442-6.
133. Berckmans, R.J., et al., *Cell-derived vesicles exposing coagulant tissue factor in saliva.* Blood, 2011. **117**(11): p. 3172-80.

A Additional experiments – Protein deposition and cell adhesion

A.1 Fibrinogen deposition on HA-containing and epimerized microbeads

Figure A1 shows the fibrinogen deposition after incubation of microbeads and microcapsules in whole blood. The HA-mineralized microbeads appeared to induce more fibrinogen deposition than the control Ca-bead. The epimerized microbeads as well as TAM and AP all showed high amounts of fibrinogen adsorption. However, due to substantial background fluorescence as seen for the negative control antibody, the results were not considered to be reliable. Furthermore, fibrinogen was not seen on AP and TAM capsules after incubation in plasma (figure 3.6), which further supports the implications that the present results may not be trustworthy.

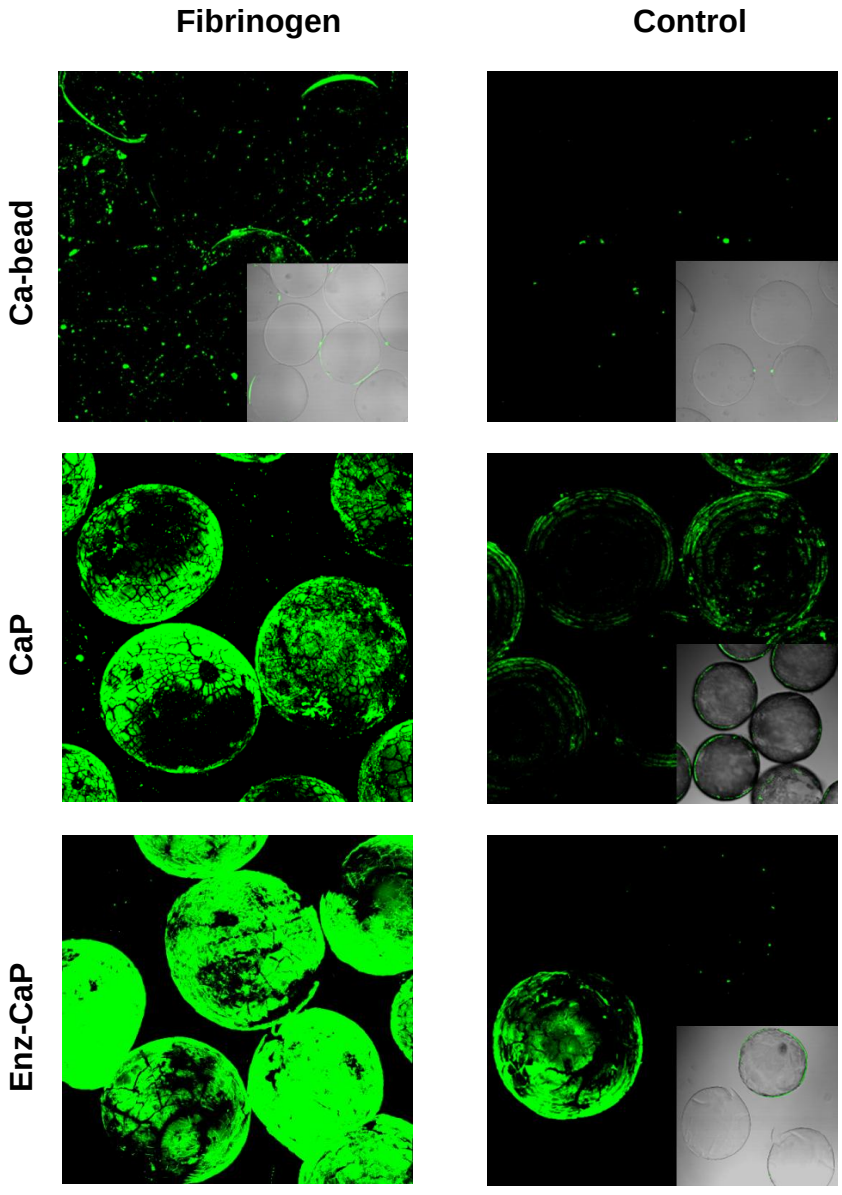

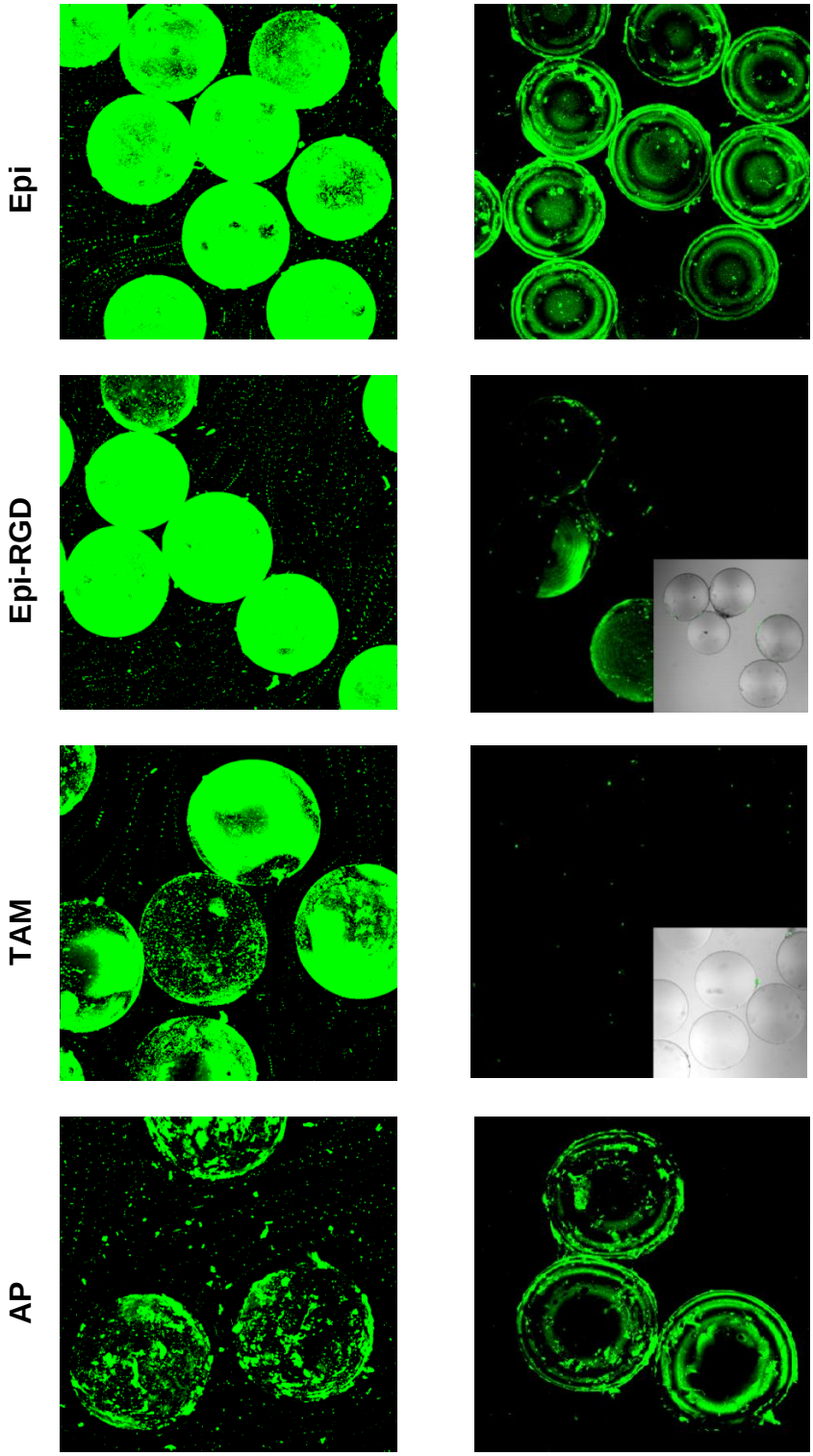

Figure A1. Fibrinogen adsorption after incubation 4 hours in whole blood on HA-containing and epimerized microbeads, with AP and TAM as positive and negative controls, respectively.

A.2 Cell adhesion on hollow versus solid microcapsules

Figure A2 shows the cell adhesion on microcapsules with a hollow and a solid core after incubation in whole blood. Some of the hollow microcapsules were burst, containing large amounts of cells inside. The solid microcapsules did not appear to suffer osmotic swelling. The hollow microcapsules showed lower amounts of attached leukocytes on their surface as compared with the solid microcapsules.

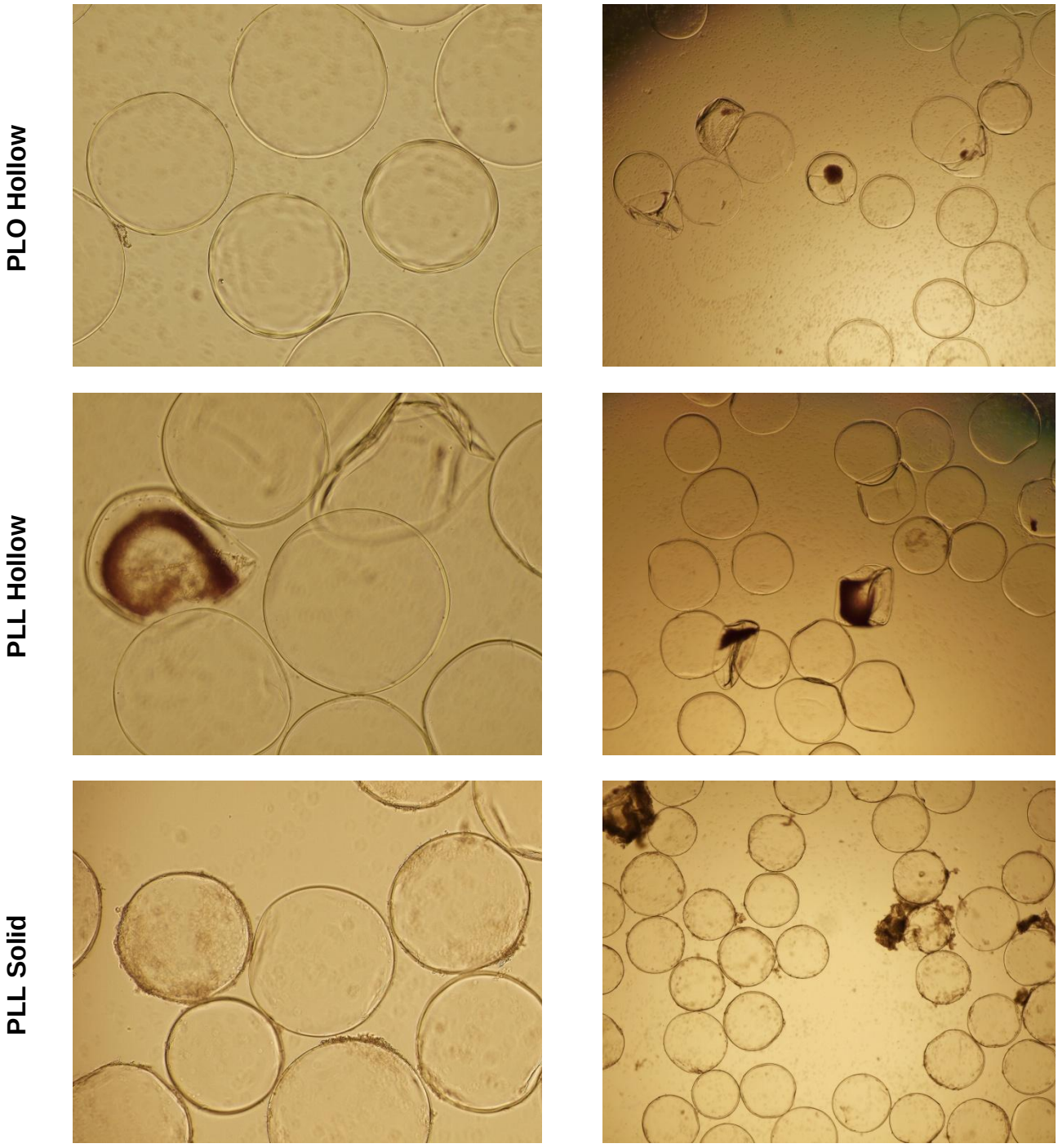

Figure A2. Cell adhesion on hollow versus solid capsules after incubation 4 hours in whole blood.

A.3 Cell adhesion and receptor expression

In order to explore capsule-cell-interactions at the alginate microcapsule surface, AP-capsules were incubated in whole blood and stained for different cellular markers. These experiments aimed to give an indication of which cell types are present, and in what numbers, in addition to the overall level of cell adhesion on the capsule surfaces. We also aimed to establish a protocol for examining the expression patterns of tissue factor (TF) on attached cells, which is expressed by monocytes upon activation. Furthermore, a time study was performed to explore potential time-dependent cell events on the capsules. To do this, AP-microcapsules exposed to anticoagulated whole blood were stained for different cellular markers with fluorochrome-labeled αCD11b, αCD14 and αTF antibodies as well as the corresponding negative control antibodies (see table 2.5). Results from the confocal imaging of the capsules are shown in figures A3-A4, in which FITC-fluorescence is shown in green, PE in red, and APC in blue. The results show signs of the fact that the employed method was not fully established and needs optimization in order to produce more reliable and informative results.

Figure A3 illustrates the responses for AP-microcapsules incubated 4 hours in whole blood before staining with specific antibodies towards CD14, CD11b and TF. The results indicated that the microcapsules had a substantial amount of CD11b-positive cells attached, which is consistent with previous findings [45]. For the microcapsules stained for αTF-FITC, a considerable amount of FITC-fluorescence was generally detected, also on areas of the microcapsule surface with no cells attached. The exception to this was when the αTF antibody was co-incubated with αCD11b antibody, for which a minor amount of TF-positive cells were observed. Fluorescence from antibodies specific for TF as well as CD14 did generally not appear to overlap on the same cells. This was in contrast to expectations, as activated monocytes express both these cellular markers. Regardless, it appeared that the antibodies were specific towards their respective markers, as demonstrated by the negative controls.

Figure A4 shows the results for the time study in which AP-microcapsules were incubated in whole blood for 3, 6 and 24 hours, respectively. For the microcapsules stained for both αCD11b and αCD14, a fair amount of CD11b-positive cells were detected after 3 and 6 hours, but not after 24 hours. Furthermore, a minor amount of CD14-positive cells were seen after 3 and 6 hours, with slightly more after 24 hours. However, the microcapsules generally showed a much larger amount of CD14-detection when stained only with αCD14 antibody, than when co-stained with αCD11b-antibody. Microcapsules stained only for αCD14 showed fair amounts of CD14-positive cells after 3 and 24 hours, but not after 6 hours. This was likely due to an error performed during the experiment which led to no antibody being added to the respective sample. The samples stained with negative control antibodies indicated that the employed antibodies were specific towards their respective cellular markers.

To sum up, the results were variable and implied that the outcome depended on the specific combination of antibodies. A reason for the substantial TF-detection on areas of the microcapsules surfaces with no cells attached could potentially be due to the adsorption of intravascular TF, which is present on circulating cell-derived vesicles [133]. It generally appeared that many of the antibodies employed in these studies had a counteracting effect on

each other, leading to ambiguous results. A possible reason for the observed results could be that the antibodies influenced each other's binding specificity, or – in the case of using antibodies specific towards the same marker – that one antibody outcompeted the other in pursuit of the same epitope. Moreover, another reason for the variable results in the present study might have been some degree of spectral overlap between the employed fluorochromes, with associated difficulties with the confocal settings. This might have led to a misrepresentation of the actual cell adhesion and surface receptor profiles.

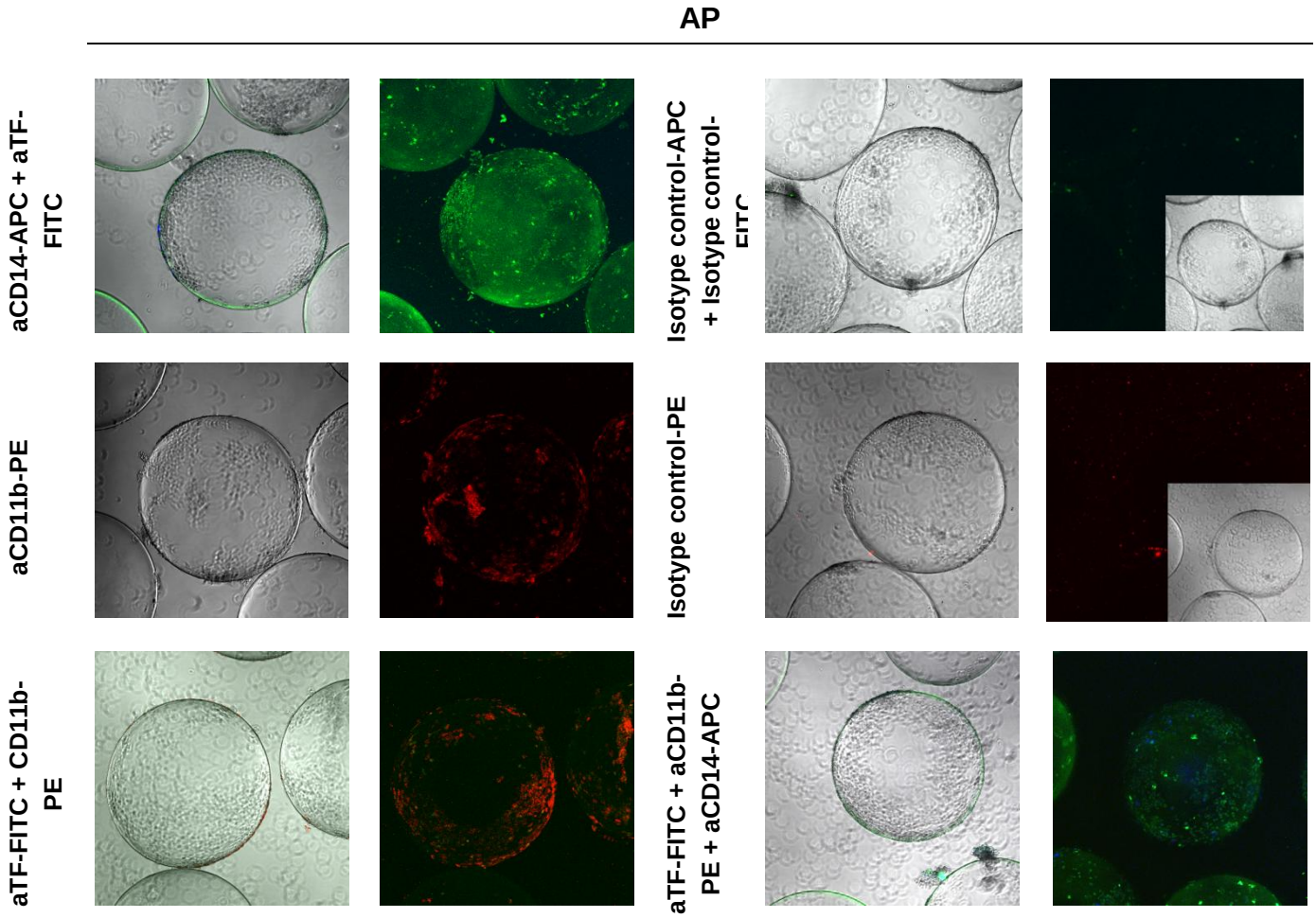

Figure A3. AP-microcapsules are incubated in whole blood for 4 hours before fixing attached cells. Microcapsules are stained with aCD14-APC, aTF-FITC, aCD11b-PE and isotype controls. Blue fluorescence is APC, red fluorescence is PE and green fluorescence is FITC. Microcapsules are displayed as equatorial section through the capsules, and as 3D projections.

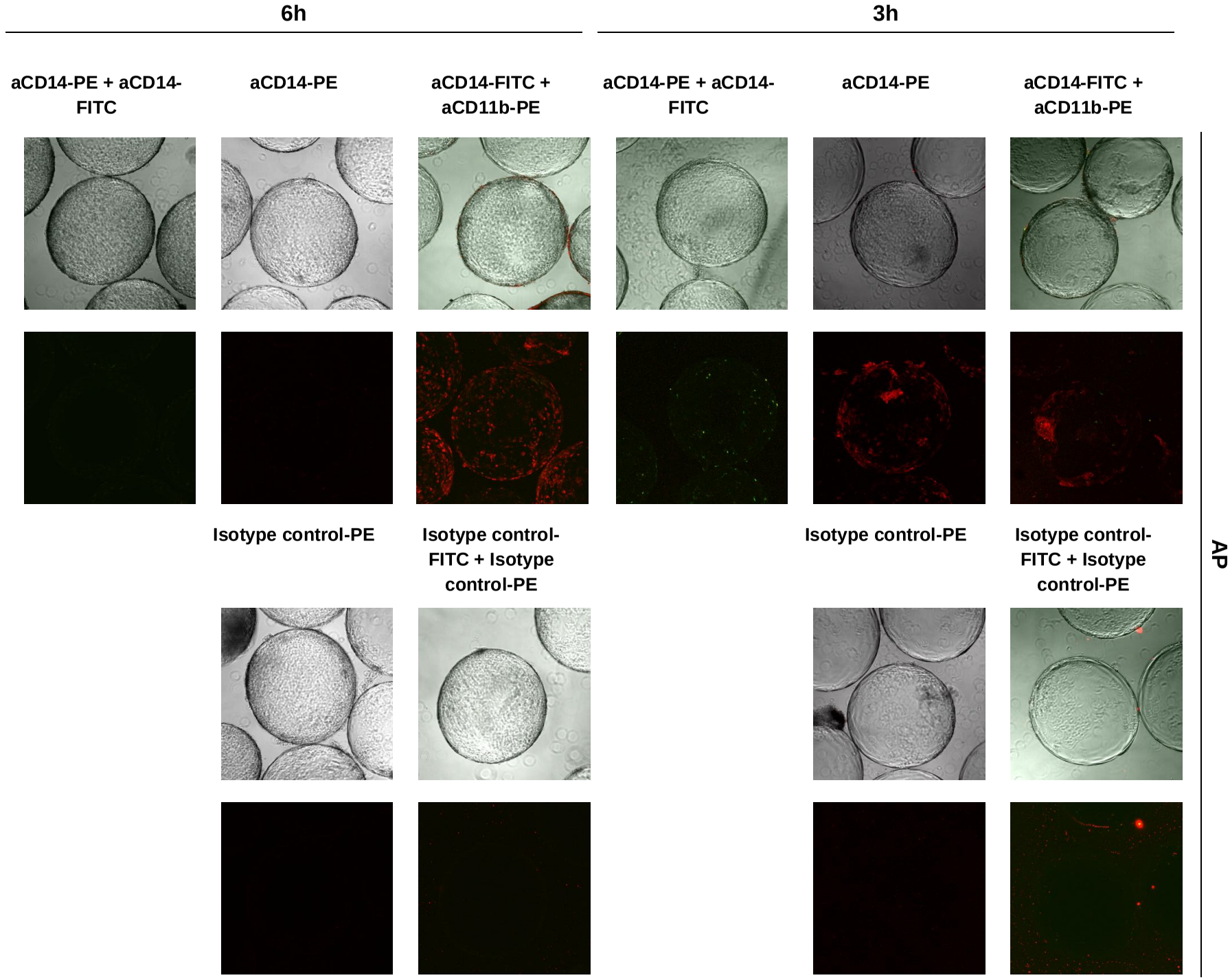
6h
3h
aCD14-PE + aCD14-FITC
aCD14-PE
aCD14-FITC + aCD11b-PE
aCD14-PE + aCD14-FITC
aCD14-PE
aCD14-FITC + aCD11b-PE
Isotype control-PE
Isotype control-FITC + Isotype control-PE
Isotype control-PE
Isotype control-FITC + Isotype control-PE
AP

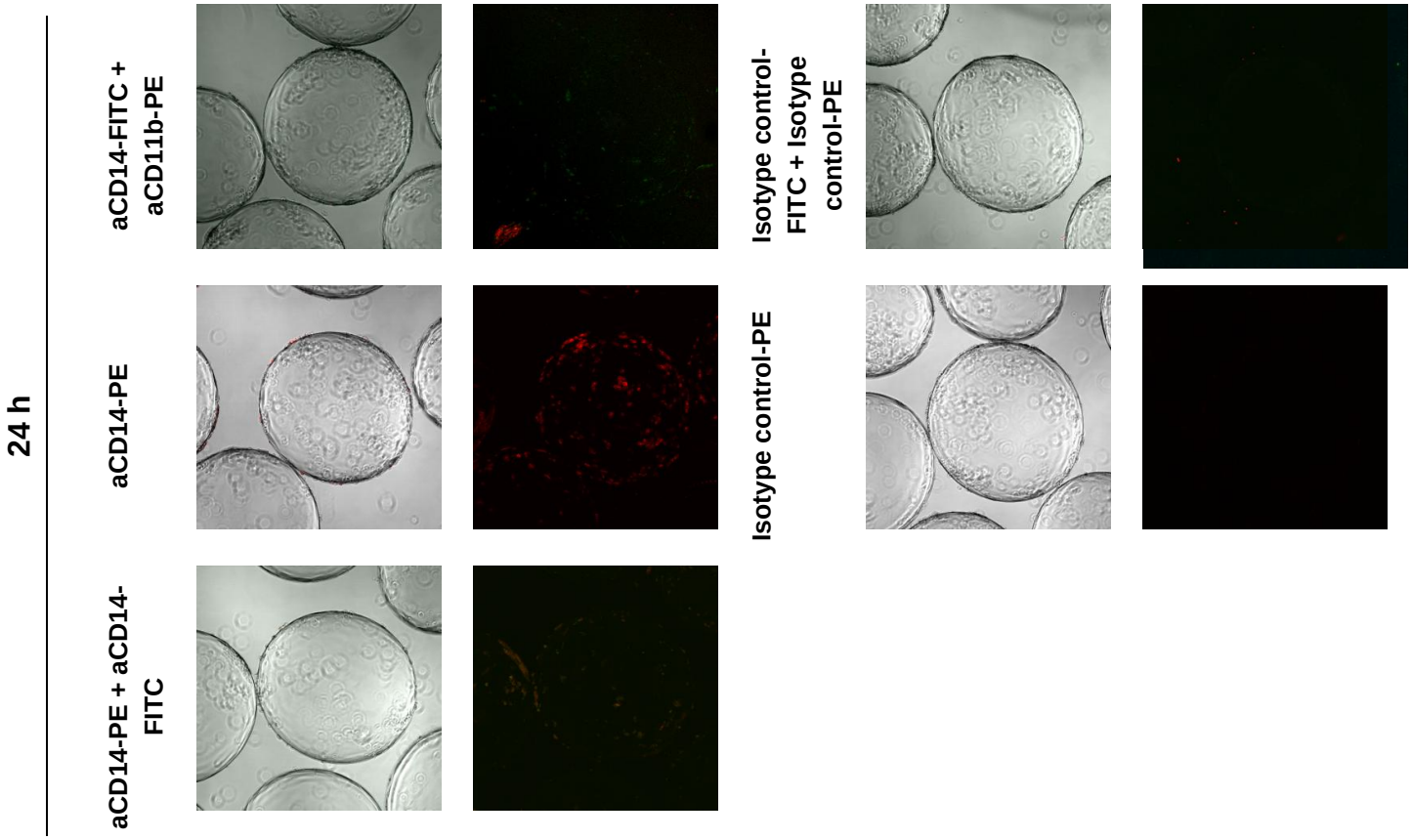

Figure A4. AP-microcapsules are incubated in whole blood for 3, 6 and 24 hours. Microcapsules are stained with αCD14-PE, αCD14-FITC and αCD11b-PE as well as isotype controls. Red fluorescence is PE, green fluorescence is FITC. Microcapsules are displayed as equatorial section through the capsules, and as 3D projections.

B Flow cytometry data

Tables B1-B2 below shows the CD11b expression levels measured as median fluorescence intensity (MFI) for the individual donors for the preliminary and main study, respectively.

B.1 Preliminary study

Table B1. CD11b expression on leukocytes for one donor after incubation of capsules 1 hour in whole blood, measured as MFI.

Sample	**Monocytes**	**Granulocytes**
T0	68,2	38,2
Saline	371,8	361,9
Ca-bead	269	25,3
CaP	437,1	465,6
Enz-CaP	276,3	266,6
TAM	216,7	181,1
AP	385,4	465,6
Epi	850,5	827,9
Epi-RGD	763,5	770,4
Zymosan	296,9	491,4

B.2 Main study – Peptide-coupled and hydroxyapatite-containing capsules

Donor 5 has several values substantially higher than those of the other four donors, thereby demonstrating biological differences between individuals. However, the baseline values (T0) for donor 5 are similar to T0 for the other donors, implicating that donor 5 is healthy.

Table B2. CD11b expression on leukocytes for five donors after incubation of capsules 1 hour in whole blood, measured as MFI. Values for the AP-sample for donor 2 were lost. Mono = monocytes; gran = granulocytes.

	Donor 1		**Donor 2**		**Donor 3**		**Donor 4**		**Donor 5**	
Sample	Mono	Gran	Mono	Gran	Mono	Gran	Mono	Gran	Mono	Gran
T0	199	131	479	157	133	85	160	146	173	150
Saline	478	526	539	266	519	792	245	231	1566	2344
M REDV	423	480	579	286	230	258	407	234	1629	2083
VAPG	1984	1287	5360	3770	1734	2183	3432	2660	3443	3693
G RGD	487	383	641	275	280	657	259	210	1274	1747
M RGD	707	595	822	318	288	503	234	204	471	587
UP-MVM	725	421	730	284	259	343	300	206	816	1380
Ca	476	504	720	292	400	1064	269	210	613	1161
CaP	524	751	1423	940	457	1245	819	1011	877	1198
Enz-CaP	569	426	479	288	410	1077	440	335	623	1049
TAM4	536	486	616	245	245	242	292	247	1655	2119
APA	504	631	908	402	825	1597	310	294	1388	1713
AP	690	968	-	-	438	1454	1029	1141	1191	1726
PMCG	1189	1197	1849	1258	905	1797	1852	1545	1644	2400
Zymosan	1653	2715	2813	4489	951	3125	1338	2374	1810	2800

C ELISA data

Tables C1-C5 below shows the ELISA data for the individual donors for the preliminary and main study, as well as the complement and leukocyte inhibition studies, respectively.

C.1 Preliminary study

Table C1. sTCC, IL-8 and TNF-α data for one donor after incubation of capsules 4 hours in whole blood, measured in AU/ml, pg/ml and pg/ml, respectively.

Sample	**sTCC**	**IL-8**	**TNF-α**
T0	0,41	60	16,7
Saline	12,4	1460	32,7
Ca-bead	5,9	360	31,5
CaP	48,9	1951	43,8
Enz-CaP	15,4	1059	30,4
TAM	3,7	615	34
AP	42,7	448	107
Epi	4,6	5656	1703
Epi-RGD	5,02	4523	1049
Zymosan	217,9	13163,2	22045,6

C.2 Main study – Peptide-coupled and hydroxyapatite-containing capsules

Table C2. sTCC data for five donors after incubation of capsules 4 hours in whole blood, measured in AU/ml. APA and AP values are lacking for donor 4.

Sample	**Donor 1**	**Donor 2**	**Donor 3**	**Donor 4**	**Donor 5**
T0	0,445	0,421	0,494	0,479	0,522
Saline	14,083	5,311	20,859	11,591	14,778
M REDV	4,672	3,727	6,286	4,037	5,472
G VAPG	4,266	3,016	4,217	3,540	3,887
G RGD	4,417	3,335	5,673	3,603	5,052
M RGD	4,551	3,549	4,145	3,253	4,625
UP-MVM	5,851	2,350	7,504	17,037	5,734
Ca	11,636	5,764	9,776	6,047	5,137
CaP	26,245	31,063	19,564	30,356	13,255
Enz-CaP	12,702	9,529	17,840	10,783	17,143
TAM4	4,016	2,028	7,642	3,316	4,741
APA	104,378	85,235	100,416	-	41,577
AP	145,066	163,597	167,525	-	145,798
PMCG	44,185	32,805	32,872	34,306	42,794
Zymosan	171,458	129,768	171,489	151,297	147,941

C.3 Complement inhibition study with compstatin

The trends in the sTCC data below are generally stable, with two exceptions for donor B, which are marked in red. These values are significantly higher than the corresponding values from donor A and C, and are excluded from the figures in the results section. One explanation may be that the PLL Solid microcapsules used in the whole blood experiment with donor B had swelled and become partly hollow, with fragments leaking out of the capsule evoking a more hollow-like response. Furthermore, it cannot be excluded that a mistake of contents had occurred and that the PLL Solid microcapsules for donor B were actually the PLL Hollow microcapsules. In terms of the IL-8 responses, these data also showed some variation, with donor C in many cases inducing noticeably lower responses than donor A and B.

Table C3. sTCC data for three donors after incubation of capsules 4 hours in whole blood containing no additive, compstatin or control peptide, measured in AU/ml. Aberrant values are shown in red.

Sample	**Donor A**	**Donor B**	**Donor C**
T0	0,445	0,663	0,660
Saline	10,454	11,899	14,289
PLO Hollow	30,811	23,618	31,044
PLL Hollow	112,399	160,830	128,935
PLL Solid	29,462	168,472	35,326
PLO Hollow + Compstatin	1,782	1,237	1,369
PLL Hollow + Compstatin	8,511	2,366	2,579
PLL Solid + Compstatin	1,385	1,091	1,052
PLO Hollow + Control peptide	18,600	13,038	17,479
PLL Hollow + Control peptide	109,157	155,829	103,769
PLL Solid + Control peptide	32,889	114,159	23,769
Zymosan	80,862	180,763	133,877

Table C4. IL-8 data for three donors after incubation of capsules 4 hours in whole blood containing no additive, compstatin or control peptide, measured in pg/ml.

Sample	**Donor A**	**Donor B**	**Donor C**
T0	23,329	26,728	23,072
Saline	1771,965	2607,721	1333,238
PLO Hollow	2103,623	2193,643	884,489
PLL Hollow	2145,279	2775,249	365,877
PLL Solid	6981,986	4133,645	4303,089
PLO Hollow + Compstatin	956,333	1048,312	139,471
PLL Hollow + Compstatin	2707,770	1511,487	155,346
PLL Solid + Compstatin	998,970	1284,237	151,833
PLO Hollow + Control peptide	3573,094	4251,042	1065,555
PLL Hollow + Control peptide	3845,863	2484,036	762,567
PLL Solid + Control peptide	11155,790	4898,502	4500,146
Zymosan	9475,244	8607,940	6467,596

C.4 Leukocyte inhibition study with cytochalasin D and CD11b-inhibiton

The data from this experiment demonstrates the importance of using the same volume proportions between blood and microcapsules throughout the assays. For donor A only 125 µl blood was employed, as opposed to the normal amount of 500 µl as for donor B and C, in order to reduce the spending of expensive materials (cytochalasin D and CD11b-inhibitory antibody). This appeared to produce noticeably different responses as the normal amount of microcapsules was present, leading to a very different blood/microcapsule ratio for the samples for donor A. This demonstrates that consistency is essential when performing parallel whole blood assays.

Table C4. IL-8 data for three donors after incubation of capsules 4 hours in whole blood containing no additive, CD11b-inhibitor, cytochalasin D or controls with ethanol or BSA + ethanol, measured in pg/ml. No APA + ethanol control was employed for donor A.

Sample	**Donor A**	**Donor B**	**Donor C**
T0	117,052	25,086	27,329
Saline	4152,109	2709,899	1599,622
APA + No additive	10160,980	3154,003	2436,991
APA + CD11b-inhibitor	8542,436	3239,585	4060,589
APA + 20 µM cytochalasin D	3039,211	1505,325	406,281
APA + 40 µM cytochalasin D	1993,775	744,364	247,565
APA + BSA control for 20 µM cytochalasin D	4656,133	2803,030	1610,509
APA + BSA control for 40 µM cytochalasin D	4151,218	1556,901	641,238
APA + ethanol	-	1180,494	683,549
Zymosan	10036,070	9063,117	4216,435

D Bio-Plex data

Cytokine levels in plasma after incubating alginate capsules in whole blood for 4 hours as measured by Bio-Plex are shown in tables D1-D12.

D.1 IL-8

Table D1. IL-8 levels for 5 donors. Values are in pg/ml. Values designated with an asterisk (*) are extrapolated beyond the standard range.

Sample	Donor 1	Donor 2	Donor 3	Donor 4	Donor 5
T0	2,78	1,88	*0,98	2,78	3,68
Saline	962,23	118,76	1101,12	551,99	1304,18
M REDV	638,56	99,47	273,13	205,35	1150,42
G VAPG	6831,23	1214,88	4357,96	3236,78	4030,99
G RGD	463,96	26,43	475,44	152,13	1075,25
M RGD	1166,34	60,63	687,74	225,41	826,81
UP-MVM	877,13	80,09	317,23	334,43	699,19
Ca	955,21	111,03	1963,35	406,92	1337,92
CaP	1160,23	735,9	1037,8	1519,57	1238,38
Enz-CaP	1254,36	67,02	1334,35	544,14	1163,62
TAM	554,52	44,39	580,2	270,06	911,53
APA	1592,1	1354,02	2055,75	1576,79	2266,38
AP	1535,02	2179,11	2757,07	4922,2	2897,69
PMCG	836,01	289,04	837,86	1334	1539,93
Zymosan	8593,65	2329,86	7237,88	3158,3	2527,21

D.2 MCP-1

Table D2. MCP-1 levels for 5 donors. Values are in pg/ml.

Sample	Donor 1	Donor 2	Donor 3	Donor 4	Donor 5
T0	33,01	22,04	17,2	26,83	43,83
Saline	90,89	20,78	81,28	48,46	83,48
M REDV	145,35	27,76	20,64	36,35	109,11
G VAPG	389,22	184,71	149,17	306,36	132,8
G RGD	65,01	23,7	23,7	31,85	80,18
M RGD	198,09	23,98	71,93	47,98	67,4
UP-MVM	129,73	26,42	21,9	33,53	80,84
Ca	171,01	30,41	51,34	41,74	117,26
CaP	412,56	168,05	34,82	256,31	85,24
Enz-CaP	198,28	16,91	111,42	54,43	91,97
TAM	66,26	20,08	39,62	45,79	91,32
APA	127,48	148,97	47,49	116,01	176,41
AP	194,81	112,68	70,46	119,13	169,63
PMCG	120,58	40,74	46,28	99,06	72,15
Zymosan	411,18	195,1	553,04	474,66	163,71

D.3 MIP-1α

Table D3. MIP-1α levels for 5 donors. Values are in pg/ml. Values designated with an asterisk (*) are extrapolated beyond the standard range.

Sample	Donor 1	Donor 2	Donor 3	Donor 4	Donor 5
T0	9,05	*1,05	*0,35	2,79	*0,35
Saline	143,68	36,29	89,07	36,37	138,73
M REDV	162,16	26,4	57,32	22,66	231,66
G VAPG	4499,48	1014,84	1706,86	1425,52	1814,29
G RGD	130,85	8,03	51,29	19,83	157,97
M RGD	232,49	19,83	77,22	23,85	130,21
UP-MVM	158,04	20,68	40,88	23,33	129,39
Ca	228,55	41,09	136,54	40,01	255,01
CaP	296,35	120,37	63,17	42,35	187,65
Enz-CaP	212,02	16,92	100,1	30,58	194,98
TAM	160,53	15,83	44,52	28,01	154,01
APA	276,36	97,48	84,27	66,6	187,79
AP	542,97	107,74	218,07	126,61	234,39
PMCG	973,44	82,35	220,27	248,01	577,38
Zymosan	2808,26	397,23	540,2	407,71	764,35

D.4 IL-1β

Table D4. IL-1β levels for 5 donors. Values are in pg/ml. Values designated with an asterisk (*) are extrapolated beyond the standard range.

Sample	Donor 1	Donor 2	Donor 3	Donor 4	Donor 5
T0	*0,18	*0,18	*0,02	*0,10	*0,02
Saline	6,04	1,79	2,59	3,29	4,94
M REDV	5,15	0,64	1,11	1,5	2,89
G VAPG	3859,6	512,09	1647,41	536,93	616,11
G RGD	2,69	*0,36	2,14	1,3	3,96
M RGD	8,98	0,45	2,84	2,39	2,09
UP-MVM	6,94	0,45	0,92	6,94	2,14
Ca	5,47	1,01	4,11	4,01	5,47
CaP	7,32	1,69	3,04	2,09	3,55
Enz-CaP	12,24	1,01	3,09	3,91	7,9
TAM	3,7	0,45	2,99	3,7	2,99
APA	8,76	3,5	5,68	8,33	9,52
AP	10,93	2,89	9,41	12,85	7,8
PMCG	144,94	36,98	36,68	52,05	165,97
Zymosan	209,24	10,39	30,84	36,86	83,55

D.5 IL-6

Table D5. IL-6 levels for 5 donors. Values are in pg/ml.

Sample	Donor 1	Donor 2	Donor 3	Donor 4	Donor 5
T0	0,81	0,49	5,11	0,49	0,49
Saline	101,6	5,64	23,32	16,11	32,88
M REDV	90,67	4,24	16,11	11,73	23,32
G VAPG	14456,54	11395,12	11160,07	10210,51	6358,9
G RGD	57,75	1,48	16,29	6,35	23,88
M RGD	71,57	4,24	35,71	14,64	21,65
UP-MVM	93,84	2,85	20,53	10,65	26,12
Ca	102,2	7,77	38,18	12,46	33,07
CaP	105,2	6,0	19,79	4,41	24,99
Enz-CaP	93,45	2,85	38,56	8,85	31,75
TAM	39,13	2,16	32,88	10,65	22,76
APA	141,72	10,11	37,42	13,19	23,88
AP	201,55	17,58	57,36	19,05	33,82
PMCG	1393,04	685,01	774,09	492,11	1083,34
Zymosan	3874,9	257,28	784,68	508,18	643,8

D.6 TNF-α

Table D6. TNF-α levels for 5 donors. Values are in pg/ml. Values designated with an asterisk (*) are extrapolated beyond the standard range. Values designated OOR < = out of range below.

Sample	Donor 1	Donor 2	Donor 3	Donor 4	Donor 5
T0	OOR <	OOR <	OOR <	9,21	OOR <
Saline	121,02	*0,14	46,58	37,86	157,4
M REDV	525,82	*2,45	40,04	40,04	118,88
G VAPG	22973,84	9464,73	10234,89	7682,57	6507,2
G RGD	343,25	OOR <	26,91	20,31	96,32
M RGD	198,99	20,31	13,67	40,04	122,09
UP-MVM	389,75	OOR <	*2,45	32,39	134,95
Ca	162,74	OOR <	122,09	92,01	167,01
CaP	83,39	*0,14	70,43	29,1	156,34
Enz-CaP	421,43	6,97	87,7	33,48	137,09
TAM	163,81	11,44	6,97	22,51	126,38
APA	227,71	40,04	OOR <	36,76	119,95
AP	676,39	*0,14	126,38	94,16	133,88
PMCG	3692,46	102,77	170,22	760,58	1402,37
Zymosan	426,7	18,1	171,28	820,55	1549,43

D.7 IL-10

Table D7. IL-10 levels for 5 donors. Values are in pg/ml. Values designated with an asterisk (*) are extrapolated beyond the standard range.

Sample	Donor 1	Donor 2	Donor 3	Donor 4	Donor 5
T0	*0,64	*0,19	2,37	*0,41	*0,41
Saline	*0,99	*0,41	1,61	*1,36	1,73
M REDV	*1,36	*0,64	5,17	1,61	3,15
G VAPG	3,95	4,22	4,76	4,35	6,98
G RGD	*1,11	*0,87	2,37	*1,11	*1,11
M RGD	2,11	*0,87	4,22	*1,11	2,11
UP-MVM	1,61	*0,52	4,49	*1,36	*1,11
Ca	1,61	*0,64	3,15	*1,36	1,86
CaP	1,86	*0,87	4,22	2,63	1,61
Enz-CaP	*1,36	*0,64	3,41	*1,11	1,86
TAM	1,61	*0,64	2,89	1,61	1,86
APA	1,61	*1,36	*1,36	1,61	1,61
AP	*1,36	*1,11	2,63	2,11	2,37
PMCG	*0,87	*1,36	5,31	2,37	3,41
Zymosan	2,37	*1,23	2,63	2,11	3,95

D.8 IL-1ra

Table D8. IL-1ra levels for 5 donors. Values are in pg/ml. Values designated with an asterisk (*) are extrapolated beyond the standard range.

Sample	Donor 1	Donor 2	Donor 3	Donor 4	Donor 5
T0	*4,23	19,16	76,73	19,16	OOR <
Saline	244,83	327,99	133,19	189,16	327,99
M REDV	438,49	175,2	355,65	272,59	383,28
G VAPG	2270,73	2298,9	851,77	1252,12	645,17
G RGD	383,28	62,49	314,15	217,02	272,59
M RGD	576,32	161,22	397,09	272,59	272,59
UP-MVM	438,49	133,19	410,89	355,65	189,16
Ca	410,89	410,89	286,45	327,99	300,3
CaP	576,32	383,28	300,3	397,09	244,83
Enz-CaP	521,21	33,75	244,83	327,99	272,59
TAM	327,99	48,17	534,99	355,65	258,71
APA	383,28	300,3	383,28	410,89	244,83
AP	410,89	410,89	327,99	548,77	161,22
PMCG	658,94	1072,43	603,86	631,4	410,89
Zymosan	438,49	300,3	355,65	300,3	355,65

D.9 PDGF-BB

Table D9. PDGF-BB levels for 5 donors. Values are in pg/ml. Values designated with an asterisk (*) are extrapolated beyond the standard range. Values designated OOR < = out of range below.

Sample	Donor 1	Donor 2	Donor 3	Donor 4	Donor 5
T0	*3,65	OOR <	OOR <	118,87	OOR <
Saline	239,72	62,67	95,72	319,54	1452,08
M REDV	364,63	59,2	93,21	389,45	1330,99
G VAPG	1317,33	28,77	371,61	606,12	1224,43
G RGD	163,48	37,04	706,91	325,77	635,55
M RGD	1218,04	87,35	432,83	244,44	737,99
UP-MVM	931,64	90,71	225,53	483,89	634,78
Ca	409,6	85,67	531,07	181,89	1117,79
CaP	458,37	752,76	395,65	685,95	825,22
Enz-CaP	790,13	39,76	629,35	578,26	1195,71
TAM	189,86	44,24	1116,21	927,71	1498,35
APA	238,15	425,09	490,08	776,89	1630,66
AP	197,02	624,71	769,1	840,84	1187,74
PMCG	140,07	124,6	598,38	513,28	616,19
Zymosan	1087,68	117,23	131,13	131,13	1937,42

D.10 VEGF

Table D10. VEGF levels for 5 donors. Values are in pg/ml. Values designated with an asterisk (*) are extrapolated beyond the standard range.

Sample	Donor 1	Donor 2	Donor 3	Donor 4	Donor 5
T0	50,03	9,44	*3,33	12,48	*0,22
Saline	36,57	50,53	54,51	37,57	42,56
M REDV	23,55	39,56	48,54	17,52	42,06
G VAPG	19,54	16,52	53,52	7,92	48,54
G RGD	21,55	*1,26	72,89	15	25,06
M RGD	18,53	27,06	86,28	16,52	30,57
UP-MVM	24,56	39,56	62,47	39,56	34,57
Ca	33,57	64,45	104,61	32,57	45,55
CaP	27,06	118,96	71,4	28,57	37,57
Enz-CaP	22,55	45,55	93,22	31,57	40,56
TAM	21,04	21,55	74,88	27,57	20,54
APA	50,53	108,07	43,55	73,89	55,51
AP	49,53	66,44	107,58	89,26	49,53
PMCG	45,55	81,33	85,29	46,54	72,4
Zymosan	15,51	146,65	39,56	35,57	47,54

D.11 RANTES

Table D11. RANTES levels for 5 donors. Values are in pg/ml. Values designated OOR < = out of range below.

Sample	Donor 1	Donor 2	Donor 3	Donor 4	Donor 5
T0	249,18	39,24	417,43	2965,39	45,32
Saline	962,65	149,97	1417,46	1197,97	3152,47
M REDV	1449,16	135,14	1449,05	1561,42	2644,03
G VAPG	6004,08	154,41	2907,19	2734,09	3580,51
G RGD	1004,98	107,57	3315,17	1443,13	1332,82
M RGD	3409,41	297,65	1829,3	1461,06	1969,62
UP-MVM	1841,07	634,58	1932,01	1939,91	1340
Ca	1596,08	357,82	3131,58	848,83	2203,52
CaP	1158,48	1640,95	3755,19	2045,94	2005,88
Enz-CaP	1867,35	121,45	4196,7	1410,98	2077,15
TAM	787,71	118,23	3147,14	1559,27	1530,27
APA	1660,33	307,46	OOR <	1085,75	3634,83
AP	1420,97	484,33	3490,7	2842,08	3418,35
PMCG	713,2	221,47	1035,15	1453,59	1894,03
Zymosan	4300,67	258,16	1375,32	978,02	5488,58

D.12 IFN-γ

Table D12. IFN-γ levels for 5 donors. Values are in pg/ml. Values designated with an asterisk (*) are extrapolated beyond the standard range. Values designated OOR < = out of range below.

Sample	Donor 1	Donor 2	Donor 3	Donor 4	Donor 5
T0	4,43	OOR <	OOR <	4,43	OOR <
Saline	16,29	16,29	16,29	OOR <	35,53
M REDV	26,31	26,31	56,64	16,29	87,24
G VAPG	72,31	44,24	68,47	35,53	52,58
G RGD	16,29	OOR <	35,53	4,43	16,29
M RGD	48,45	4,43	26,31	4,43	44,24
UP-MVM	16,29	4,43	35,53	16,29	4,43
Ca	4,43	16,29	56,64	26,31	16,29
CaP	35,53	OOR <	64,58	16,29	26,31
Enz-CaP	16,29	OOR <	44,24	OOR <	26,31
TAM	4,43	OOR <	44,24	16,29	26,31
APA	16,29	10,75	35,53	OOR <	16,29
AP	4,43	OOR <	35,53	4,43	4,43
PMCG	16,29	4,43	44,24	4,43	4,43
Zymosan	16,29	OOR <	16,29	OOR <	52,58

E Statistical analysis

Statistical analysis for the main study with the hydroxyapatite-containing and peptide-coupled microbeads was performed on the cytokine and sTCC levels as well as leukocyte activation in terms of CD11b expression after incubating the different capsules in whole blood for 4 hours. The software SPSS Statistics (v. 21, IBM) was used to perform Wilcoxon signed-rank tests. Differences were considered significant at $P < 0.05$. The output from SPSS Statistics is shown in tables E1-E30.

E.1 CD11b – monocytes

Table E1. Descriptive statistics – monocytes, CD11b-expression. n=5

Sample	Mean	Std. Deviation	Minimum	Maximum
T0	228,8	141,9	133,0	479,0
Saline	669,4	514,8	245,0	1566,0
M REDV	653,6	559,1	230,0	1629,0
G VAPG	3190,6	1449,6	1734,0	5360,0
G RGD	588,2	414,3	259,0	1274,0
M RGD	504,4	256,4	234,0	822,0
UP-MVM	566,0	264,4	259,0	816,0
Ca	495,6	176,8	269,0	720,0
CaP	820,0	382,8	457,0	1423,0
Enz-CaP	504,2	89,4	410,0	623,0
TAM	668,8	573,3	245,0	1655,0
APA	787,0	413,8	310,0	1388,0
AP	669,6	475,2	0,0	1191,0
PMCG	1487,8	423,2	905,0	1852,0
Zymosan	1713,0	697,2	951,0	2813,0

Table E2. Test statistics – monocytes, CD11b-expression. Wilcoxon signed ranks test, b=based on negative ranks, c=based on positive ranks.

	Saline-M REDV	Saline-G VAPG	Saline-G RGD	Saline-M RGD	Saline-UP-MVM	Saline-Ca-bead	Saline-CaP
Z	-0,135[c]	-2,023[c]	-0,405[b]	-0,405[b]	-0,405[b]	-0,405[b]	-0,405[c]
Asymp. Sign.	0,893	0,043	0,686	0,686	0,686	0,686	0,686

	Saline-Enz-CaP	Saline-TAM	Saline-APA	Saline-AP	Saline-PMCG	Saline-Zymosan	Ca-bead-PMCG
Z	-0,405[b]	-0,674[c]	-1,214[c]	-0,135[b]	-2,023[c]	-2,023[c]	-2,023[b]
Asymp. Sign.	0,686	0,500	0,225	0,893	0,043	0,043	0,043

	UP-MVM -M REDV	TAM - G VAPG	TAM - G RGD	UP-MVM -M RGD	Ca-bead - CaP	Ca-bead - Enz-CaP	Ca-bead-APA
Z	-0,135[b]	-2,023[b]	-0,944[c]	-0,405[b]	-2,023[c]	-0,677[c]	-2,023[b]
Asymp. Sign.	0,893	0,043	0,345	0,686	0,043	0,498	0,043

	Ca-bead-AP
Z	-0,944[b]
Asymp. Sign.	0,345

E.2 CD11b – granulocytes

Table E3. Descriptive statistics – granulocytes, CD11b-expression. n=5

Sample	Mean	Std. Deviation	Minimum	Maximum
T0	133,8	28,9	85,0	157,0
Saline	831,8	875,1	231,0	2344,0
M REDV	668,2	796,9	234,0	2083,0
G VAPG	2718,6	1048,2	1287,0	3770,0
G RGD	654,4	634,2	210,0	1747,0
M RGD	441,4	173,3	204,0	595,0
UP-MVM	526,8	483,4	206,0	1380,0
Ca	646,2	440,3	210,0	1161,0
CaP	1029,0	200,5	751,0	1245,0
Enz-CaP	635,0	394,0	288,0	1077,0
TAM	667,8	818,0	242,0	2119,0
APA	927,4	676,5	294,0	1713,0
AP	1057,8	659,1	0,0	1726,0
PMCG	1639,4	488,2	1197,0	2400,0
Zymosan	3100,6	820,9	2374,0	4489,0

Table E4. Test statistics – granulocytes, CD11b-expression. Wilcoxon signed ranks test, b=based on negative ranks, c=based on positive ranks.

	Saline-M REDV	Saline-G VAPG	Saline-G RGD	Saline-M RGD	Saline-UP-MVM	Saline-Ca-bead	Saline-CaP
Z	-1,214[b]	-2,023[c]	-1,753[b]	-0,674[b]	-1,753[b]	-0,135[b]	-0,674[c]
Asymp. Sign.	0,225	0,043	0,080	0,500	0,080	0,893	0,500

	Saline-Enz-CaP	Saline-TAM	Saline-APA	Saline-AP	Saline-PMCG	Saline-Zymosan	Ca-bead-PMCG
Z	-0,135[c]	-1,753[b]	-0,944[c]	-0,944[c]	-2,023[c]	-2,023[c]	-2,023[b]
Asymp. Sign.	0,893	0,080	0,345	0,345	0,043	0,043	0,043

	UP-MVM -M REDV	TAM - G VAPG	TAM - G RGD	UP-MVM -M RGD	Ca-bead - CaP	Ca-bead - Enz-CaP	Ca-bead-APA
Z	-0,944[c]	-2,023[b]	-0,405[c]	-0,405[c]	-2,023[c]	-0,135[b]	-2,023[b]
Asymp. Sign.	0,345	0,043	0,686	0,686	0,043	0,893	0,043

	Ca-bead-AP
Z	-1,753[b]
Asymp. Sign.	0,080

E.3 sTCC

Table E5. Descriptive statistics – sTCC. n=5

Sample	Mean	Std. Deviation	Minimum	Maximum
T0	0,472	0,040	0,421	0,522
Saline	13,325	5,628	5,311	20,859
M REDV	4,839	1,049	3,727	6,286
G VAPG	3,785	0,519	3,016	4,266
G RGD	4,416	0,977	3,335	5,673
M RGD	4,024	0,607	3,253	4,625
UP-MVM	7,695	5,548	2,350	17,037
Ca	7,672	2,866	5,137	11,636
CaP	24,097	7,590	13,255	31,063
Enz-CaP	13,600	3,737	9,529	17,840
TAM	4,349	2,095	2,028	7,642
APA	66,321	44,663	0,000	104,378
AP	124,397	70,279	0,000	167,525
PMCG	37,393	5,620	32,805	44,185
Zymosan	154,391	17,615	129,768	171,489

Table E6. Test statistics – sTCC. Wilcoxon signed ranks test, b=based on negative ranks, c=based on positive ranks.

	Saline-M REDV	Saline-G VAPG	Saline-G RGD	Saline-M RGD	Saline-UP-MVM	Saline-Ca-bead	Saline-CaP
Z	-2,023[b]	-2,023[b]	-2,023[b]	-2,023[b]	-1,483[b]	-1,753[b]	-1,214[c]
Asymp. Sign.	0,043	0,043	0,043	0,043	0,138	0,080	0,225

	Saline-Enz-CaP	Saline-TAM	Saline-APA	Saline-AP	Saline-PMCG	Saline-Zymosan	Ca-bead-PMCG
Z	-0,135[c]	-2,023[b]	-1,753[c]	-1,753[c]	-2,023[c]	-2,023[c]	-2,023[b]
Asymp. Sign.	0,893	0,043	0,080	0,080	0,043	0,043	0,043

	UP-MVM -M REDV	TAM - G VAPG	TAM - G RGD	UP-MVM -M RGD	Ca-bead - CaP	Ca-bead - Enz-CaP	Ca-bead-APA
Z	-0,944[b]	-0,135[b]	-0,674[c]	-1,483[b]	-2,023[c]	-2,023[c]	-1,753[b]
Asymp. Sign.	0,345	0,893	0,500	0,138	0,043	0,043	0,080

	Ca-bead-AP
Z	-1,753[b]
Asymp. Sign.	0,080

E.4 IL-8

Table E7. Descriptive statistics – IL-8. n=5

Sample	Mean	Std. Deviation	Minimum	Maximum
T0	2,420	1,026	0,980	3,680
Saline	807,656	473,417	118,760	1304,180
M REDV	473,386	429,365	99,470	1150,420
G VAPG	3934,368	2028,720	1214,880	6831,230
G RGD	438,642	405,978	26,430	1075,250
M RGD	593,386	450,250	60,630	1166,340
UP-MVM	461,614	320,811	80,090	877,130
Ca	954,886	737,576	111,030	1963,350
CaP	1138,376	286,308	735,900	1519,570
Enz-CaP	872,698	547,835	67,020	1334,350
TAM	472,140	329,899	44,390	911,530
APA	1769,008	377,511	1354,020	2266,380
AP	2858,218	1273,170	1535,020	4922,200
PMCG	967,368	488,979	289,040	1539,930
Zymosan	4769,380	2927,998	2329,860	8593,650

Table E8. Test statistics – IL-8. Wilcoxon signed ranks test, b=based on negative ranks, c=based on positive ranks.

	Saline-M REDV	Saline-G VAPG	Saline-G RGD	Saline-M RGD	Saline-UP-MVM	Saline-Ca-bead	Saline-CaP
Z	-2,023[b]	-2,023[c]	-2,023[b]	-1,483[b]	-2,023[b]	-,135[c]	-1,214[c]
Asymp. Sign.	0,043	0,043	0,043	0,138	0,043	0,893	0,225

	Saline-Enz-CaP	Saline-TAM	Saline-APA	Saline-AP	Saline-PMCG	Saline-Zymosan	Ca-bead-PMCG
Z	-0,405[c]	-2,023[b]	-2,023[c]	-2,023[c]	-0,674[c]	-2,023[c]	-0,405[b]
Asymp. Sign.	0,686	0,043	0,043	0,043	0,500	0,043	0,686

	UP-MVM -M REDV	TAM - G VAPG	TAM - G RGD	UP-MVM -M RGD	Ca-bead - CaP	Ca-bead - Enz-CaP	Ca-bead-APA
Z	-0,405[b]	-2,023[b]	-0,674[c]	-1,214[c]	-0,674[c]	-0,405[b]	-2,023[b]
Asymp. Sign.	0,686	0,043	0,500	0,225	0,500	0,686	0,043

	Ca-bead-AP
Z	-2,023[b]
Asymp. Sign.	0,043

E.5 MCP-1

Table E9. Descriptive statistics – MCP-1. n=5

Sample	Mean	Std. Deviation	Minimum	Maximum
T0	28,582	10,338	17,200	43,830
Saline	64,978	29,605	20,780	90,890
M REDV	67,842	55,984	20,640	145,350
G VAPG	232,452	110,888	132,800	389,220
G RGD	44,888	26,069	23,700	80,180
M RGD	81,876	67,667	23,980	198,090
UP-MVM	58,484	46,274	21,900	129,730
Ca	82,352	59,975	30,410	171,010
CaP	191,396	149,547	34,820	412,560
Enz-CaP	94,602	68,353	16,910	198,280
TAM	52,614	27,195	20,080	91,320
APA	123,272	48,211	47,490	176,410
AP	133,342	49,189	70,460	194,810
PMCG	75,762	34,133	40,740	120,580
Zymosan	359,538	172,302	163,710	553,040

Table E10. Test statistics – MCP-1. Wilcoxon signed ranks test, b=based on negative ranks, c=based on positive ranks.

	Saline-M REDV	Saline-G VAPG	Saline-G RGD	Saline-M RGD	Saline-UP-MVM	Saline-Ca-bead	Saline-CaP
Z	-0,135[c]	-2,023[c]	-1,753[b]	-0,135[b]	-0,405[b]	-0,944[c]	-1,483[c]
Asymp. Sign.	0,893	0,043	0,080	0,893	0,686	0,345	0,138

	Saline-Enz-CaP	Saline-TAM	Saline-APA	Saline-AP	Saline-PMCG	Saline-Zymosan	Ca-bead-PMCG
Z	-1,753[c]	-1,214[b]	-1,753[c]	-1,753[c]	-0,674[c]	-2,023[c]	-0,135[c]
Asymp. Sign.	0,080	0,225	0,080	0,080	0,500	0,043	0,893

	UP-MVM -M REDV	TAM - G VAPG	TAM - G RGD	UP-MVM -M RGD	Ca-bead - CaP	Ca-bead - Enz-CaP	Ca-bead-APA
Z	-1,753[c]	-2,023[c]	-1,214[b]	-1,483[b]	-1,214[c]	-0,674[c]	-1,214[b]
Asymp. Sign.	0,080	0,043	0,225	0,135	0,225	0,500	0,225

	Ca-bead-AP
Z	-2,023[b]
Asymp. Sign.	0,043

E.6 MIP-1α

Table E11. Descriptive statistics – MIP-1α. n=5

Sample	Mean	Std. Deviation	Minimum	Maximum
T0	2,718	3,678	0,350	9,050
Saline	88,828	52,467	36,290	143,680
M REDV	100,040	92,761	22,660	231,660
G VAPG	2092,198	1380,750	1014,840	4499,480
G RGD	73,594	67,239	8,030	157,970
M RGD	96,720	88,257	19,830	232,490
UP-MVM	74,464	64,492	20,680	158,040
Ca	140,240	101,071	40,010	255,010
CaP	141,978	103,102	42,350	296,350
Enz-CaP	110,920	90,409	16,920	212,020
TAM	80,580	70,782	15,830	160,530
APA	142,500	88,244	66,600	276,360
AP	245,956	174,983	107,740	542,970
PMCG	420,290	358,659	82,350	973,440
Zymosan	983,550	1030,720	397,230	2808,260

Table E12. Test statistics – MIP-1α. Wilcoxon signed ranks test, b=based on negative ranks, c=based on positive ranks.

	Saline-M REDV	Saline-G VAPG	Saline-G RGD	Saline-M RGD	Saline-UP-MVM	Saline-Ca-bead	Saline-CaP
Z	-0,135[c]	-2,023[c]	-1,214[b]	-0,674[b]	-1,214[b]	-2,023[c]	-1,483[c]
Asymp. Sign.	0,893	0,043	0,225	0,500	0,225	0,043	0,138

	Saline-Enz-CaP	Saline-TAM	Saline-APA	Saline-AP	Saline-PMCG	Saline-Zymosan	Ca-bead-PMCG
Z	-0,944[c]	-0,674[b]	-1,753[c]	-2,023[c]	-2,023[c]	-2,023[c]	-2,023[c]
Asymp. Sign.	0,345	0,500	0,080	0,043	0,043	0,043	0,043

	UP-MVM -M REDV	TAM - G VAPG	TAM - G RGD	UP-MVM -M RGD	Ca-bead - CaP	Ca-bead - Enz-CaP	Ca-bead-APA
Z	-1,753[c]	-2,023[c]	-1,214[b]	-1,214[c]	-0,405[c]	-2,023[b]	-0,135[b]
Asymp. Sign.	0,080	0,043	0,225	0,225	0,686	0,043	0,893

	Ca-bead-AP
Z	-1,753[c]
Asymp. Sign.	0,080

E.7 IL-1β

Table E13. Descriptive statistics – IL-1β. n=5

Sample	Mean	Std. Deviation	Minimum	Maximum
T0	0,100	0,080	0,020	0,180
Saline	3,730	1,736	1,790	6,040
M REDV	2,258	1,822	0,640	5,150
G VAPG	1434,428	1436,373	512,090	3859,600
G RGD	2,090	1,367	0,360	3,960
M RGD	3,350	3,274	0,450	8,980
UP-MVM	3,478	3,220	0,450	6,940
Ca	4,014	1,822	1,010	5,470
CaP	3,538	2,240	1,690	7,320
Enz-CaP	5,630	4,461	1,010	12,240
TAM	2,766	1,342	0,450	3,700
APA	7,158	2,504	3,500	9,520
AP	8,776	3,783	2,890	12,850
PMCG	87,324	62,945	36,680	165,970
Zymosan	74,176	80,108	10,390	209,240

Table E14. Test statistics – IL-1β. Wilcoxon signed ranks test, b=based on negative ranks, c=based on positive ranks, d=the sum of negative ranks equals the sum of positive ranks.

	Saline-M REDV	Saline-G VAPG	Saline-G RGD	Saline-M RGD	Saline-UP-MVM	Saline-Ca-bead	Saline-CaP
Z	-2,023[b]	-2,023[c]	-2,023[b]	-0,405[b]	-0,405[b]	-0,405[c]	-0,405[b]
Asymp. Sign.	0,043	0,043	0,043	0,686	0,686	0,686	0,686

	Saline-Enz-CaP	Saline-TAM	Saline-APA	Saline-AP	Saline-PMCG	Saline-Zymosan	Ca-bead-PMCG
Z	-1,214[c]	-1,214[b]	-2,023[c]	-2,023[c]	-2,023[c]	-2,023[c]	-2,023[b]
Asymp. Sign.	0,225	0,225	0,043	0,043	0,043	0,043	0,043

	UP-MVM -M REDV	TAM - G VAPG	TAM - G RGD	UP-MVM -M RGD	Ca-bead - CaP	Ca-bead - Enz-CaP	Ca-bead-APA
Z	-0,406[b]	-2,023[c]	-1,214[b]	0,000[d]	-0,948[b]	-0,730[c]	-2,023[b]
Asymp. Sign.	0,684	0,043	0,225	1,000	0,343	0,465	0,043

	Ca-bead-AP
Z	-2,023[b]
Asymp. Sign.	0,043

E.8 IL-6

Table E15. Descriptive statistics – IL-6. n=5

Sample	Mean	Std. Deviation	Minimum	Maximum
T0	1,478	2,035	0,490	5,110
Saline	35,910	38,050	5,640	101,600
M REDV	29,214	35,045	4,240	90,670
G VAPG	10716,228	2910,751	6358,900	14456,540
G RGD	21,150	22,229	1,480	57,750
M RGD	29,562	26,120	4,240	71,570
UP-MVM	30,798	36,362	2,850	93,840
Ca	38,736	37,780	7,770	102,200
CaP	32,078	41,814	4,410	105,200
Enz-CaP	35,092	35,906	2,850	93,450
TAM	21,516	15,278	2,160	39,130
APA	45,264	54,971	10,110	141,720
AP	65,872	77,512	17,580	201,550
PMCG	885,518	355,001	492,110	1393,040
Zymosan	1213,768	1500,277	257,280	3874,900

Table E16. Test statistics – IL-6. Wilcoxon signed ranks test, b=based on negative ranks, c=based on positive ranks.

	Saline-M REDV	Saline-G VAPG	Saline-G RGD	Saline-M RGD	Saline-UP-MVM	Saline-Ca-bead	Saline-CaP
Z	-2,023[b]	-2,023[c]	-2,023[b]	-0,944[b]	-2,032[b]	-0,944[c]	-0,944[b]
Asymp. Sign.	0,043	0,043	0,043	0,345	0,042	0,345	0,345

	Saline-Enz-CaP	Saline-TAM	Saline-APA	Saline-AP	Saline-PMCG	Saline-Zymosan	Ca-bead-PMCG
Z	-0,674[b]	-1,214[b]	-0,944[c]	-2,023[c]	-2,023[c]	-2,023[c]	-2,023[b]
Asymp. Sign.	0,500	0,225	0,345	0,043	0,043	0,043	0,043

	UP-MVM -M REDV	TAM - G VAPG	TAM - G RGD	UP-MVM -M RGD	Ca-bead - CaP	Ca-bead - Enz-CaP	Ca-bead-APA
Z	-1,214[b]	-2,023[c]	-0,135[b]	-0,135[b]	-1,483[b]	-1,753[b]	-0,405[b]
Asymp. Sign.	0,225	0,043	0,893	0,893	0,138	0,080	0,686

	Ca-bead-AP
Z	-2,023[b]
Asymp. Sign.	0,043

E.9 TNF-α

Table E17. Descriptive statistics –TNF-α. n=5

Sample	Mean	Std. Deviation	Minimum	Maximum
T0	1,842	4,119	0,000	9,210
Saline	72,600	64,556	0,140	157,400
M REDV	145,446	216,829	2,450	525,820
G VAPG	11372,646	6648,525	6507,200	22973,840
G RGD	97,358	142,164	0,000	343,250
M RGD	79,020	79,820	13,670	198,990
UP-MVM	111,908	164,738	0,000	389,750
Ca	108,770	68,180	0,000	167,010
CaP	67,880	59,508	0,140	156,340
Enz-CaP	137,334	166,549	6,970	421,430
TAM	66,222	73,425	6,970	163,810
APA	84,892	91,051	0,000	227,710
AP	206,190	268,185	0,140	676,390
PMCG	1225,680	1475,421	102,770	3692,460
Zymosan	597,212	612,875	18,100	1549,430

Table E18. Test statistics – TNF-α. Wilcoxon signed ranks test, b=based on negative ranks, c=based on positive ranks.

	Saline-M REDV	Saline-G VAPG	Saline-G RGD	Saline-M RGD	Saline-UP-MVM	Saline-Ca-bead	Saline-CaP
Z	-0,135[c]	-2,023[c]	-0,674[b]	-0,135[c]	-0,674[b]	-1,753[c]	-0,730[b]
Asymp. Sign.	0,893	0,043	0,500	0,893	0,500	0,080	0,465

	Saline-Enz-CaP	Saline-TAM	Saline-APA	Saline-AP	Saline-PMCG	Saline-Zymosan	Ca-bead-PMCG
Z	-0,944[c]	-0,405[b]	-0,135[c]	-1,461[c]	-2,023[c]	-2,023[c]	-2,023[c]
Asymp. Sign.	0,345	0,686	0,893	0,144	0,043	0,043	0,043

	UP-MVM -M REDV	TAM - G VAPG	TAM - G RGD	UP-MVM -M RGD	Ca-bead - CaP	Ca-bead - Enz-CaP	Ca-bead-APA
Z	-1,214[c]	-2,023[c]	-0,135[c]	-0,135[b]	-1,753[b]	-0,405[b]	-0,674[b]
Asymp. Sign.	0,225	0,043	0,893	0,893	0,080	0,686	0,500

	Ca-bead-AP
Z	-0,944[c]
Asymp. Sign.	0,345

E.10 IL-10

Table E19. Descriptive statistics – IL-10. n=5

Sample	Mean	Std. Deviation	Minimum	Maximum
T0	0,804	0,890	0,190	2,370
Saline	1,220	0,534	0,410	1,730
M REDV	2,386	1,805	0,640	5,170
G VAPG	4,852	1,225	3,950	6,980
G RGD	1,314	0,599	0,870	2,370
M RGD	2,084	1,322	0,870	4,220
UP-MVM	1,818	1,547	0,520	4,490
Ca	1,724	0,918	0,640	3,150
CaP	2,064	1,539	0,000	4,220
Enz-CaP	1,676	1,065	0,640	3,410
TAM	1,594	1,036	0,000	2,890
APA	1,510	0,137	1,360	1,610
AP	1,916	0,654	1,110	2,630
PMCG	2,664	1,772	0,870	5,310
Zymosan	2,458	0,986	1,230	3,950

Table E20. Test statistics – IL-10. Wilcoxon signed ranks test, b=based on negative ranks, c=based on positive ranks, d=the sum of negative ranks equals the sum of positive ranks.

	Saline-M REDV	Saline-G VAPG	Saline-G RGD	Saline-M RGD	Saline-UP-MVM	Saline-Ca-bead	Saline-CaP
Z	-2,023[c]	-2,023[c]	-0,405[c]	-1,753[c]	-0,921[c]	-1,826[c]	-1,214[c]
Asymp. Sign.	0,043	0,043	0,686	0,080	0,357	0,068	0,225

	Saline-Enz-CaP	Saline-TAM	Saline-APA	Saline-AP	Saline-PMCG	Saline-Zymosan	Ca-bead-PMCG
Z	-1,214[c]	-1,214[c]	-1,084[c]	-2,023[c]	-1,753[c]	-2,023[c]	-1,483[c]
Asymp. Sign.	0,225	0,225	0,279	0,043	0,080	0,043	0,138

	UP-MVM -M REDV	TAM - G VAPG	TAM - G RGD	UP-MVM -M RGD	Ca-bead - CaP	Ca-bead - Enz-CaP	Ca-bead-APA
Z	-1,355[c]	-2,023[c]	-0,677[b]	-1,214[c]	-0,813[c]	0,000[d]	-0,184[b]
Asymp. Sign.	0,176	0,043	0,498	0,225	0,416	1,000	0,854

	Ca-bead-AP
Z	-0,674[c]
Asymp. Sign.	0,500

E.11 IL-1ra

Table E21. Descriptive statistics – IL-1ra. n=5

Sample	Mean	Std. Deviation	Minimum	Maximum
T0	23,856	30,798	0,000	76,730
Saline	244,632	85,723	133,190	327,990
M REDV	325,042	102,960	175,200	438,490
G VAPG	1463,738	780,716	645,170	2298,900
G RGD	249,906	121,075	62,490	383,280
M RGD	335,962	158,173	161,220	576,320
UP-MVM	305,476	136,505	133,190	438,490
Ca	347,304	59,942	286,450	410,890
CaP	380,364	125,963	244,830	576,320
Enz-CaP	280,074	174,940	33,750	521,210
TAM	305,102	176,135	48,170	534,990
APA	344,516	69,468	244,830	410,890
AP	371,952	141,984	161,220	548,770
PMCG	675,504	242,344	410,890	1072,430
Zymosan	350,078	56,645	300,300	438,490

Table E22. Test statistics – IL-1ra. Wilcoxon signed ranks test, b=based on negative ranks, c=based on positive ranks, d=the sum of negative ranks equals the sum of positive ranks.

	Saline-M REDV	Saline-G VAPG	Saline-G RGD	Saline-M RGD	Saline-UP-MVM	Saline-Ca-bead	Saline-CaP
Z	-1,214[c]	-2,023[c]	-0,135[c]	-0,944[c]	-0,674[c]	-1,753[c]	-1,483[c]
Asymp. Sign.	0,225	0,043	0,893	0,345	0,500	0,080	0,138

	Saline-Enz-CaP	Saline-TAM	Saline-APA	Saline-AP	Saline-PMCG	Saline-Zymosan	Ca-bead-PMCG
Z	-0,405[c]	-0,674[c]	-1,214[c]	-1,214[c]	-2,023[c]	-1,483[c]	-2,023[c]
Asymp. Sign.	0,686	0,500	0,225	0,225	0,043	0,138	0,043

	UP-MVM -M REDV	TAM - G VAPG	TAM - G RGD	UP-MVM -M RGD	Ca-bead - CaP	Ca-bead - Enz-CaP	Ca-bead-APA
Z	0,000[d]	-2,023[c]	-0,405[b]	-0,944[c]	-0,674[c]	-0,730[b]	-0,135[b]
Asymp. Sign.	1,000	0,043	0,686	0,345	0,500	0,465	0,893

	Ca-bead-AP
Z	-0,535[c]
Asymp. Sign.	0,593

E.12 PDGF-BB

Table E23. Descriptive statistics – PDGF-BB. n=5

Sample	Mean	Std. Deviation	Minimum	Maximum
T0	24,504	52,776	0,000	118,870
Saline	433,946	578,717	62,670	1452,080
M REDV	447,496	516,500	59,200	1330,990
G VAPG	709,652	552,915	28,770	1317,330
G RGD	373,750	291,301	37,040	706,910
M RGD	544,130	447,936	87,350	1218,040
UP-MVM	473,310	333,177	90,710	931,640
Ca	465,204	405,466	85,670	1117,790
CaP	623,590	187,405	395,650	825,220
Enz-CaP	646,642	416,937	39,760	1195,710
TAM	755,274	619,966	44,240	1498,350
APA	712,174	548,691	238,150	1630,660
AP	723,882	359,968	197,020	1187,740
PMCG	398,504	246,131	124,600	616,190
Zymosan	680,918	816,476	117,230	1937,420

Table E24. Test statistics – PDGF-BB. Wilcoxon signed ranks test, b=based on negative ranks, c=based on positive ranks.

	Saline-M REDV	Saline-G VAPG	Saline-G RGD	Saline-M RGD	Saline-UP-MVM	Saline-Ca-bead	Saline-CaP
Z	-0,135[c]	-1,214[c]	-0,674[b]	-0,405[c]	-0,674[c]	-0,405[c]	-0,944[c]
Asymp. Sign.	0,893	0,225	0,500	0,686	0,500	0,686	0,345

	Saline-Enz-CaP	Saline-TAM	Saline-APA	Saline-AP	Saline-PMCG	Saline-Zymosan	Ca-bead-PMCG
Z	-1,214[c]	-0,944[c]	-1,753[c]	-1,214[c]	-0,135[c]	-1,214[c]	-0,135[c]
Asymp. Sign.	0,225	0,345	0,080	0,225	0,893	0,225	0,893

	UP-MVM -M REDV	TAM - G VAPG	TAM - G RGD	UP-MVM -M RGD	Ca-bead - CaP	Ca-bead - Enz-CaP	Ca-bead-APA
Z	-0,674[b]	-0,674[b]	-2,023[b]	-0,674[c]	-0,674[c]	-1,753[c]	-1,483[b]
Asymp. Sign.	0,500	0,500	0,043	0,500	0,500	0,080	0,138

	Ca-bead-AP
Z	-1,214[b]
Asymp. Sign.	0,225

E.13 VEGF

Table E25. Descriptive statistics – VEGF. n=5

Sample	Mean	Std. Deviation	Minimum	Maximum
T0	15,100	20,118	0,220	50,030
Saline	44,348	7,923	36,570	54,510
M REDV	34,246	13,113	17,520	48,540
G VAPG	29,208	20,448	7,920	53,520
G RGD	27,152	27,138	1,260	72,890
M RGD	35,792	28,818	16,520	86,280
UP-MVM	40,144	13,902	24,560	62,470
Ca	56,150	29,981	32,570	104,610
CaP	56,712	39,141	27,060	118,960
Enz-CaP	46,690	27,456	22,550	93,220
TAM	33,116	23,520	20,540	74,880
APA	66,310	25,909	43,550	108,070
AP	72,468	25,512	49,530	107,580
PMCG	66,222	19,005	45,550	85,290
Zymosan	56,966	51,506	15,510	146,650

Table E26. Test statistics – VEGF. Wilcoxon signed ranks test, b=based on negative ranks, c=based on positive ranks.

	Saline-M REDV	Saline-G VAPG	Saline-G RGD	Saline-M RGD	Saline-UP-MVM	Saline-Ca-bead	Saline-CaP
Z	-2,023[b]	-1,483[b]	-1,214[b]	-0,674[b]	-1,214[b]	-0,674[c]	-0,405[c]
Asymp. Sign.	0,043	0,138	0,225	0,500	0,225	0,500	0,686

	Saline-Enz-CaP	Saline-TAM	Saline-APA	Saline-AP	Saline-PMCG	Saline-Zymosan	Ca-bead-PMCG
Z	-0,674[b]	-1,214[b]	-1,753[c]	-2,023[c]	-2,023[c]	-0,135[b]	-0,944[b]
Asymp. Sign.	0,500	0,225	0,080	0,043	0,043	0,893	0,345

	UP-MVM -M REDV	TAM - G VAPG	TAM - G RGD	UP-MVM -M RGD	Ca-bead - CaP	Ca-bead - Enz-CaP	Ca-bead-APA
Z	-1,095[b]	-0,674[b]	-0,944[b]	-0,674[b]	-0,674[b]	-2,023[b]	-0,674[b]
Asymp. Sign.	0,273	0,500	0,345	0,500	0,500	0,043	0,500

	Ca-bead-AP
Z	-2,023[b]
Asymp. Sign.	0,043

E.14 RANTES

Table E27. Descriptive statistics – RANTES. n=5

Sample	Mean	Std. Deviation	Minimum	Maximum
T0	743,312	1252,089	39,240	2965,390
Saline	1376,104	1102,641	149,970	3152,470
M REDV	1447,760	889,797	135,140	2644,030
G VAPG	3076,056	2092,204	154,410	6004,080
G RGD	1440,734	1171,790	107,570	3315,170
M RGD	1793,408	1117,089	297,650	3409,410
UP-MVM	1537,514	562,138	634,580	1939,910
Ca	1627,566	1096,980	357,820	3131,580
CaP	2121,288	980,606	1158,480	3755,190
Enz-CaP	1934,726	1475,096	121,450	4196,700
TAM	1428,524	1130,111	118,230	3147,140
APA	1337,674	1440,070	0,000	3634,830
AP	2331,286	1325,404	484,330	3490,700
PMCG	1063,488	647,008	221,470	1894,030
Zymosan	2480,150	2279,212	258,160	5488,580

Table E28. Test statistics – RANTES. Wilcoxon signed ranks test, b=based on negative ranks, c=based on positive ranks.

	Saline-M REDV	Saline-G VAPG	Saline-G RGD	Saline-M RGD	Saline-UP-MVM	Saline-Ca-bead	Saline-CaP
Z	-0,405[c]	-2,023[c]	-0,405[c]	-0,944[c]	-0,674[c]	-0,405[c]	-1,214[c]
Asymp. Sign.	0,686	0,043	0,686	0,345	0,500	0,686	0,225

	Saline-Enz-CaP	Saline-TAM	Saline-APA	Saline-AP	Saline-PMCG	Saline-Zymosan	Ca-bead-PMCG
Z	-0,674[c]	-0,135[c]	-0,405[c]	-2,023[c]	-0,944[b]	-0,944[c]	-1,214[c]
Asymp. Sign.	0,500	0,893	0,686	0,043	0,345	0,345	0,225

	UP-MVM -M REDV	TAM - G VAPG	TAM - G RGD	UP-MVM -M RGD	Ca-bead - CaP	Ca-bead - Enz-CaP	Ca-bead-APA
Z	-0,674[b]	-1,483[c]	-0,135[c]	-0,405[c]	-1,214[c]	-1,214[c]	-0,405[b]
Asymp. Sign.	0,500	0,138	0,893	0,686	0,225	0,225	0,686

	Ca-bead-AP
Z	-1,483[b]
Asymp. Sign.	0,138

E.15 IFN-γ

Table E29. Descriptive statistics – IFN-γ. n=5

Sample	Mean	Std. Deviation	Minimum	Maximum
T0	1,772	2,426	0,000	4,430
Saline	16,880	12,588	0,000	35,530
M REDV	42,558	29,210	16,290	87,240
G VAPG	54,626	15,661	35,530	72,310
G RGD	14,508	13,787	0,000	35,530
M RGD	25,572	21,014	4,430	48,450
UP-MVM	15,394	12,723	4,430	35,530
Ca	23,992	19,828	4,430	56,640
CaP	28,542	24,069	0,000	64,580
Enz-CaP	17,368	18,752	0,000	44,240
TAM	18,254	17,807	0,000	44,240
APA	15,772	12,893	0,000	35,530
AP	9,764	14,531	0,000	35,530
PMCG	14,764	17,259	4,430	44,240
Zymosan	17,032	21,476	0,000	52,580

Table E30. Test statistics – IFN-γ. Wilcoxon signed ranks test, b=based on negative ranks, c=based on positive ranks, d=the sum of negative ranks equals the sum of positive ranks.

	Saline-M REDV	Saline-G VAPG	Saline-G RGD	Saline-M RGD	Saline-UP-MVM	Saline-Ca-bead	Saline-CaP
Z	-2,032[c]	-2,023[c]	-0,184[b]	-0,944[c]	0,000[d]	-0,730[c]	-1,084[c]
Asymp. Sign.	0,042	0,043	0,854	0,345	1,000	0,465	0,279

	Saline-Enz-CaP	Saline-TAM	Saline-APA	Saline-AP	Saline-PMCG	Saline-Zymosan	Ca-bead-PMCG
Z	0,000[d]	-0,271[c]	-0,272[b]	-0,674[b]	-0,365[b]	-0,447[c]	-1,511[b]
Asymp. Sign.	1,000	0,786	0,785	0,500	0,715	0,655	0,131

	UP-MVM -M REDV	TAM - G VAPG	TAM - G RGD	UP-MVM -M RGD	Ca-bead - CaP	Ca-bead - Enz-CaP	Ca-bead-APA
Z	-1,826[c]	-2,023[c]	-0,552[b]	-0,730[c]	-0,271[c]	-1,214[b]	-1,095[b]
Asymp. Sign.	0,068	0,043	0,581	0,465	0,786	0,225	0,273

	Ca-bead-AP
Z	-1,826[b]
Asymp. Sign.	0,068